MASTERARBEIT | MASTER'S THESIS

Titel | Title

Optimization of purification methods for PEGylated-polymer conjugates

verfasst von | submitted by

Akinalp Ismet Saglam BSc

angestrebter akademischer Grad | in partial fulfilment of the requirements for the degree of

Magister pharmaciae (Mag. pharm.)

Wien | Vienna, 2026

Studienkennzahl lt. Studienblatt | Degree programme code as it appears on the student record sheet:	UA 066 605
Studienrichtung lt. Studienblatt | Degree programme as it appears on the student record sheet:	Masterstudium Pharmazie
Betreut von | Supervisor:	Univ.-Prof. Dipl.-Ing. Dr. Manfred Ogris
Mitbetreut von | Co-Supervisor:	Haider Sami Ph.D.

1 Abstract (English)

Cancer treatment remains one of the most challenging areas of biomedical research, with substantial societal relevance given the growing number of patients requiring effective therapies. Beyond conventional treatment modalities, cancer research has advanced innovative therapeutic strategies, including immunotherapy and gene-based approaches. In this context, gene therapy and mRNA technologies have emerged as versatile platforms for the development of novel treatments. However, the intrinsic physicochemical properties of mRNA pose significant challenges for efficient and targeted delivery, necessitating the use of specialized drug delivery systems such as polymer-based carriers. PEGylated linear polyethylenimine (LPEI), when further functionalized with targeting moieties to form LPEI-PEG tri-conjugates, represents a promising carrier system for the targeted in vivo delivery of nucleic acids. The synthesis process, and in particular the downstream purification strategy, plays a critical role in determining the quality, reproducibility, and functional performance of these polymeric conjugates. The primary objective of this study was to optimize the synthesis and purification of LPEI10kDa-PEG2k-based tri-conjugates. Tri-conjugate synthesis involved the initial conjugation of LPEI (10 kDa) to a heterobifunctional PEG2k linker to form an LPEI10kDa-PEG2k-OPSS bi-conjugate, followed by purification via cation-exchange chromatography and desalting either via centrifugal filtration or dialysis. The purified bi-conjugate was subsequently reacted with cysteine to generate the corresponding tri-conjugate, which was again purified chromatographically and desalted either via centrifugal filtration or dialysis. A central focus of this work was the optimization of purification strategies for LPEI10kDa-based bi- and tri-conjugates through a comparative evaluation of centrifugal filtration and dialysis. This comparison demonstrated that dialysis was superior with respect to desalting efficiency and overall yield, whereas centrifugal filtration offered significantly higher time efficiency and resulted in higher OPSS/CYS-to-LPEI molar ratios. To support this optimization, LPEI quantification using a copper-based assay was systematically evaluated with respect to reagent shelf-life, assay variability, and polymer or conjugate loss during purification. The reagent shelf life was determined to be 41 days. Assay variability ranged from 2-18% and decreased to below 7% across all dilutions when reagent concentrations exceeded 30 µg/mL. This suggests that in order to reduce variability in the copper assay results, a standard curve with dilutions above 30 µg/mL should be utilized. With regard to conjugate loss during purification, higher dilution prior to cation-exchange chromatography resulted in reduced yield loss. Based on these findings, a single centrifugal filtration step was selected as the standard desalting procedure. This approach achieved adequate salt removal while preserving acceptable yield and reduced processing time relative to a five-cycle washing protocol, which required approximately one additional hour. Additionally, as part of the characterization and as an initial application trial, dynamic light scattering measurements were performed using both pDNA- and mRNA-based polyplexes with sole LPEI and the synthesized tri-conjugate to compare particle size and homogeneity.

2 Abstract (German)

Die Krebsbehandlung ist nach wie vor einer der anspruchsvollsten Bereiche der biomedizinischen Forschung und hat angesichts der wachsenden Zahl von Patienten, die wirksame Therapien benötigen, eine erhebliche gesellschaftliche Relevanz. Über die konventionellen Behandlungsmethoden hinaus hat die Krebsforschung innovative therapeutische Strategien vorangetrieben, darunter Immuntherapien und genbasierte Ansätze. In diesem Zusammenhang haben sich Gentherapie und mRNA-Technologien als vielseitige Plattformen für die Entwicklung neuartiger Behandlungen herausgestellt. Die intrinsischen physikalisch-chemischen Eigenschaften von mRNA stellen jedoch erhebliche Herausforderungen für eine effiziente und gezielte Verabreichung dar, sodass der Einsatz spezieller Wirkstofffreisetzungssysteme wie polymerbasierter Träger erforderlich ist. PEGyliertes lineares Polyethylenimin (LPEI) stellt, wenn es mit Zielmolekülen weiter funktionalisiert wird, um LPEI-PEG-Tri-Konjugate zu bilden, ein vielversprechendes Trägersystem für die gezielte In-vivo-Verabreichung von Nukleinsäuren dar. Der Synthesevorgang und insbesondere die nachgeschaltete Reinigungsstrategie spielen eine entscheidende Rolle bei der Bestimmung der Qualität, Reproduzierbarkeit und Funktionsleistung dieser polymeren Konjugate. Das primäre Ziel dieser Studie war die Optimierung der Synthese und Reinigung von LPEI10kDa-PEG2k-basierten Tri-Konjugaten. Die Tri-Konjugat-Synthese umfasste die anfängliche Konjugation von LPEI (10 kDa) mit einem heterobifunktionellen PEG2k-Linker zur Bildung eines LPEI10kDa-PEG2k-OPSS-Bi-Konjugats, gefolgt von einer Reinigung mittels Kationenaustauschchromatographie und Entsalzung entweder durch Zentrifugalfiltration oder Dialyse. Das gereinigte Bi-Konjugat wurde anschließend mit Cystein zur Reaktion gebracht, um das entsprechende Tri-Konjugat zu erzeugen, welches erneut chromatographisch gereinigt und entweder durch Zentrifugalfiltration oder Dialyse entsalzt wurden. Ein zentraler Schwerpunkt dieser Arbeit war die Optimierung von Reinigungsstrategien für LPEI10kDa-basierte Bi- und Tri-Konjugate durch eine vergleichende Bewertung von Zentrifugalfiltration und Dialyse. Dieser Vergleich zeigte, dass die Dialyse hinsichtlich der Entsalzungseffizienz und der Gesamtausbeute überlegen war, während die Zentrifugalfiltration eine deutlich höhere Zeiteffizienz bot und zu höheren OPSS/CYS-zu-LPEI-Molverhältnissen führte. Zur Unterstützung dieser Optimierung wurde die LPEI-Quantifizierung unter Verwendung einer kupferbasierten Analyse systematisch hinsichtlich der Haltbarkeit der Reagenzien, der Analysen-Variabilität und des Polymer- oder Konjugatverlusts während der Reinigung bewertet. Die Haltbarkeit der Reagenzien wurde auf 41 Tage festgelegt. Die Analysen-Variabilität lag zwischen 2 und 18 % und sank bei allen Verdünnungen unter 7%, wenn die Reagenzienkonzentrationen 30 µg/ml überschritten. Dies deutet darauf hin, dass zur Verringerung der Variabilität der Kupfer-Analysen-Ergebnisse eine Standardkurve mit Verdünnungen über 30 µg/ml verwendet werden sollte. In Bezug auf den Konjugatverlust während der Reinigung führte eine höhere Verdünnung vor der Kationenaustauschchromatographie zu einem geringeren Ertragsverlust. Auf der Grundlage dieser Ergebnisse wurde ein einziger Zentrifugalfiltrationsschritt als Standardverfahren zur Entsalzung ausgewählt. Mit diesem Ansatz wurde eine ausreichende Salz Entfernung bei akzeptablem Ertrag und reduzierter Verarbeitungszeit im Vergleich zu einem Waschprotokoll mit fünf Zyklen erreicht, das etwa eine zusätzliche Stunde erforderte. Zusätzlich wurden im Rahmen der Charakterisierung und als erster Anwendungsversuch dynamische Lichtstreuungsmessungen mit pDNA- und mRNA-basierten Polyplexen aus reinem LPEI sowie dem synthetisierten Tri-Konjugat durchgeführt, um Partikelgröße und Homogenität zu vergleichen.

Table of Contents

1 Abstract (English) 2

2 Abstract (German) 3

List of Abbreviations 7

3 Introduction 8

3.1 Cancer – a complex disease 8

3.2 Status-quo of cancer treatment 9

3.2.1 Traditional Therapy 9

3.2.2 Immunotherapy 9

3.2.3 Targeted Therapies 10

3.2.3.1 Gene Therapy 10

3.2.3.1.1 mRNA-based Cancer Therapy 10

3.3 Nanomedicine and Drug Delivery Systems 10

3.3.1 LPEI 11

3.3.1.1 PEGylation and Targeting 11

3.3.1.2 Branched and linear PEI 11

3.3.1.3 Determination of LPEI-content 11

3.3.2 Purification of LPEI 11

3.3.2.1 Cation Exchange Chromatography 11

3.3.2.1.1 Purification of the LPEI-PEG-OPSS Bi-Conjugate 11

3.3.2.1.2 Purification of the LPEI-PEG-Peptide Tri-Conjugate 12

3.3.2.2 Desalting and Isolation 12

3.3.2.2.1 Desalting via Dialysis 12

3.3.2.2.2 Desalting via Centrifugal Filtration 12

3.3.3 Polyplex-Characterization using Dynamic-Light-Scattering-Measurement 12

4 Aims of this study 13

5 Materials and methods 14

5.1 Materials 14

5.1.1 Chemicals 14

5.1.2 Materials 15

5.1.3 Devices 16

5.1.4 Software 16

5.2 Methods 16

5.2.1 Nomenclature 16

5.2.1.1 Nomenclature – Purification 16

5.2.1.2 Nomenclature – DLS Characterization 17

5.2.2 Assays for Characterization of LPEI-Conjugates 17

5.2.2.1 Copper Assay 17

5.2.2.1.1 Preparation of the LPEI10kDa for the copper assay standard curve 17

5.2.2.1.2 Execution of the copper assay 17

5.2.2.1.3 Shelf-Life validation of the copper-acetic-buffer 18

5.2.2.1.4 Evaluation of Copper Assay Variability 18

5.2.2.2 DTT Assay 18

5.2.2.2.1 DTT Assay for the Bi-Conjugate 18

5.2.2.2.2 DTT Assay for the Tri-Conjugate 19

5.2.2.3 Determination of the molar ratio 19

5.2.3 Optimizing Purification of LPEI-Conjugates 19

5.2.3.1 ÄKTA Purification of LPEI 10 kDa 19

5.2.3.1.1 Eluent Buffer Production for the Polymer and Bi-Conjugate 19

5.2.3.1.2 Eluent Buffer Production for the Tri-Conjugate 20

5.2.3.1.3 Execution of CEX Purification using the ÄKTA-System 20
5.2.3.1.4 Conductivity measurement using the ÄKT-System 21
5.2.3.2 LPEI10kDa Desalting via Centrifugal Filtration Purification 21
5.2.3.2.1 Mock Synthesis and Purification 1 21
5.2.3.2.2 Mock Synthesis and Purification 2.1 22
5.2.3.2.3 Mock Synthesis and Purification 2.2 23
5.2.3.2.4 Mock Synthesis and Purification 3 23
5.2.4 Synthesis of the LPEI-PEG-OPSS bi-conjugate 24
5.2.5 Purification of the LPEI-PEG-OPSS Bi-Conjugate 24
5.2.5.1 ÄKTA Purification 24
5.2.5.2 Desalting via Centrifugal Filtration Purification 25
5.2.5.3 Desalting via Dialysis and Lyophilization 25
5.2.6 Synthesis of the LPEI-PEG-CYS Tri-Conjugate 26
5.2.7 Purification of the LPEI-PEG-CYS Tri-Conjugate 27
5.2.7.1 CEX Purification using the ÄKTA-System 27
5.2.7.2 Desalting via Centrifugal Filtration Purification 27
5.2.7.3 Desalting via Dialysis and Lyophilization 28
5.2.8 DLS Characterization 29
5.2.8.1 LPEI10kDa-pDNA-Polyplexes 29
5.2.8.2 Tri-Conjugate-mRNA-Polyplexes 29
5.2.9 AI declaration and Illustrations 30
6 Results & Discussion 30
6.1.1 Copper Assay Optimization 30
6.1.1.1 Preparation of the LPEI10kDa for the copper assay standard curve 30
6.1.1.2 Shelf-Life validation of the copper-acetic-buffer 31
6.1.1.3 Evaluation of Copper Assay Variability 31
6.1.2 CEX Purification of LPEI 10 kDa and Desalting using Centrifugal Filtration 32
6.1.2.1 Mock Synthesis and Purification 1 32
6.1.2.2 Mock Synthesis and Purification 2.1 33
6.1.2.3 Mock Synthesis and Purification 2.2 34
6.1.2.4 Mock Synthesis and Purification 3 36
6.1.2.5 Discussion – Mock Syntheses and Purifications 1-3 39
6.1.3 Synthesis of the LPEI-PEG-OPSS bi-conjugate 39
6.1.4 Purification of the LPEI-PEG-OPSS Bi-Conjugate 39
6.1.4.1 ÄKTA Purification of LPEI-PEG-OPSS 39
6.1.4.2 Desalting of LPEI-PEG-OPSS 40
6.1.4.3 Discussion – LPEI-PEG-OPSS Bi-Conjugate Synthesis and Purification 41
6.1.5 Synthesis of the LPEI-PEG-CYS Tri-Conjugate 41
6.1.6 Purification of the LPEI-PEG-CYS Tri-Conjugate 42
6.1.6.1 ÄKTA Purification of LPEI-PEG-CYS 42
6.1.6.2 Desalting of LPEI-PEG-CYS 43
6.1.6.3 Discussion – LPEI-PEG-CYS Tri-Conjugate Synthesis and Purification 44
6.1.7 DLS Characterization 44
6.1.7.1 LPEI-pDNA-Polyplexes 44
6.1.7.1.1 LPEI10kDa-pDNA-Polyplexes with a pDNA concentration of 40 µg/mL 44
6.1.7.1.2 LPEI10kDa-pDNA-Polyplexes with a pDNA concentration of 10 µg/mL 45
6.1.7.2 Tri-Conjugate-mRNA-Polyplexes 46
6.1.7.2.1 LPEI-mRNA-Polyplexes with a N/P ratio of 12 46
6.1.7.2.2 LPEI-mRNA-Polyplexes with a N/P ratio of 120 47
7 Conclusion and Outlook 48
8 List of figures 50
9 List of Tables 56
10 References 58
11 Appendix 61

11.1 Ad Mock Synthesis and Purification 2.1_____ 61

11.2 Ad Mock Synthesis and Purification 3 _____ 61

11.3 Ad ÄKTA Purification of LPEI-PEG-OPSS _____ 62

11.4 Ad Purification of the LPEI-PEG-CYS Tri-Conjugate _____ 65

List of Abbreviations

ACT	Adoptive Cell Therapy
ADC	Antibody-Drug-Conjugates
ATP	Adenosin-Tri-Phosphate
bPEI	branched Polyethylenimine
CAR-T	Chimeric Antigen-Receptor T-cell
CEX	Cation Exchange Chromatography
CF	Centrifugal FIltration
CRS	Cytokine Release Syndrome
DDS	Drug Delivery System
DLS	Dynamic Light Scattering
DTT	DL-Dithiothreitol
EGFR	Endothelial Growth Factor Receptor
EMT	Epithelial–Mesenchymal Transition
EPR	Enhanced Permeability and Retention
GLuc	Gaussia Luciferase
kDa	kilo Dalton
LPEI	linear Polyethylenimine
MDR	Multidrug Resistance
MDSC	Myeloid-derived Suppressor Cells
MPS	Mononuclear Phagocyte System
mRNA	messenger RNA
MWCO	Molecular Weight Cut-Off
PDI	Polydispersity Index
PEI	Polyethylenimine
RES	Reticulo-Endothelial System
siRNA	small interfering RNA
TAA	Tumor-associated Antigens
TME	Tumor Microenvironment
TSA	Tumor-specific Antigens
VEGF	Vasculo-Endothelial Growth Factor

3 Introduction

Cancer remains one of the most significant global health challenges, causing approximately ten million deaths each year and ranking as the second leading cause of mortality worldwide after cardiovascular disease.[1] A recent assessment estimates that by 2040, new cases will reach 28 million with 16,2 million deaths globally.[2] These numbers make it clear of what significance cancer research and in consequence therapy options are in regards to the millions of patients who are and will be in need for them. Prior to discussing the current trends in cancer therapy research, it is important to have a fundamental understanding regarding the complexity of cancer as a disease.

3.1 Cancer – a complex disease

Cancer as a severe health condition is characterized by complex biological heterogeneity where the breakdown of the mechanisms that regulate the cell cycle, leads to the unchecked survival and proliferation of malignant cells. The tumorigenesis itself involves the acquisition of different capabilities which aid and abet its progression. This set of functional capabilities, which will be further elaborated in the section below, are summarized as the hallmarks of cancer.[3]

Four of the cancer hallmarks relate to growth- or replication-promoting capacities: sustaining proliferative signaling, evading growth suppression, resisting apoptosis, and enabling replicative immortality. Sustained proliferative signaling arises from deregulated growth-promoting pathways that are tightly controlled in normal tissues. At the molecular level, this may involve overexpression of growth-factor receptors, such as the epidermal growth factor receptor (EGFR) in various cancer types, which heightens cellular responsiveness to mitogenic cues, or constitutive activation of downstream signaling cascades.[4,5] In addition, cancer cells circumvent growth-inhibitory mechanisms by inactivating tumor suppressor genes such as RB or TP53. They further resist apoptosis, the programmed cell-death process that normally prevents malignant transformation, by upregulating anti-apoptotic regulators or downregulating pro-apoptotic factors. Whereas normal cells can divide only a finite number of times due to progressive telomere shortening that triggers senescence or cell death, cancer cells acquire an unlimited replicative capacity. This is typically achieved through upregulation of telomerase, an enzyme that elongates telomeric DNA, allowing cells to bypass the crisis phase and maintain telomere length sufficient for continuous proliferation.[4]

The hallmarks vascularization, invasion and metastasis, reprogramming cellular metabolism and avoiding the immune system can be attributed as crucial for the survival of the tumor.[4] Tumors are able to facilitate angiogenesis by expression of angiogenic factors such as VEGF-A after oncogene signaling or hypoxia. This is essential in order for the tumor to meet its metabolic demands such as nutrient supply, dispose of catabolic products and overcoming hypoxia.[6] Furthermore, tumors must activate an "angiogenic switch" to transition from a microscopic, quiescent state to a macroscopic, malignant state. This switch allows the tumor to recruit endothelial cells and sprout new vessels, thereby unlocking the potential for indefinite growth.[7] As cancers progress, they acquire the ability to invade surrounding tissues and disseminate to distant organs. A key facilitator of this transition is the epithelial-mesenchymal transition (EMT), during which tumor cells lose adhesion molecules such as E-cadherin and adopt enhanced motility and invasiveness.[8] Metastatic spread involves a multi-step cascade encompassing local invasion, intravasation into blood or lymphatic vessels, survival during systemic transit, extravasation into distant tissues, and eventual colonization.[9] Another emerging hallmark of cancer is the reprogramming of cellular metabolism. Tumor cells frequently shift their energy production toward glycolysis even in the presence of oxygen, a phenomenon known as the Warburg effect. Although aerobic glycolysis is less efficient at generating ATP, it enables the diversion of glycolytic intermediates into biosynthetic pathways essential for supporting rapid cell growth and proliferation. A further critical hallmark is the ability of cancer cells to evade immune destruction. Despite continuous immune surveillance, tumors evolve mechanisms to escape detection or disable key immune components. They may secrete immunosuppressive molecules such as TGF-β or recruit suppressive immune cell populations, including regulatory T-cells (Tregs) and myeloid-derived suppressor cells (MDSCs), which collectively inhibit immune response. Together, these strategies allow malignant cells to persist and expand within an otherwise hostile immunological environment.[10]

In order for cells to be able to acquire these aforementioned capabilities, there has to be some genetic

diversity which is provided by genome instability. Genome instability accelerates the rate at which premalignant cells accumulate these favorable genotypes, conferring selective advantages that allow for their outgrowth and dominance in the tissue environment. Cancer cells achieve this mutability through increased sensitivity to mutagenic agents or a breakdown in the genomic maintenance machinery. In addition, inflammation within the tumor microenvironment enhances tumorigenesis and progression by supplying bioactive molecules that support multiple hallmark capabilities.[4]

Considering all established hallmarks, the profound biological complexity of cancer becomes evident and helps to explain the persistent challenges in achieving effective therapeutic control. Ongoing research continues to refine our understanding of tumorigenesis, and several additional, potentially emerging hallmarks, such as phenotypic plasticity, non-mutational epigenetic reprogramming, polymorphic microbiomes, and senescent cell-associated processes, are currently under active investigation.[11] Broadening our understanding of disease is essential for accelerating the development of innovative therapeutic strategies. Over the past decades, major scientific advances have driven the emergence of novel cancer therapies, leading to improved patient survival and a broader range of treatment options. The following section outlines the current landscape of cancer therapy.

3.2 Status-quo of cancer treatment

Broadly, contemporary cancer treatment strategies can be categorized into three major classes: traditional therapies, immunotherapies, and targeted therapies.

3.2.1 Traditional Therapy

Conventional cancer therapies primarily consist of surgery and radiotherapy for localized, non-metastatic tumors, and systemic chemotherapy for metastatic disease.[5] To this day, surgery is typically the initial intervention, when detected early, and is often complemented by adjuvant radiotherapy or chemotherapy.[12] Despite their widespread use, these modalities have substantial limitations: Surgery is largely confined to localized disease and becomes ineffective once malignant cells have disseminated.[5] Radiotherapy, although potent for local tumor control, can cause collateral damage to adjacent healthy tissues.[12] Also, chemotherapy, which exerts its effects by targeting rapidly dividing cells, lacks specificity, thereby harming normal proliferative cell populations.[5] The result: systemic toxicities such as acute and delayed nausea, mucositis, and cognitive impairments, with long-term risks such as secondary malignancies.[13] Moreover, the emergence of multidrug resistance (MDR) significantly compromises chemotherapeutic efficacy.[3] Consequently, while conventional therapies remain the clinical standard, their limited curative potential, high toxicity, and risk of recurrence underscore the need for more effective and selective treatment strategies.[10]

3.2.2 Immunotherapy

Immunotherapy represents a paradigm shift in oncology, moving away from therapies that directly target tumor cells with toxins (like chemotherapy) toward strategies that mobilize the patient's own immune system to recognize and eradicate malignancy. Recent decades have seen exponential progress, establishing immunotherapy as a pillar of cancer treatment alongside surgery, chemotherapy, and radiotherapy.[14] The objective is to induce a robust, specific, and long-lasting immune response that can target primary tumors and metastases while establishing immunological memory to prevent recurrence.[15] For that purpose, different approaches have been established to address cancer: monoclonal antibodies target specific antigens on cancer cells[5]; adoptive cell therapy (ACT) involves the isolation, modification, and expansion of immune cells ex vivo, followed by reinfusion into the patient[16]; cancer vaccines aim to stimulate an active immune response against tumor-associated antigens (TAAs) or tumor-specific antigens (TSAs)[17]; oncolytic viruses are genetically modified to selectively replicate within and lyse tumor cells while sparing normal tissue[18] and antibody-drug-conjugates (ADCs) combine the targeting specificity of monoclonal antibodies with the cytotoxicity of chemotherapy.[5] Despite clinical successes, immunotherapy faces significant hurdles that limit its universal application: The TME is often immunosuppressive, populated by regulatory T-cells (Tregs) and MDSCs that inhibit effector T-cells.[19] Cytokine release syndrome (CRS) remains a challenge when utilizing therapies like chimeric-antigen-receptor T-cell (CAR-T).[2] Also, personalized therapies involve complex, labor-intensive manufacturing processes with high costs and long turnaround times, which can be prohibitive for patients with rapidly progressing disease.[20]

3.2.3 Targeted Therapies

Targeted therapy represents a revolutionary approach in cancer treatment, seeking to eliminate malignancies through specific molecular interventions rather than relying on the indiscriminate toxicity associated with conventional chemotherapy.[5] Targeted treatments are designed to block specific biologic transduction pathways or cancer proteins essential for tumor growth and progression. These molecular targets, such as receptors, growth factors, kinase cascades, or molecules related to angiogenesis and apoptosis, are often found to be overexpressed or mutated in cancer cells compared to normal tissues. The potential of targeted therapies lies in their ability to achieve high specificity and reduced toxicity compared to traditional chemotherapy.[2] This shift involves focusing on molecular traits, rather than just the tumor's physical location (organ-centric paradigm).[12,16] By matching treatment to a patient's unique genomic and molecular profile (precision medicine), targeted therapies have shown superior clinical outcomes compared to non-matched treatments.[16]

3.2.3.1 Gene Therapy

Gene therapy plays a critical role by utilizing genetic material (DNA or RNA) to precisely modify cells, aiming for a cure.[2] In the context of targeted therapy, gene therapy strategies focus on fine-tuning molecular processes by gene silencing, gene transfer or immunotherapy engineering. The silencing of a specific gene is achieved by utilizing small interfering RNAs (siRNAs) which target genes that promote tumor growth, survival, metastasis, or chemotherapy resistance.[3,12] Introducing functional genes, such as wild-type tumor suppressors or pro-apoptotic and chemosensitizing genes, directly into cancerous cells allow the inhibition of growth or induction of death.[3,12]

3.2.3.1.1 mRNA-based Cancer Therapy

In connection to immunotherapy options discusses in 3.2.2 and the goals of gene therapy above, messenger RNA (mRNA) is increasingly used to encode tumor antigens for personalized vaccines, cytokines for immune modulation, or CARs or T-cell Receptors (TCRs) for engineering the patient's own immune cells.[21] This approach represents a shift toward personalized medicine, as mRNA can be rapidly customized to match the unique mutational profile of an individual patient's tumor.[10,15,17] mRNA-based therapeutics offer several key advantages as a platform for cancer treatment, including a favorable safety profile due to the absence of genomic integration, high potency and versatility through the ability of a single mRNA construct to encode multiple antigens, rapid and scalable manufacturing, and transient yet controllable expression.[17,22] The temporary nature of mRNA expression reduces the risk of prolonged or chronic inflammation, enhancing overall safety and tolerability.[17] However, one of the major challenges limiting its clinical application is the inherent instability of mRNA and its susceptibility to enzymatic degradation, which necessitates efficient and protected delivery into the cytoplasm of target cells.[17,21] For that reason, drug delivery systems (DDS), especially those utilizing nanoscale carriers, are essential for implementing gene therapy and other targeted strategies.[5]

3.3 Nanomedicine and Drug Delivery Systems

DDS and nanocarriers enable two main mechanisms for achieving tumor targeting: passive and active targeting. Passive targeting exploits the enhanced permeability and retention (EPR) effect, which results from the highly permeable vasculature and poor lymphatic drainage typical of solid tumors. Carriers between approximately 30 to 200 nm accumulate selectively in the tumor interstitium.[3,5,23] Active targeting, on the other hand, is achieved by conjugating specific targeting moieties (ligands, peptides, antibodies) to the surface of the nanocarrier. These moieties bind selectively to receptors overexpressed on tumor cell surfaces, enhancing internalization.[5,12,23]

Current gene therapy strategies for cancer are diverse, utilizing various biological and synthetic vehicles to deliver therapeutic payloads. Viruses are inherently efficient at infecting cells. Oncolytic viruses (e.g., T-VEC, H101) are genetically engineered to selectively replicate in and lyse tumor cells while stimulating an anti-tumor immune response. Adenoviruses and lentiviruses are also used to transduce immune cells in adoptive cell therapies. [18,21] To overcome safety concerns associated with viral vectors (such as immunogenicity and insertional mutagenesis), non-viral vectors have been developed. [10,24] The most clinically advanced non-viral systems are composed of ionizable lipids, helper lipids, cholesterol, and PEG-lipids. They protect nucleic acids from degradation and facilitate endosomal escape. [1,22]

3.3.1 LPEI

Polyethylenimine (PEI) is considered as a "gold standard" of cationic polymers.[25] It is characterized by a strong DNA condensation via high charge density and electrostatic interaction.[24] PEI contains amine groups that are protonated at physiological pH, allowing it to bind electrostatically to negatively charged nucleic acids. Its high buffering capacity leads to the "proton sponge effect": Once the so called polyplex is endocytosed, PEI absorbs protons in the acidic environment of the endosome, causing an influx of chloride ions and water. This results in osmotic swelling and subsequent rupture of the endosome, releasing the nucleic acid payload into the cytoplasm. [24,26,27]

3.3.1.1 PEGylation and Targeting

PEI is also widely used in conjugation for targeted delivery e.g. PEG-PEI. The PEGylation (covalently binding polyethylene glycol or PEG) is a crucial modification that imparts several significant benefits by providing a shielding and stealth property to the PEI-Nucleic-Acid complex.[24] PEGylation significantly reduces protein binding and interactions with blood components, preventing aggregation and clearance by the reticulo-endothelial system (RES) and mononuclear phagocyte system (MPS). However, excessive PEGylation comes with the downside of negatively affecting the endosomal release of polyplexes and reducing the efficiency of cellular uptake. To enable specific targeting PEI is often chemically coupled with specific targeting ligands like protein- or peptide-based ligands. These conjugates form nanosized polyplexes that deliver their payload into target cells through receptor-mediated endocytosis.[26]

3.3.1.2 Branched and linear PEI

PEI exists in a branched (bPEI) and linear (LPEI) form. bPEI contains primary, secondary, and tertiary amines and forms very stable complexes with DNA. The heterogeneous distribution of amine groups confers bPEI with an exceptional proton-absorption capacity, leading to enhanced buffering performance. However, high molecular weight bPEI is often associated with significant cytotoxicity. [24,28] LPEI is synthesized via the hydrolysis of poly(2-ethyl-2-oxazoline) precursors and contains secondary amines and is often preferred because it exhibits improved transfection performance in vivo and in vitro compared to bPEI. LPEI polyplexes also tend to dissociate more easily within intracellular vesicles, releasing the payload more efficiently. [26,28]

3.3.1.3 Determination of LPEI-content

Another important aspect during the production of targeting polymers like LPEI is the determination of its content throughout different stages of the process.[26] Since LPEI itself lacks chromophores, quantification via ordinary spectrophotometry alone is impossible. Therefore, a spectrophotometric method that relies on forming a detectable complex or analyzing specific functional groups in modified LPEI such as in the copper assay is essential. This method enables the rapid, sensitive, and reproducible quantitative determination of LPEI by forming a blue cuprammonium complex upon adding copper (II) ions (Cu2+), that can be detected at λ max of 285 nm by UV-VIS spectrophotometry.[29]

3.3.2 Purification of LPEI

The purification of polyethylenimine PEI-based conjugates, particularly LPEI functionalized with polyethylene glycol and targeting ligands, is a multistep process that is critical for ensuring the safety, reproducibility, and therapeutic efficacy of the resulting gene delivery vehicles.[26] Purification focuses on removing unreacted components, such as excess PEG or peptide, which can otherwise interfere with polyplex formation and increase toxicity.[26,30]

3.3.2.1 Cation Exchange Chromatography

Cation exchange chromatography (CEX) is an efficient, low-pressure aqueous separation technique that leverages molecular charge differences. In this process, positively charged molecules bind to a negatively charged resin.[31] Due to its high cationic charge density (among the highest of synthetic polymers) polyethylenimine exhibits strong affinity for cation-exchange resins such as MacroPrep™ High S.[26] In the synthesis of LPEI-based tri-conjugates, CEX is used at two critical stages.

3.3.2.1.1 Purification of the LPEI-PEG-OPSS Bi-Conjugate

Following the initial coupling reaction between LPEI and the PEG linker, the crude reaction mixture is

applied to a CEX column. Unreacted PEG and low-molecular-weight, non-polymeric by-products lack the high cationic charge density characteristic of the LPEI-modified conjugate and therefore elute early at low salt concentrations. In contrast, the desired LPEI-PEG conjugate remains strongly bound to the resin and is subsequently eluted by a stepwise or gradient increase in ionic strength using sodium chloride.[26]

3.3.2.1.2 Purification of the LPEI-PEG-Peptide Tri-Conjugate

Following conjugation of the peptide ligand to the bi-conjugate, a CEX chromatography step is required to remove unreacted peptide and reaction by-products. As observed during purification of the bi-conjugate, the fully functionalized LPEI-PEG-peptide conjugate remains strongly bound to the resin and typically elutes only at high salt concentrations.[26]

3.3.2.2 Desalting and Isolation

After the conjugate is eluted from the CEX column, the resulting solution contains a high concentration of NaCl, which must be removed before the conjugate can be used to form polyplexes with nucleic acids.[26] Proper desalting is vital because high salt concentrations can cause excessive particle aggregation during the polyplex mixing process, resulting in unstable nanoparticles that fail to transfect cells effectively.[32] Centrifugal filtration and dialysis are both established techniques used in biochemical processes for sample preparation, including the essential function of desalting:[33,34]

3.3.2.2.1 Desalting via Dialysis

Dialysis is a separation process that relies on passive diffusion across a semipermeable membrane. The sample solution is separated from a dilute receiving solution by a membrane. The concentration gradient drives the diffusion of smaller molecules, like salts, across the membrane into the dialysate, while larger macromolecules are retained. Conventional dialysis typically uses a relatively thick polymer layer with tortuous pores. This design results in slow diffusion rates and low rates of diffusion, often leading to extremely long process times.[34]

3.3.2.2.2 Desalting via Centrifugal Filtration

Centrifugal filtration (CF), on the other hand, utilizes force to drive the separation process, often providing a different balance of speed and selectivity than traditional dialysis. While their performance can vary widely between brands and design iterations, they offer a method of separation that relies on mechanical force rather than simple diffusion, typically leading to faster process times than conventional dialysis.[33]

3.3.3 Polyplex-Characterization using Dynamic-Light-Scattering-Measurement

As mentioned in 3.3, the size of nanoparticles plays a significant role in their ability to target the cancer specifically. Therefore, dynamic light scattering (DLS) is an essential technique for characterizing the resulting particle complexes, known as polyplexes, formed between LPEI and nucleic acids (DNA/RNA). Since DLS calculates the size from the translational diffusion coefficient rather than measuring it directly, accurate data collection and analysis are paramount. In this context, the Z-average and polydispersity index (PDI) are commonly reported parameters derived from the correlation function. The Z-average (Zav), or cumulant mean, is a statistical measure of the overall size of the particles in a suspension and is often the most reported particle size in DLS studies. For monomodal (single-peak) particle size distributions, the Z-average size is typically close to the intensity-weighted hydrodynamic size (Dh). The PDI is a dimensionless parameter derived alongside the Z-average from the cumulant analysis of the DLS correlation function. It serves as a measure of the width of the particle size distribution or the heterogeneity of the sample. PDI values can range from 0 (perfectly monodisperse, uniform sample) up to 1 (highly polydisperse or aggregated sample). Many papers state that a PDI value below 0.3 indicates low polydispersity of nanoparticles. [35]

4 Aims of this study

Linear polyethylenimine, when PEGylated and conjugated to a targeting moiety to form LPEI-PEG conjugates, emerges as a promising carrier for the targeted delivery of nucleic acids for in vivo applications. In this context, the production process, and consequently the purification strategy, plays a critical role in determining the quality and performance of these polymer tri-conjugates.

The primary objectives of this study were to optimize synthesis and purification of LPEI10k-PEG2k based tri-conjugates. Synthesis of tri-conjugate starts with conjugating LPEI-10kDa to PEG2k-heterobifunctional linker to form LPEI10kDa-PEG2k-OPSS bi-conjugate, followed by cation-exchange chromatography and desalting. This purified LPEI10kDa-PEG2k-OPSS bi-conjugate is then used for preparation of tri-conjugate by coupling it to targeting peptide or cysteine amino acid. Tri-conjugate synthesis is also followed by chromatography and desalting. One of the main goals of this work was optimization of LPEI10kDa-based bi- and tri-conjugate purification by comparing centrifugation filtration and dialysis. Towards this, LPEI quantification by copper assay was investigated for shelf-life of assay reagent, evaluation of assay variability and loss of polymer/conjugate during the purification process. The second main goal was the characterization of cysteine-LPEI molar ratio of conjugates as a function of purification method, which is an important parameter for targeting applications. Furthermore, dynamic light scattering measurements were performed to characterize LPEI-PEG-CYS-mRNA polyplexes prepared from purified tri-conjugates, to assess their ability to complex nucleic acids.

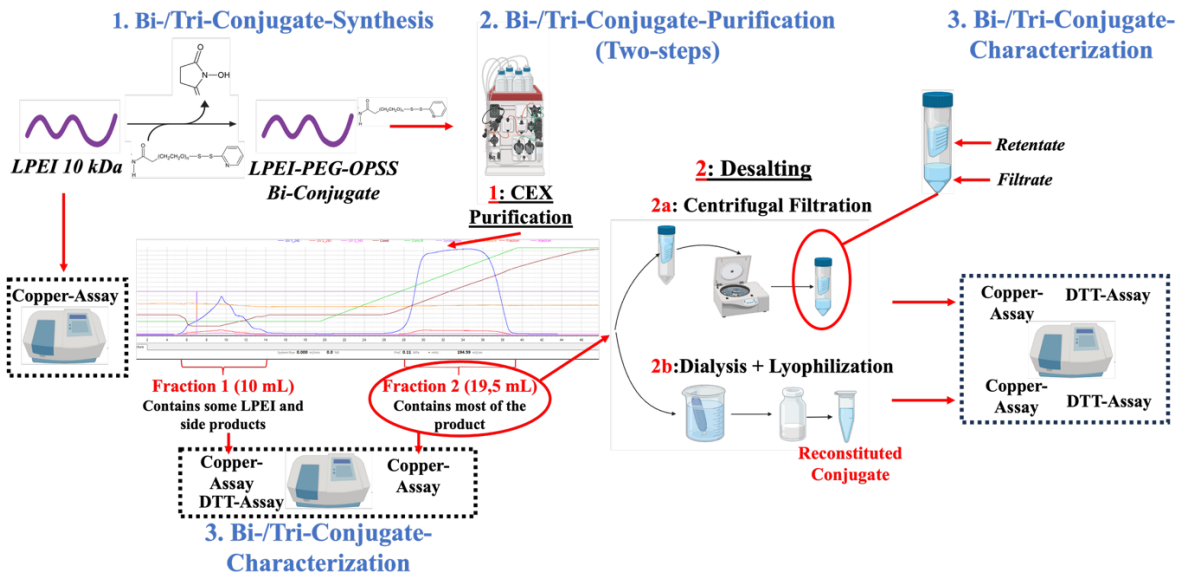

Figure 1 *Schematic illustration of the aims subject to this master's thesis; Created with BioRender.com*

5 Materials and methods

This section lists all the materials and methods which were utilized in the scope of this master's thesis.

5.1 Materials

The subsequent section outlines the materials organized into chemicals (***Table 1***), materials (***Table 2***), devices (***Table 3***) and software (***Table 4***).

5.1.1 Chemicals

Table 1 *List of used chemicals*

Chemical	Manufacturer	Usage
Ethanol	Merck; CAS: 1.00983.2511; REF: 64-17-5	Various
DMSO (Dimethyl sulfoxide)	MERCK; CAS: D5879-500ML; REF: 67-68-5	LPEI bi-conjugate
Py-S-S-PEG-NHS (alpha-Butyric Acid NHS Ester-omega-Pyridyldithiopropanamido PEG)	Rapp Polymer; CS: 132000-44-35; LOT: 1224.324	LPEI bi-conjugate
Tris buffer (2-Amino-2-hydroxymethyl-propane-1,3-diol)	Roche; CAS: 0497-1KG; REF: 7786-1	LPEI bi-conjugate
L-cysteine	Merck; CAS: J994-100G; REF: 52-90-4	LPEI tri-conjugate
Argon	Air Liquide; Alphagaz 1 Ar	LPEI tri-conjugate
HEPES (2-[4-(2-hydroxyethyl)piperazin-1-yl]ethanesulfonic acid)	Merck; CAS: A3724,0259; REF: 7365-45-9	Chromatographic purification
Milli-Q Water	in-house	Various
ACN	Merck; CAS: 34851-1L; REF: 75-05-8	Various
NaCl (Sodium Chloride)	Carl Roth; CAS: P029.3; REF: 7647-14-5	Various
Molecular sieve	Merck; CAS: 334286-1KG; REF: 30880-99-1	Various
HBG buffer (HEPES-buffered-Glucose)	pH: 7.421 (20 mM HEPES, 5 % [w/V] Glucose) in MQ-water, 0.1 µm filtered; house-made	Polyplexing
Plasmid DNA (pCMV-GLuc)	House-made	Dynamic Light Scattering
mRNA (GLuc mRNA)	House-made	Dynamic Light Scattering
Sodium acetate anhydrous	Carl Roth; CAS: A4555,025; REF: 127-09-3	Copper assay
Copper(II) sulfate pentahydrate	Merck; CAS: 12849-1KG; REF7758-99-8	Copper assay
Acetic Acid	Merck; CAS: 20104-334; REF: 64-19-7	Copper assay
LPEI (free base) 10 kDa	House-made: 241114-66 AT	Copper assay, LPEI synthesis
NaOH (Sodium Hydroxide)	Merck: CAS: S5881-1KG; REF: 1310-73-2	Set pH
HCl (Hydrochloric Acid)	Carl- Roth; CAS: 30721-2.5L-M; REF: 7647-01-0	Set pH

DL-Dithiothreitol	Merck; CAS: D9779-5G; REF. 3483-12-3	DTT assay

5.1.2 Materials

Table 2 *List of used materials*

Material	Manufacturer	Usage
Eppendorf tube (0.2-2 mL)	Eppendorf	Various
Pipettes	Eppendorf	Various
Pipette tips	Eppendorf	Various
Parafilm	Carl Roth; H951.1	Various
Pipette boy	Integra Pipetboy 2	Various
Serological Pipette	Sarstedt; Seroligcal pipette	Various
Centrifugal Tube 50	Sarstedt; REF: 62.548.004	Various
Centrifugal Tube 25	Eppendorf; DNA LoBind	Various
Centrifugal Tube 15	Sarstedt; REF: 62.554.502	Various
Centrifugal Tube 5	Eppendorf; DNA LoBind	Various
Gloves	Dermagrip; nitrile examination gloves	Various
Thermometer	Easy-Read USA VWR; 620-0788	Synthesis LPEI bi-conjugate
Glass vile	Roth; LOT: 88705212200291	Synthesis LPEI tri-conjugate
Magnetic stirrer core	Carl Roth	Synthesis LPEI tri-conjugate
Microcuvettes	Brand; REF: 7592 30	Synthesis LPEI tri-conjugate
Volumetric flask (100 mL)	Hirschmann	Various
Filter Unit	Thermo Fisher Scientific; REF: FB12566504	Chromatographic purification
Syringe (2 mL)	Braun - Luer Solo; REF: 4606051V	Chromatographic purification
Syringe (5 mL)	Braun - Luer Solo; REF: 4606205V	Chromatographic purification
Beaker (4L)	VitLab & VWR (Material PP)	Chromatographic purification
Round-bottom flask	Hirschmann & Schott (both Duran based)	Chromatographic purification
Centrifugal filter tubes (15 mL total volume; molecular cut-off: 3 kDa)	Merck; REF: UFC900324	Desalting via Centrifugation filtration
Centrifugal filter tubes (2 mL total volume; molecular cut-off: 3 kDa)	Merck; REF: UFC200324	Desalting via Centrifugation filtration
Pre-wetted RC tubing (Dialysis bag) (molecular cut-off: 1 kDa)	Spectra/Por; REF:132640	Desalting via Dialysis

5.1.3 Devices

Table 3 *List of used devices*

Device	Manufacturer Details	Usage
Thermoshaker	Eppendorf (Thermomixer 5436)	Various
Vortex	Starlab	Various
Eppendorf-centrifuge	Sprout Plus	Various
Magnetic stirrer hot plate	Heidolph	Various
Photometer	GeneQUant (80-2120-00)	Various
MQ device	Satorium Arium pro	Various
pH meter	WTW: pH-electrode SenTix 41 (x213005080)	Various
Ultrasonic bath	VWR Ultrasonic cleaner	Various
Analytical Scale	KERN ABP 100-5DM	Various
ÄKTA purification incl. Fraction collector	ÄKTA pure incl Fraction collectore F9-C	Chromatographic purification
Freeze-dryer	CHRIST (Alpha 2-4 Ldplus)	Chromatographic purification
Centrifuge (filter tubes)	Thermo Fisher Scientific, HERAEUS Megafuge 16R	Centrifugation purification
NanoVue	NanoVue Plus (28956057)	Various
DLS	Zetasizer Nano ZS (Malvern)	DLS measurement

5.1.4 Software

Table 4 *List of used software*

Software	Device	Usage
Unicorn 6.3 (Build 6.3.2.89)	ÄKTA	Chromatographic purification
GeneQuant 4281 V1.61	Photometer (GeneQuant1300)	Various
NanoVue 4282 V2.0.4	NanoVue	Various
Alpha 2-4 V1.76	Freeze-dryer	Various
Zetasizer software V7.13	Zetasizer Nano ZS (Malvern)	DLS measurement

5.2 Methods

The subsequent section elaborates all the methods executed in this master's thesis.

5.2.1 Nomenclature

This section elaborates the nomenclature used for the purification process and DLS characterization.

5.2.1.1 Nomenclature – Purification

In order to distinguish between the different purification conditions, a nomenclature has been established which is explained using an exemplary label below:

e.g.: LPEI10kDa_ÄKTA1CF

Explanation:

ÄKTA: chromatographic purification

xCF: x washing cycles using centrifugal filters

5.2.1.2 Nomenclature – DLS Characterization

In order to distinguish between the different polyplexes, a nomenclature has been established which is explained using an exemplary label below:

e.g.: LPC_CF

Explanation:

L: LPEI 10 kDa

PC: PEG-CYS

_CF/D: Centrifugal Filtration or Dialysis

5.2.2 Assays for Characterization of LPEI-Conjugates

The characterization of the LPEI bi-conjugates includes the copper- and DTT-assay which are used to determine the concentration of LPEI and indirectly the concentration of OPSS/amino-acid groups after synthesis of the bi/tri-conjugate. This information is afterwards used to calculate the ratio of PEG-OPSS bound to LPEI which is needed for the synthesis of the tri-conjugate and also to calculate the ratio of amino-acid bound to the bi-conjugate. Please note, that for the characterization it was crucial to use micro-cuvettes with a measuring chamber height of Z = 15 mm and to ensure that micro-cuvettes with the same reference number were used for accurate, side-by-side results.

5.2.2.1 Copper Assay

The copper assay is utilized to determine the LPEI concentration via complexation of the amine groups with copper-(II)-ions which leads to absorption of light at 285 nanometers.

5.2.2.1.1 Preparation of the LPEI10kDa for the copper assay standard curve

The calculations of this assay are based on the line equation of a LPEI standard curve. Therefore, a LPEI 10kDa stock solution with a concentration of 10 mg/mL is produced as following: 199,46 mg LPEI were weighed and 16 mL of MQ-water added. In order to dissolve the LPEI and set the pH to 8, 1 molar HCl was added dropwise using a pipette and the pH was monitored using a pH-meter at room temperature. Afterwards, the volume was made up to 20 mL by adding the needed amount of MQ-water, also considering the volume of HCl added. To ascertain the concentration of the produced stock, a copper assay was performed according 5.2.2.1.2 using the stock for the establishing of the standard curve as well as an unknown sample. This LPEI 10 kDa stock was used for all standard curves of further copper assays subject to this thesis.

5.2.2.1.2 Execution of the copper assay

In order to prepare the acetic buffer, 0,821 g Na-acetate were weighed and dissolved in 80 mL MQ-water. Before filling up to 100 mL with MQ-water, the pH was set to 5,4 by adding acetic acid and measuring via pH-meter at room temperature. 100 mL of Cu^{2+} solution was prepared by dissolving 23 mg of $CuSO_4$ in 0,1 M Na-acetate buffer. For creating a standard curve, unfiltered LPEI 10 kDa (10 mg/mL) was used. Standard solutions were made in MQ-water with a final volume of 100 µL at concentrations ranging from 10-100 µg/mL (***Table 5***). 100 µL water was used as a blank. Standard solutions were analyzed in duplicates. The LPEI sample to be analyzed was also diluted to a final volume of 100 µL with MQ-water. Duplicates and different dilutions of samples were produced using MQ-water. The standard solution set as well as samples were mixed with 100 µL of the copper solution. They were incubated at room temperature for 5 minutes and the absorption wavelength set to 285 nm (***Figure 2***). The absorption of LPEI solutions and LPEI samples to be analyzed were measured and concentrations calculated with the help of the standard curve equation.

Table 5 *Dilution Table used for the Copper Assay Standard Curve*

Concentration [µg/mL]	Amount of 1000 µg/mL LPEI standard stock [µL]	Amount of MQ-water [µL]
10	3	297
20	6	294
30	9	291

50	15	285
70	21	279
90	27	273
100	30	270

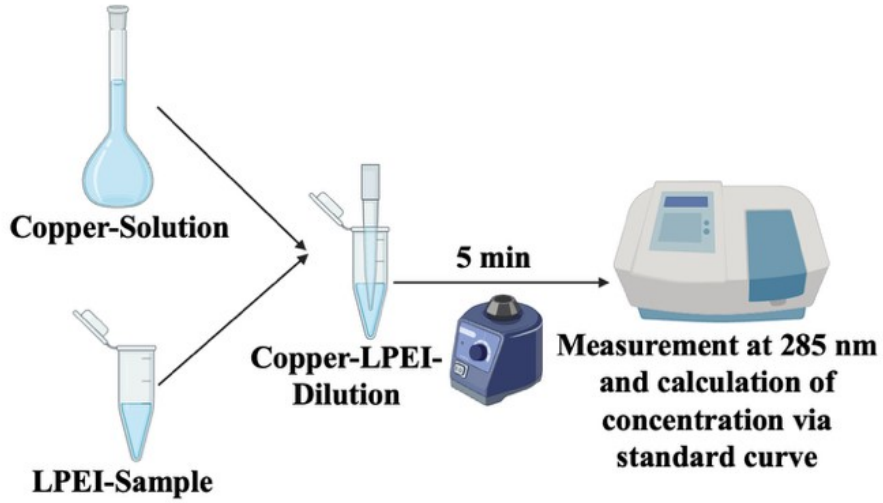

Figure 2 *Schematic-Execution of the Copper Assay: Copper solution was added to the sample and the mixture was incubated for five minutes; absorption was measured at 285 nm using a spectrophotometer; created with BioRender.com*

5.2.2.1.3 Shelf-Life validation of the copper-acetic-buffer

Since the copper assay is essential to determine the LPEI concentration which forms the basis for all further calculation regarding the molar ratio and yield, it was performed often during this research project. In order to increase time efficiency and reduce unnecessary reagent usage, an experiment to determine the shelf-life of the copper-acetic-buffer at room temperature has been done. For this purpose, the standard curve produced as described in 5.2.2.1 from a copper-acetic-buffer, which was stored at room temperature for 17, 20 and 41 days, was compared with a freshly produced copper-acetic-buffer.

5.2.2.1.4 Evaluation of Copper Assay Variability

Another subject of investigation was the evaluation of variability in regards to the copper assay method in order to ensure accurate LPEI-content calculations. For this purpose, a total of four standard curves which were produced with the exact same copper solution and LPEI standard have been compared in regards to their respective standard curve.

5.2.2.2 DTT Assay

The DTT assay is based on the reduction of the pyridyl-disulfide group of the NHS-PEG-OPSS group by DTT, releasing 2-thiopyridone whose increase in absorbance at 343 nm indicates the extent of disulfide reduction. The amount of split of 2-thiopyridone indicates indirectly the amount of PEG-OPSS bound after bi-conjugate synthesis or amount of amino acid bound after tri-conjugate synthesis.

5.2.2.2.1 DTT Assay for the Bi-Conjugate

To reduce the pyridyl-disulfide group, a Dithiothreitol (DTT) reagent was freshly prepared by dissolving 0,154 g of DL-Dithiothreitol in 1 mL of MQ-water, with its primary function being the cleavage of the 2-thiopyridone group from the NHS-PEG-OPSS. Prior to measurement, the samples required dilution with MQ-water to ensure that the absorption fell within the photometer's measurable range. For the measurement procedure, 150 µL of each dilution was combined with 15 µL of the DTT reagent, thoroughly mixed, and subsequently incubated for 10 minutes at room temperature (***Figure 3***). Following incubation, 100 µL of each mixture was transferred into micro-cuvettes, and the absorption was recorded at a single wavelength of 343 nm, using pure MQ-water to set the photometer's zero point. A blank solution, consisting of 150 µL of MQ-water and 15 µL of DTT reagent, was measured in duplicates. For data analysis, the mean value of the absorption readings for each duplicate was first determined, and the averaged blank value was subtracted. Subsequently, the concentration of the OPSS content in the sample was calculated using the Beer-Lambert Law (Eq. 1):

$$A = \varepsilon \cdot c \cdot d \qquad \text{Eq. 1}$$

A… Absorption
ε… Molar absorption coefficient [L/mol·cm]
c… Concentration [mol/L]
d… Path length in solution [cm]

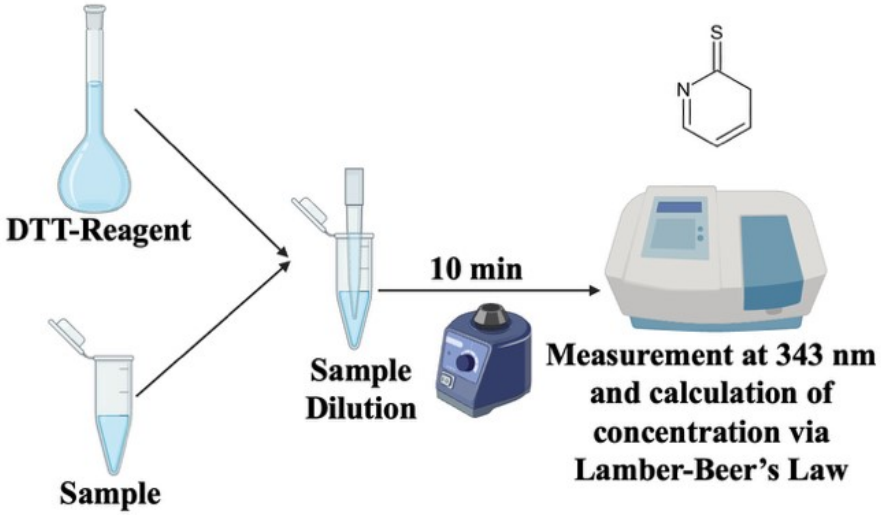

Figure 3 *Schematic-Execution of the DTT Assay: DTT reagent was added to the sample and the mixture was incubated for ten minutes; absorption was measured at 343 nm using a spectrophotometer; created with BioRender.com*

5.2.2.2.2 DTT Assay for the Tri-Conjugate

The DTT assay for the tri-conjugate is slightly different since after coupling of the amino acid to the bi-conjugate, the 2-thiopyridone group is split of without the need for a DTT reagent. Therefore, the determination of the coupled amino acid is executed via using the fraction 1 (exemplary fraction 1: ***Figure 13***) received after CEX purification which contains the 2-thiopyridone. As a blank, a solution of 150 µL of MQ-water was used. Prior to measurement, the sample needed to be diluted in MQ-water to fall within the photometer's measurable range. 100 µL of each dilution was transferred into micro-cuvettes (in duplicates for each measurement), and the absorption was subsequently measured at a single wavelength of 343 nm, with MQ-water serving to zero the photometer. The calculation was performed as described in 5.2.2.2.1.

5.2.2.3 Determination of the molar ratio

The molar ratio is a mean to characterize the efficiency of bi/tri-conjugate synthesis in regards to PEG-OPSS/amino-acid coupling to LPEI. For this purpose, the concentration of the LPEI calculated via the copper assay and split of 2-thiopyridone concentration calculated via the DTT assay were converted to µmol and divided in following manner (Eq. 2):

$$Molar\ Ratio = \frac{(2)thiopyridone\ content\ [\mu mol]}{LPEI\ content\ [\mu mol]} \qquad \text{Eq. 2}$$

5.2.3 Optimizing Purification of LPEI-Conjugates

In order to gain insights as to how cation-exchange chromatography purification and subsequent centrifugal filtration purification performs in regards to LPEI-conjugates, a series of mock syntheses and purifications were performed using LPEI 10 kDa without the PEG-OPSS linker being attached.

5.2.3.1 ÄKTA Purification of LPEI 10 kDa

5.2.3.1.1 Eluent Buffer Production for the Polymer and Bi-Conjugate

Prior to purification, two 20 mM HEPES (2-[4-(2-hydroxyethyl)piperazin-1-yl]ethanesulfonic acid) buffer solutions were prepared: For the 20 mM HEPES eluent 4,78g of HEPES were dissolved in 1 L MQ-water using a magnet stirrer, whereas, for the 20 mM HEPES/3 M NaCl eluent 4,81g HEPES and

175,4g of NaCl were dissolved in the same manner in 1 L MQ-water. Subsequently, the pH was adjusted to 7,4 utilizing solid NaOH, after which the solution was freed from gas as well as filtered under vacuum with filters yielding a 200 µm aPES membrane.

5.2.3.1.2 Eluent Buffer Production for the Tri-Conjugate

Prior to purification, two 20 mM HEPES (2-[4-(2-hydroxyethyl)piperazin-1-yl]ethanesulfonic acid) buffer solutions were prepared: For the 20 mM HEPES eluent 4,78g of HEPES were dissolved in 900 mL MQ-water + 100 mL acetonitrile using a magnet stirrer, whereas, for the 20 mM HEPES/3 M NaCl eluent 4,81g HEPES and 175,4g of NaCl were dissolved in the same manner in 900 mL MQ-water and 100 mL acetonitrile. Subsequently, the pH was adjusted to 7,4 utilizing solid NaOH, after which the solution was freed from gas as well as filtered under vacuum with filters yielding a 200 µm aPES membrane.

5.2.3.1.3 Execution of CEX Purification using the ÄKTA-System

Table 6 *Amounts of Reagents used in each Mock Synthesis and Purification*

Experiment	LPEI [mg]	Ethanol [mL]	HEPES / HEPES-NaCl [mL]	DMSO [mL]	TRIS [mL]	1 M HCl [mL]	Applied amount of Crude Polymer [mL]	Runs performed to apply Crude Polymer
Mock Synthesis and Purification 1	150,38	3	2,00 / 2,00	0,2	0,2	1	5	1
Mock Synthesis and Purification 2.1*	50,4	1	6,66 /1,67	0,1	0,1	0,33	9,86	2
Mock Synthesis and Purification 2.2	50,4	1	6,66 /1,67	0,1	0,1	0,33	9,86	2
Mock Synthesis and Purification 3^{+}	50,09	1	6,66 /1,67	0,1	0,1	0,36	9,9	2

**Higher dilutions of the crude polymer were produced prior CEX purification from mock synthesis 2 onwards*
$^{+}$0,5 mL of the resulting fraction 2 was used for conductivity measurement via ÄKTA as described in 5.2.3.1.4

After LPEI was weighed according ***Table 6*** and dissolved completely in Ethanol, it was incubated for 15 minutes at 35°C / 800 rpm on a Thermoshaker. Following that, DMSO was added, which under normal circumstances would be used to dissolve the NHS-PEG-OPSS linker, and the mixture was incubated again for 10 minutes at 35°C / 800 rpm. Lastly, TRIS was added, which under real synthesis conditions would have quenched the reaction, the mixture incubated for a third time for 15 minutes at 35°C / 800 rpm and the salt concentration adjusted to 0,5 M using 20 µM HEPES and 20 µM HEPES + 3M NaCl. This mixture is referred as crude polymer. 5 mL of the crude polymer were then applied onto the ÄKTA for each purification run using the settings described in ***Table 7***. The CEX purification via the ÄKTA-system provides 2 different fractions, which for simplification will be called ***fraction 1*** (containing some of the purified LPEI) and ***fraction 2*** (containing most of the purified LPEI). Both fractions were collected for each experiment and a copper assay was performed on both fractions. Also, since all calculations regarding the LPEI content are made using the copper assay, the redetermination of LPEI in the crude polymer/conjugate prior CEX was established as a mean to ensure method uniformity from mock synthesis 3 onwards.

Table 7 *ÄKTA Settings used for Mock Synthesis 1-3 and Synthesis 1 (Run 1-4)*

Gradient Time [min]	Buffer
Column equilibration	Solution A: 96,7% Solution B: 3.3%

0-30	Solution A: 96,7% Solution B: 3,3%
30-62,5	Linear gradient towards Solution B 100%
62,5-72,5	Solution B: 100%
72,5-88,5	MQ-water
Column re-equilibration	Solution A: 96,7% Solution B: 3,3%

5.2.3.1.4 Conductivity measurement using the ÄKT-System

Apart from purification purposes, the ÄKTA device's capability to detect the conductivity of applied samples were used to evaluate the salt concentration. For that purpose, a method was written with the settings described in ***Table 8***, where 0,5 mL sample were applied onto the ÄKTA.

Table 8 *ÄKTA Settings for Conductivity Measurement*

Column Volume	Buffer
1	**Solution A: 100% Solution B: 0%**
1	**Linear gradient towards Solutions B 100%**

5.2.3.2 LPEI10kDa Desalting via Centrifugal Filtration Purification

The following section illustrates the execution of the centrifugal filtration purification for the LPEI 10 kDa. Since, with each experiment and gained insights the experiment was modified, the execution for each experiment will be described individually if centrifugal filtration purification was performed.

5.2.3.2.1 Mock Synthesis and Purification 1

The centrifugal filter was conditioned with 2 mL of MQ-water at 4000 G for 10 minutes. The water was discarded afterwards. The faction 2 was applied and for the first run 4000 G for 10 minutes were used. Afterwards, before each run approximately 1,2 mL of fraction 2 was applied onto the filter and the filtrate discarded. Run 2-17 were executed with 4000 G for 15 minutes. Also, the pH of the retentate was determined via indicator paper at run 3, 6, 9, 12. Following the last filtration cycle the retentate was taken out using a pipette and the volume determined. A copper assay according 5.2.2.1.2 was executed.

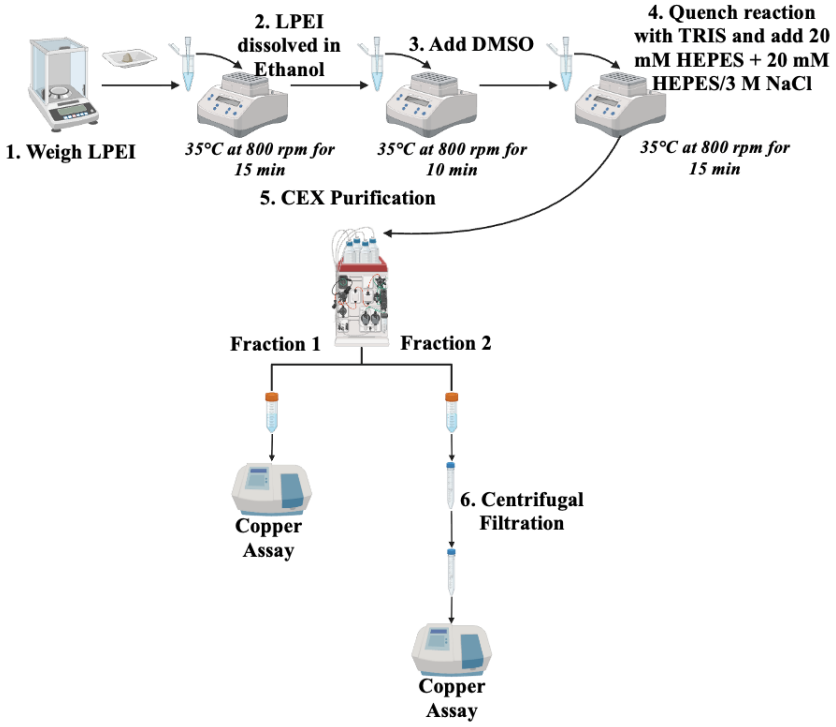

Figure 4 *Schematic-Execution of the Mock Synthesis 1 as described in 5.2.3.2.1; created with BioRender.com*

5.2.3.2.2 Mock Synthesis and Purification 2.1

For this experiment two 2 mL centrifugal filters and one 15 mL centrifugal filter were used. The centrifugal filters were conditioned with 2 mL / 15 mL of MQ-water at 4000 G for 15 minutes. The water was discarded afterwards. Fraction 2 was applied (2 mL and 15 mL) and one centrifugation cycle 4000 G for 15 minutes was executed. Afterwards, the filtrate and retentate of one of the 2 mL centrifugal filters and the 15 mL centrifugal filters were collected for copper assay evaluation. The other 2 mL centrifugal filter underwent another centrifugation washing cycle and also here filtrate and retentate were collected for copper assay evaluation. The remaining amount of the fraction 2 in the 15 mL centrifugation filter was then further concentrated 15 minutes, 4000 G. A copper assay according 5.2.2.1.2 was executed. To determine the LPEI amount bound to the filter membrane the amount of LPEI in the retentate and filtrate were subtracted from the total applied amount of LPEI onto the filter.

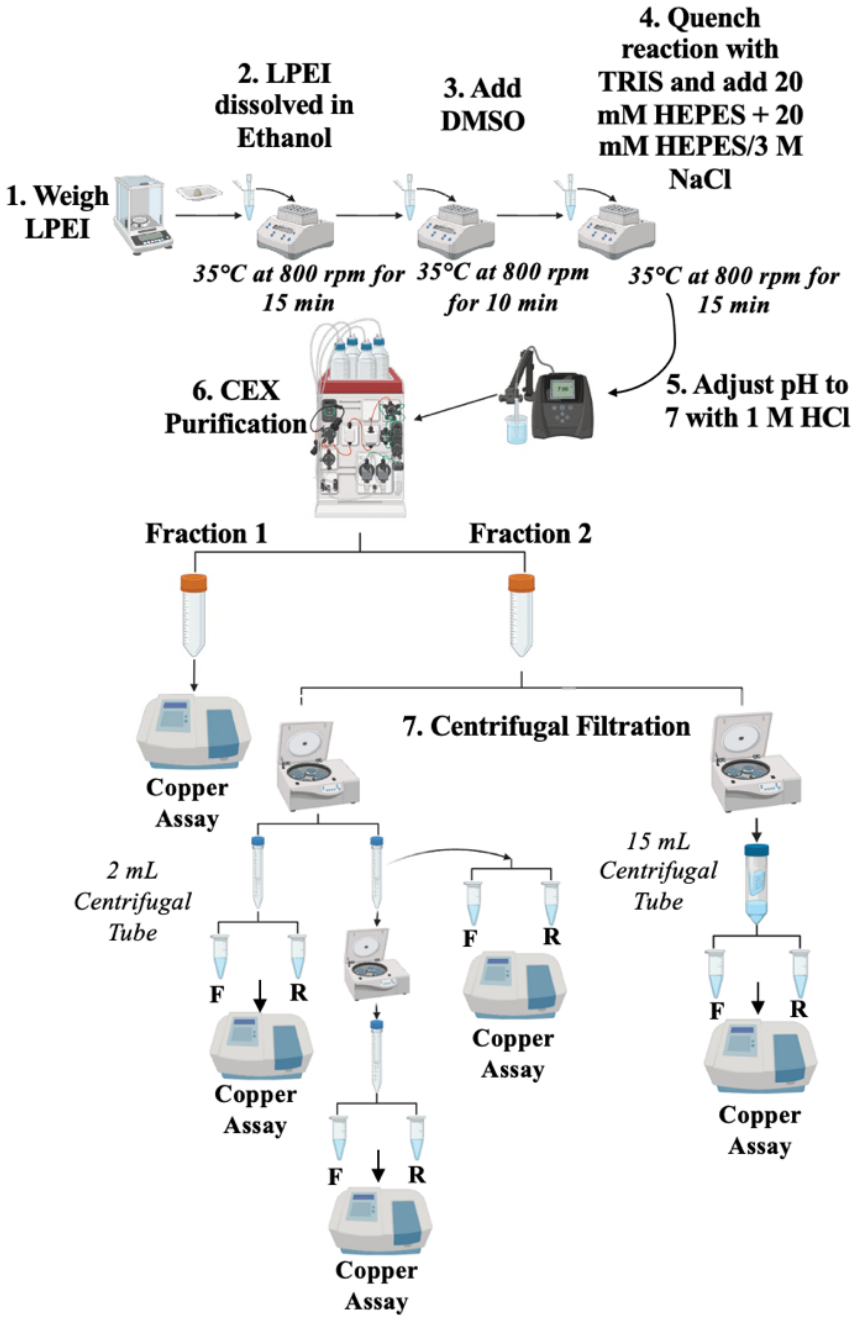

Figure 5 *Schematic-Execution of the Mock Synthesis 2.1 as described in 5.2.3.2.2; F = Filtrate and R = Retentate; created with BioRender.com*

5.2.3.2.3 Mock Synthesis and Purification 2.2

The centrifugal filter from the mock synthesis 2 was stored at 4°C with MQ-water in it and reused in this experiment. For this experiment the remaining 9,555 mL of the Fraction 2 from the mock synthesis and purification 2.1 was firstly concentrated to 0,5 mL with the 15 mL centrifugal filter. The concentrate was then washed 5 times adding 15 mL in the first run and 10 mL of MQ-water in the following 4 runs. The settings remained as 4000 G for 15 minutes. Please note that for the last (5th) run the centrifugation was done 30 minutes to further concentrate the retentate. After each washing cycle 0,5 mL of the filtrate was taken in order to apply onto the ÄKTA and evaluate conductivity (5.2.3.1.4).

5.2.3.2.4 Mock Synthesis and Purification 3

Two 15 mL centrifugal filters were used and were conditioned with 15 mL of MQ-water at 4000 G for 15 minutes. The water was afterwards discarded. 14,611 mL of fraction 2 was applied and one centrifugation cycle (4000 G for 15 minutes) was executed to concentrate the sample to approximately 0,5 mL. Afterwards, one of the filtrates was collected and 3 µL of the retentate were taken out for copper assay evaluation. Onto the retentate 10 mL of MQ-water were added and the first washing cycle performed (4000 G for 15 minutes). Again, the filtrates of both centrifugal filters were collected. The retentate of one of the filters was also taken out (concentrate: 738 µL) of which 3 µL were taken for copper assay evaluation and 0,5 mL for conductivity evaluation according ***Table 8***. Onto the other centrifugal filter 10 mL of MQ-water were added again and another washing cycle executed. In total the second centrifugal filter underwent 5 washing cycles, adding 10 mL MQ-water after each cycle and collecting the filtrate of each cycle for a copper assay and conductivity evaluation. After the last washing cycle also the retentate (654 µL) was collected for copper assay and conductivity evaluation.

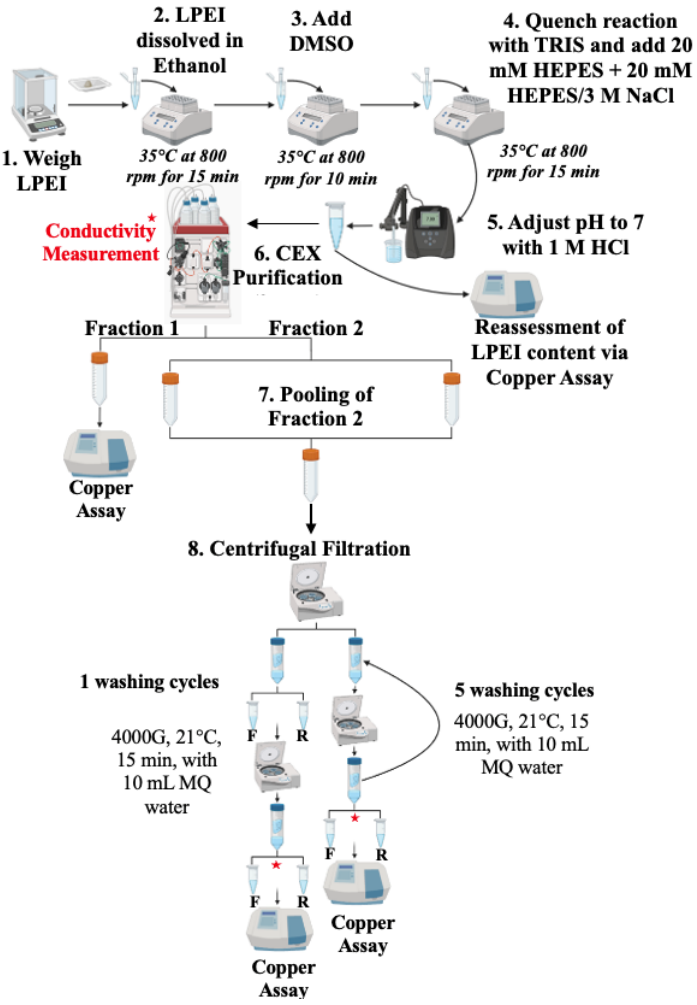

Figure 6 *Schematic-Execution of the Mock Synthesis 3 as described in 5.2.3.2.4; F = Filtrate and R = Retentate; created with BioRender.com*

5.2.4 Synthesis of the LPEI-PEG-OPSS bi-conjugate

In total two batches of the LPEI-PEG-OPSS biconjugate were synthesized (***Table 9***): 200 mg of LPEI free base was dissolved in pure ethanol and split into four 1,5 mL Eppendorf tubes before incubating in a Thermoshaker for 15 minutes at 800 rpm and 35 °C (Synthesis 1) and 37°C (Synthesis 2). The temperature was controlled with a thermostat before every incubation. In the meantime, 80 mg of NHS-PEG2kDa-OPSS was dissolved in DMSO, and was added to each tube containing the LPEI. The LPEI/NHS-PEG2kDa-OPSS mixture was again put in the Thermoshaker and incubated for another 3 hours at 35 °C/37°C with 800 rpm. Following the incubation time, the reaction of LPEI and PEG-OPSS was quenched adding 1 M Tris (pH 8.0) to each tube, vortexed and incubating for another 15 minutes at 35 °C/37°C with 800 rpm. Following that, the mixture was diluted and the salt concentration adjusted to 0,5 M using 20 µM HEPES and 20 µM HEPES + 3M NaCl. Finally, the solution was put on a magnet stirrer and the pH was set to 7,0 (Synthesis 1) / 7,4 (Synthesis 2) using 1 M HCl. A sample from the crude conjugate was taken in order to redetermine the LPEI content using copper assay.

Table 9 *Reagents used for the Bi-Conjugate Synthesis*

Experiment	LPEI [mg]	Ethanol [mL]	Py-S-S-PEG-NHS [mg]	HEPES / HEPES-NaCl [mL]	DMSO [mL]	1 M TRIS [mL]	1 M HCl [mL]	Amount of Crude Conjugate [mL]	Runs performed to apply crude conjugate
Synthesis 1[+]	200	4	80	26,66 / 6,67	0,2	0,267	1,25	38,9	8
Synthesis 2	200	5	83	26,66 / 6,46	0,3	0,267	1,05	40	8

[+] *0,5 mL of dialyzed bi-conjugate was used for conductivity measurement via ÄKTA as described in 5.2.3.1.4*

5.2.5 Purification of the LPEI-PEG-OPSS Bi-Conjugate

Both batches of bi-conjugate underwent CEX purification using the ÄKTA-system and again fraction 1 and fraction 2 were collected after each ÄKTA run. In order to compare the centrifugal filtration purification with dialysis, the fraction 2 was afterwards divided and underwent one of the both desalting methods.

5.2.5.1 ÄKTA Purification

For synthesis 1, 8 ÄKTA runs were performed and fractions collected/divided as described in ***Table 10***. Also, the gradient times have been cut in half after ÄKTA run 5 as described in ***Table 11*** to increase time efficiency. As for Synthesis 2, in total 8 ÄKTA runs were performed. However, since after ÄKTA run 7 only 3 mL of the LPEI-PEG-OPSS solution remained, it was further diluted to 5 mL again using 20 µM HEPES and 20 µM HEPES + 3M NaCl to also ensure the correct salt concentration and an 8th ÄKTA run was performed. The collected fraction 2 was collected/divided as in ***Table 10***.

Table 10 *Collected Fraction 2 from ÄKTA Purification of Synthesis 1 and 2*

Experiment	Collected Fraction 2	Amount of Fraction 2 [mL]	Method of further Purification
Synthesis 1	ÄKTA Run 1-4	67	Centrifugal Purification
	ÄKTA Run 5-7	27	Dialysis and Lyophilization
Synthesis 2	ÄKTA Run 1-4	40	Centrifugal Purification
	ÄKTA Run 5-8	40	Dialysis and Lyophilization

Table 11 *Optimized ÄKTA settings to increase time efficiency used for Synthesis 1 and 2*

Gradient Time [min]	Buffer
Column equilibration	Solution A: 96,7% Solution B: 3,3%
0-12,5	Solution B: 16,7%
12,5-32,5	Linear gradient towards Solution B: 100%
32,5-42,4	Solution B: 100%
Column re-equilibration	Solution A: 96,7% Solution B: 3,3%

5.2.5.2 Desalting via Centrifugal Filtration Purification

The fraction 2 was applied on 15 mL centrifugal filters which were conditioned with 15 mL of MQ-water. Firstly, the applied fraction 2 was concentrated to approximately 0,5 mL and afterwards 15 mL of MQ-water was added for the washing cycle. The used settings and the duration of centrifugation are depicted in ***Table 12***. In order to determine the LPEI and PEG-OPSS content, samples from the retentate were taken and a copper assay (5.2.2.1.2), as well as, DTT (5.2.2.2.1) assay was performed. Afterwards, the molar ratio was calculated as described in 5.2.2.3.

Table 12 *Centrifugal Filtration of the Bi-Conjugate from Synthesis 1 and 2*

Experiment	Applied amount of Fraction 2 [mL]	Concentration Step	Washing Step	Amount of Retentate [mL]
Synthesis 1	60	40 min, 4000 G, 21°C	40 min, 4000 G, 21°C	2,085
Synthesis 2	40	50 min, 4000 G, 21°C	60 min, 4000 G, 21°C	1,865

5.2.5.3 Desalting via Dialysis and Lyophilization

In regards to synthesis 1, fraction 2 was divided into two dialysis tubes (MWCO <1 kDa) and for synthesis 2, fraction 2 was divided into three dialysis tubes (MWCO <1 kDa) as depicted in ***Figure 7***. Each tube was put into a 5 L baker with MQ-water at 4°C and dialysis was performed for 24 hours under constant stirring using a magnet stirrer. The MQ-water was changed after approximately 12 hours. After completed dialysis, the contents of the dialysis tubes were transferred into CT 25 and the dialysis tubes were washed with 3 mL of MQ-water for thorough transfer. Also, a sample (0,5 mL) was taken out of the CT 25 for conductivity measurement as described in 5.2.3.1.4 during synthesis 1. Afterwards, lyophilization was executed for approximately 1,5 days until only a powder was seen. The powder was reconstituted using MQ-water (***Table 13***). In order to determine the LPEI and PEG-OPSS content, samples from the reconstituted bi-conjugate were taken and a copper assay (5.2.2.1.2), as well as, DTT (5.2.2.2.1) assay was performed. Afterwards, the molar ratio was calculated as described in 5.2.2.3.

Table 13 *Dialysis and Lyophilization of the Bi-Conjugate from Synthesis 1 and 2*

Experiment	Applied amount of Fraction 2 [mL]	Dialysis	Lyophilization	Amount after Reconstitution [mL]
Synthesis 1	25	24 hours at 4°C	36 hours	0,57
Synthesis 2	40	24 hours at 4°C	36 hours	1,02

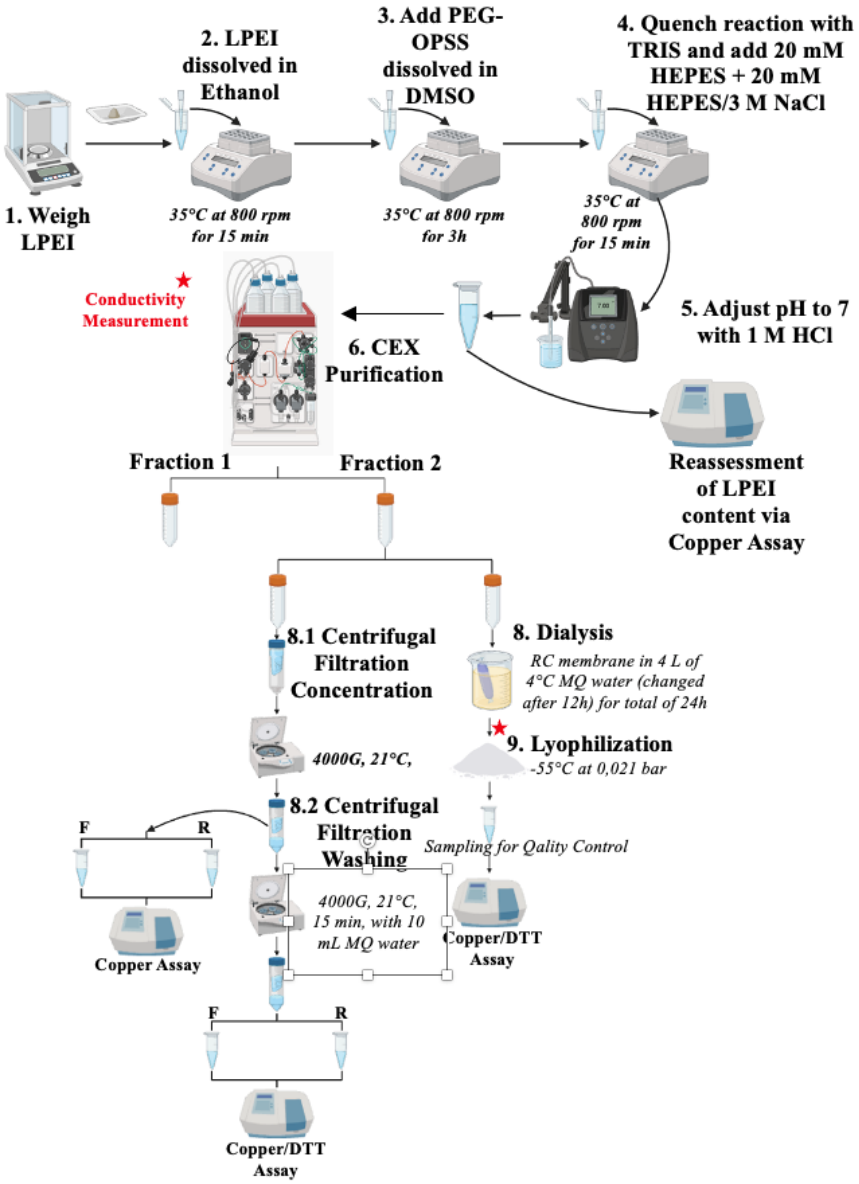

Figure 7 *Schematic-Execution of the Bi-Conjugate-Synthesis as described in 5.2.4 and 0; F = Filtrate and R = Retentate; created with BioRender.com*

5.2.6 Synthesis of the LPEI-PEG-CYS Tri-Conjugate

For the tri-conjugate synthesis, the bi-conjugates from each synthesis and, therefore, each desalting method were utilized. Please note that from synthesis 2 only half of the bi-conjugates synthesized were further processed to a tri-conjugate. The bi-conjugates were diluted using 20 mM HEPES + 10% v/v acetonitrile to a final concentration of 4-5 mg/mL. After determination of the PEG-OPSS molarity using the DTT assay, 5 equivalents of L-Cysteine were dissolved in MQ-water for synthesis. Both solutions were purged with argon gas and 0,1 mL of the bi-conjugate dilution was used as a blank for online monitoring of the synthesis via spectrophotometer. L-Cysteine was added according ***Table 14*** and the reaction mixture was stirred at room temperature. The absorption of released 2-thioyridone was measured at 343 nm for 20 minutes by taking samples out of the mixture and putting it back after measuring. After completed synthesis, the mixture was further diluted using 20 mM HEPES + 10% v/v acetonitrile and 20 mM HEPES + 3 M NaCl + 10% v/v acetonitrile mL with a salt concentration of 0,5 M. The pH was adjusted to 7,4 using HCl.

Table 14 *Reagents used for the Tri-Conjugate-Synthesis*

Experiment	Desalting Method used for Bi-conjugate	Calculated amount of Bi-Conjugate [mg]	Amount of L-Cysteine [mg]	First Dilution HEPES + ACN	Second Dilution HEPES-NaCl + ACN [mL]	Amount of Crude Conjugate [mL]	Runs performed to apply Crude Conjugate
Synthesis 1	CF	49,88	2,54	6,39	1,67	10,4	2
	DL	53,67	2,03	3,42	0,83	5,02	1
Synthesis 2	CF	20,77	3,05	3,23	0,86	5,33	1
	CL	35,83	3,32	6,8	1,5	9,13	2

5.2.7 Purification of the LPEI-PEG-CYS Tri-Conjugate

All batches of tri-conjugate underwent CEX purification using the ÄKTA-system according the described settings in ***Table 16*** and again fraction 1 and fraction 2 were collected after each ÄKTA run. In order to compare the centrifugal filtration purification with dialysis, the fraction 2 was afterwards divided and underwent one of the both desalting methods according to the desalting method used during bi-conjugate purification.

5.2.7.1 CEX Purification using the ÄKTA-System

For synthesis 1, two ÄKTA runs were performed for the tri-conjugate synthesized from the bi-conjugate desalted via centrifugal filtration and one ÄKTA run was performed for the tri-conjugate synthesized from the bi-conjugate desalted via dialysis. For synthesis 2, one ÄKTA run was performed for the tri-conjugate synthesized from the bi-conjugate desalted via centrifugal filtration and two ÄKTA runs were performed for the tri-conjugate synthesized from the bi-conjugate desalted via dialysis. The fractions were collected according ***Table 15*** and accordingly further processed.

Table 15 *Collected Fraction 1 and 2 from ÄKTA Purification of Synthesis 1 and 2*

Experiment	Desalting Method used for Bi-conjugate	Collected Fraction 2	Amount of Fraction 2 [mL]	Amount of Fraction 1 [mL]	Method of further Purification
Synthesis 1	CF	ÄKTA Run 1-2	20	26	Centrifugal Purification
	DL	ÄKTA Run 3	11,5	14	Dialysis and Lyophilization
Synthesis 2	CF	ÄKTA Run 1	10	14	Centrifugal Purification
	DL	ÄKTA Run 2-3	20	28	Dialysis and Lyophilization

Table 16 *ÄKTA settings for Tri-Conjugate-Synthesis*

Gradient Time [min]	Buffer
Column equilibration	Solution A: 96,7% Solution B: 100%
0-25	Solution B: 16,7%
25-57,5	Linear gradient towards Solution B: 100%
57,5-73,5	Solution B: 100%
Column re-equilibration	Solution A: 96,7% Solution B: 100%

5.2.7.2 Desalting via Centrifugal Filtration Purification

The fraction 2 was applied on 15 mL centrifugal filters which were conditioned with 15 mL of MQ-water. Firstly, the applied fraction 2 was concentrated to approximately 0,5 mL and afterwards 15 mL of MQ-water was added for the washing cycle. The used settings and the duration of centrifugation are depicted in ***Table 17***. In order to determine the LPEI content, a sample from the retentate was taken and a copper assay (5.2.2.1.2) was performed. Prior, the molar ratio calculation as described in 5.2.2.3, a DTT assay was performed on a sample of the according fraction 1 to determine the cysteine concentration (5.2.2.2.2).

Table 17 *Centrifugal Filtration of the Tri-Conjugate*

Experiment	Applied amount of Fraction 2 [mL]	Concentration Step	Washing Step	Amount of Retentate [mL]
Synthesis 1	20	40 min, 4000 G, 21°C	40 min, 4000 G, 21°C	0,85
Synthesis 2	10	50 min, 4000 G, 21°C	60 min, 4000 G, 21°C	0,85

5.2.7.3 Desalting via Dialysis and Lyophilization

In regards to synthesis 1, fraction 2 was transferred into one dialysis tube with a MWCO of 1 kDa and for synthesis 2, fraction 2 was divided into two dialysis bags. Each tube was put into a 5 L baker with MQ-water at 4°C and dialysis was performed for 24 hours under constant stirring using a magnet stirrer. The MQ-water was changed after approximately 12 hours. After completed dialysis, the contents of the dialysis bags were transferred into CT 25 and the dialysis tubes were washed with 3 mL of MQ-water for thorough transfer. Lyophilization was executed for approximately 1,5 days until only a powder was seen. The powder was reconstituted using MQ-water. In order to determine the LPEI content, a sample from the reconstituted tri-conjugate was taken and a copper assay (5.2.2.1.2) was performed. Prior, the molar ratio calculation as described in 5.2.2.3, a DTT assay was performed on a sample of the according fraction 1 to determine the cysteine concentration (5.2.2.2.2).

Table 18 *Dialysis and Lyophilization of the Tri-Conjugate*

Experiment	Applied amount of Fraction 2 [mL]	Dialysis	Lyophilization	Amount after Reconstitution [mL]
Synthesis 1	11,5	24 hours at 4°C	36 hours	0,52
Synthesis 2	20	24 hours at 4°C	36 hours	0,52

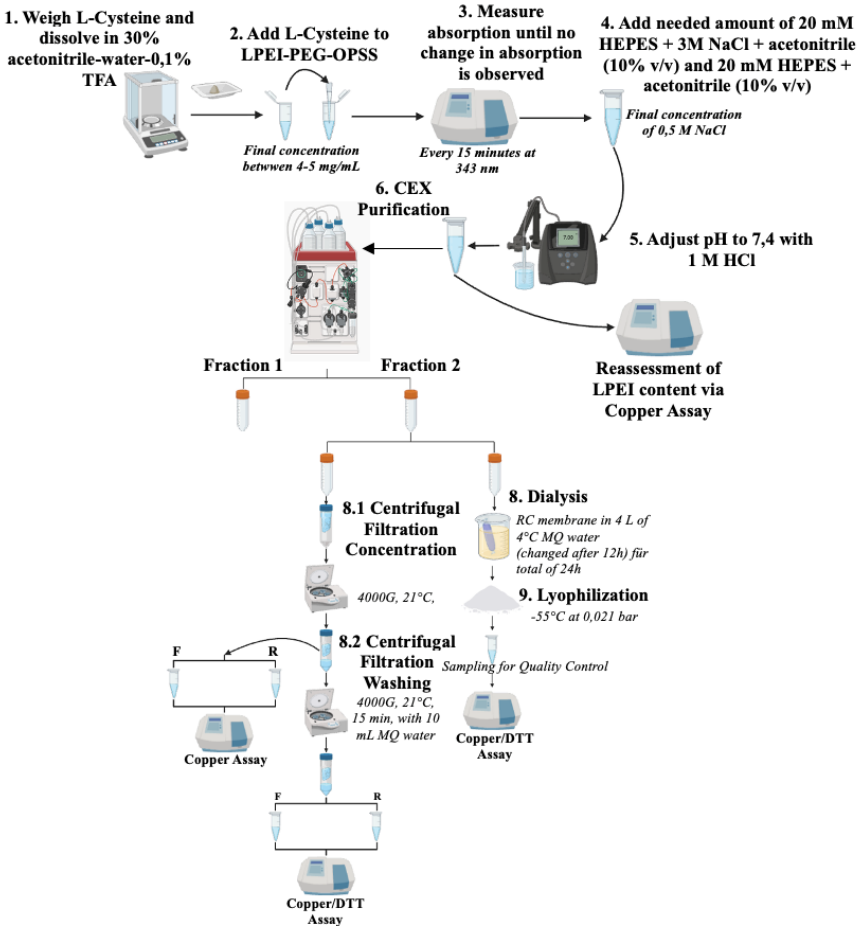

Figure 8 *Schematic-Execution of the Tri-Conjugate-Synthesis as described in 5.2.6 and 5.2.7; F = Filtrate and R = Retentate; created with BioRender.com*

5.2.8 DLS Characterization

In order to evaluate the size distribution of LPEI/LPEI-PEG-CYS-based polyplexes with pDNA/mRNA, dynamic light scattering measurements were performed using the same SOP described in ***Table 19.*** As for the cationic polymer, sole LPEI was used for pDNA polyplexes as a mean for method optimization due to limited amount of tri-conjugates from 5.2.6 for mRNA-polyplexes. The production of the polyplexes was executed using flash-pipetting of two sets of mixtures resulting in N/P ratios of 12 or 120. Also, polyplexes with pDNA concentrations of 40 µg/mL and 10 µg/mL were compared to each other for LPEI-pDNA-polyplexes. For the calculation of the needed volumes, an Excel sheet template was used and N/P ratios calculated according equation (Eq. 3). Each N/P ratio was produced by mixing the LPEI, our cationic polymer, with the nucleic acid, in different ratios. All measurements were executed on the DLS device using disposable micro cuvette and the results were analyzed using the zetasizer software (v7.13).

$$cat.Polymer\ [\mu g] = \frac{nucleic\ acid\ [\mu g] \cdot \frac{N}{P}\ ratio\ \cdot 205}{330} \qquad \text{Eq. 3}$$

Table 19 *Settings used for Dynamic-Light-Scattering Measurements*

Parameter	Value
Temperature	25°C
Viscosity (HBG)	0,99 cP
Refractive Index	1,330
Number of measurements for each dilution	4

5.2.8.1 LPEI10kDa-pDNA-Polyplexes

For the LPEI-pDNA-polyplexes a mother-stock out of LPEI 10 kDa and GLuc-pDNA in HBG buffer was produced according ***Table 20*** in a laminar airflow. The mother-stocks were then gently flipped and spun down. From these mother-stocks, a volume equivalent to the calculated mass, was put into 0,5 mL tubes, resulting in 2 different tubes (for each N/P ratio) containing either LPEI or pDNA. Afterwards, each tube was further diluted with HBG buffer to receive 20 µL of each mixture. The tubes were then gently flipped and spun down. Subsequently, the LPEI was added to the pDNA by flash-pipetting around 25 times and incubated for 5 minutes under non-sterile conditions. For this purpose, the pipette was set to 35 µL thoroughly mixing the solution. Lastly, the LPEI-pDNA-polyplex solution was further diluted and transferred into a cuvette to perform the DLS measurement.

Table 20 *LPEI-pDNA-Polyplex-Preparation*

LPEI [µg/mL]	pDNA [µg/mL]	N/P ratio	Mother-Stock of LPEI [mL]		Desired pDNA concentration for Polyplex [µg/mL]	Mother-Stock of pDNA [mL]		LPEI Dilution [mL]		pDNA Dilution [mL]	
			LPEI	HBG		pDNA	HBG	LPEI	HBG	pDNA	HBG
2282,14	3887,5	12	2,63	17,37	10	2,57	47,43	2,08	17,92	2,00	18,00
		120	3,51	6,49		2,57	47,43	7,82	12,18	2,00	18,00
2282,14	3887,5	12	2,19	17,81	40	2,57	47,43	10,01	9,99	8,00	12,00
		120	20	0		3,05	46,95	10,96	9,04	8,00	12,00

5.2.8.2 Tri-Conjugate-mRNA-Polyplexes

For the Tri-Conjugate-mRNA-polyplexes a mother-stock out of the tri-conjugates from each desalting method from synthesis 2 and GLuc-mRNA in HBG buffer was produced according ***Table 21*** in a laminar airflow. The mother-stocks were then gently flipped and spun down. From these mother-stocks, a volume equivalent to the calculated mass, was put into 0,5 mL tubes, resulting in 2 different tubes (for each N/P ratio) containing either tri-conjugate or mRNA. Afterwards, each tube was further diluted with HBG buffer to receive 20 µL of each mixture. The tubes were then gently flipped and spun down. Subsequently, the tri-conjugate was added to the mRNA by flash-pipetting around 25 times and incubated for 5 minutes under non-sterile conditions. For this purpose, the pipette was set to 35 µL

thoroughly mixing the solution. Lastly, the Tri-Conjugate-mRNA-polyplex solution was further diluted and transferred into a cuvette to perform the DLS measurement.

Table 21 *Tri-Conjugate-Polyplex-Preparation*

LPEI Type	LPEI [µg/mL]	mRNA [µg/mL]	N/P ratio	Mother-Stock of LPEI [mL]		Mother-Stock of mRNA [mL]		LPEI Dilution [mL]		pDNA Dilution [mL]	
				LPEI	HBG	mRNA	HBG	LPEI	HBG	mRNA	HBG
L	9147,17	1528	12	2,19	77,81	6,54	93,46	10,01	9,99	16	4
			120	5,47	14,53						
LPC - CF	5586,35		12	2,69	57,31						
			120	8,95	11,5						
LPC - D	4708,87		12	3,19	56,81						
			120	10,62	9,38						

5.2.9 AI declaration and Illustrations

In the preparation of this thesis, AI-based tools were used in a supportive manner. NotebookLM (https://notebooklm.google) was employed to assist with the organization, navigation, and summarization of academic sources. Additionally, ChatGPT (https://chat.openai.com) and Gemini (https://gemini.google.com) were used exclusively to improve the clarity, structure, and linguistic quality of formulations based on my original drafts. No confidential research data was processed by these tools. None of the AI tools were used to generate original scientific content, research data, hypotheses, interpretations, or conclusions. All AI-generated suggestions were carefully reviewed and proofread before inclusion to ensure accuracy and adherence to scientific standards. Schematic figures were created using BioRender (https://biorender.com).

6 Results & Discussion

This section elaborates and discusses the results of the different methods described in 5.2 which were utilized as part of this master's thesis.

6.1.1 Copper Assay Optimization

In the following section the results of the LPEI-standard production as well as copper assay shelf-life validation and assay variability as described in 5.2.2.1.1, 5.2.2.1.3 and 5.2.2.1.4 will be discussed.

6.1.1.1 Preparation of the LPEI10kDa for the copper assay standard curve

After establishing the standard curve using the unfiltered LPEI, an error rate of R^2= 0,9992 was achieved suggesting high reliability in regards to the calculated concentrations using the standard curve equation shown in ***Figure 9*** below. A concentration of 9685 µg/mL was determined for the concentration of the unfiltered LPEI which was used as the standard for all following copper assay evaluations. This was intended since using the exact same standard stock ensures well comparable and reliable results across all copper assays executed as part of this thesis.

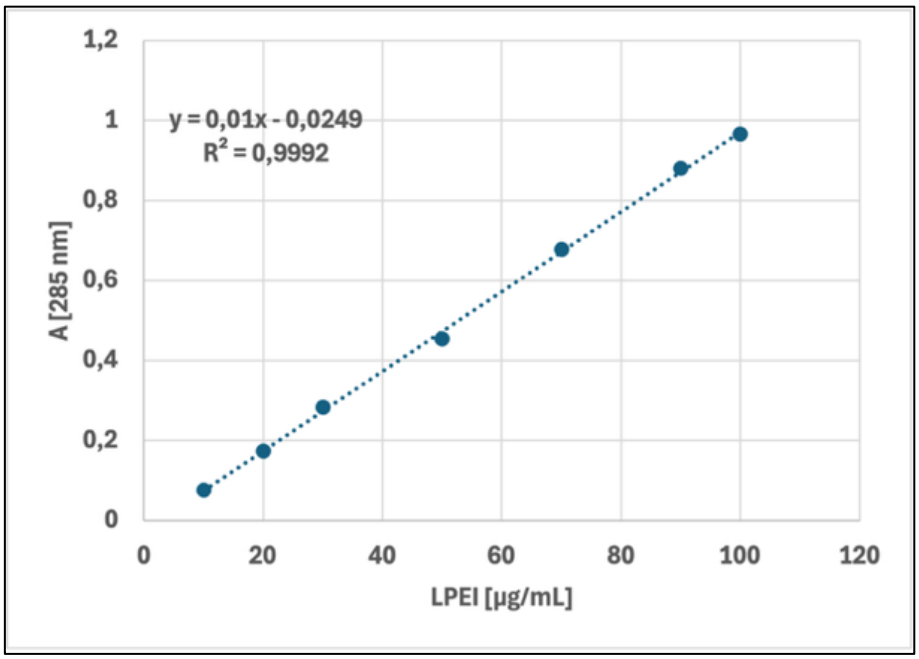

Figure 9 *Standard Curve of produced LPEI-Stock by measuring absorption of each dilution at 285 nm using a spectrophotometer*

6.1.1.2 Shelf-Life validation of the copper-acetic-buffer

After comparing the standard curves produced with the old copper-acetic-buffer with the ones produced with the freshly produced buffer, it is evident that there are no observable changes in regards to absorption properties. Therefore, a shelf-life of 41 days was validated, increasing overall efficiency and sustainability as can be seen in ***Figure 10***.

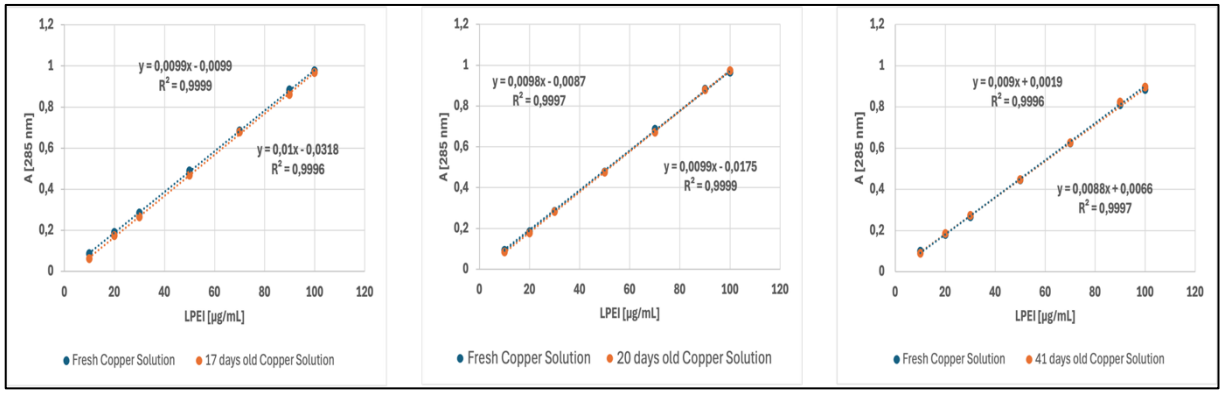

Figure 10 *Comparison of 17-, 20- and 41-days old copper-acetic-buffer with freshly produced copper-acetic-buffer; measured absorption of each dilution at 285 nm using a spectrophotometer*

6.1.1.3 Evaluation of Copper Assay Variability

This experiment shows that the variation of absorption for each dilution ranges between 2-18% (***Figure 12***) even though the error rates for all of the compared standard curves are well above 0,999 (***Figure 11***). This suggests a variation in the method itself which should be considered when comparing the results of different copper assays.

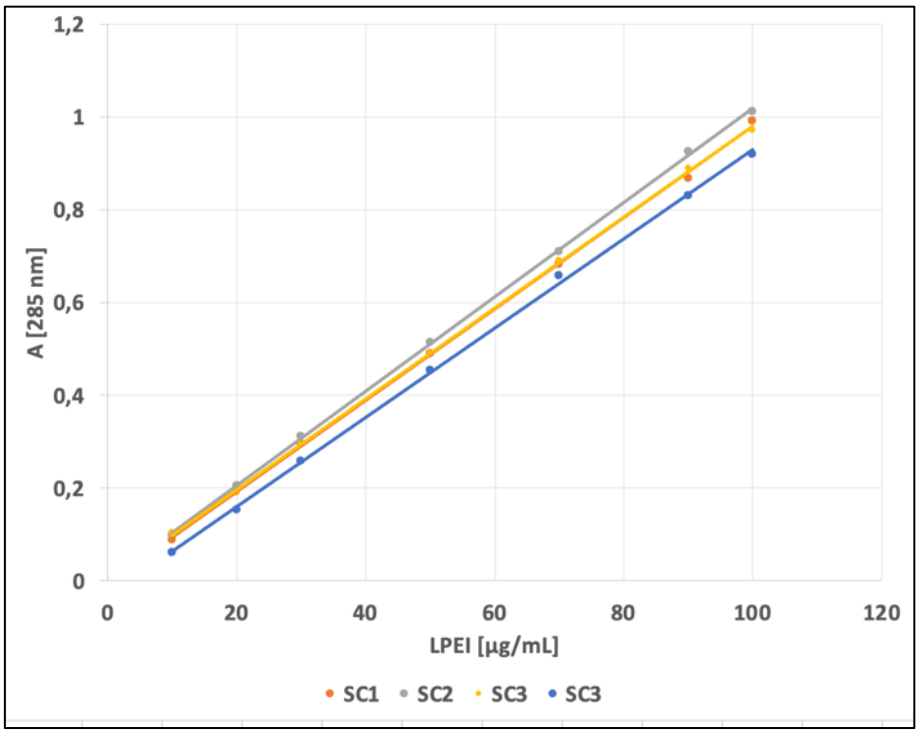

Figure 11 *Comparison of 4 different standard curves produced at different time points with the exact same LPEI-standard which was produced as described in 5.2.2.1.1 in regards to variation in absorption at 285 nm using a spectrophotometer; SC = Standard Curve*

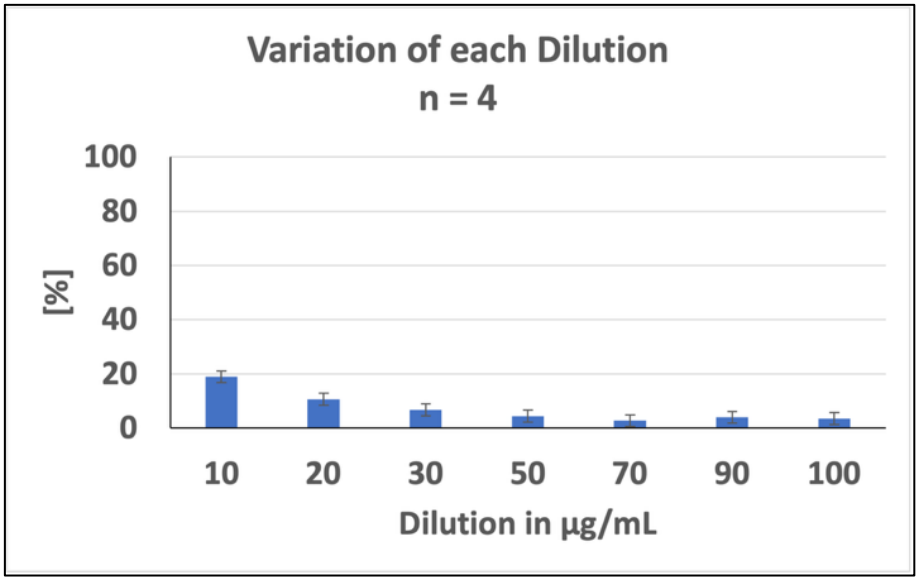

Figure 12 *Calculated variation of absorption for each dilution from all 4 standard curves shown in* ***Figure 11***

6.1.2 CEX Purification of LPEI 10 kDa and Desalting using Centrifugal Filtration

This chapter illustrates the results of the three mock syntheses which underwent CEX using the ÄKTA-system and subsequent centrifugal filtration by providing their respective ÄKTA-graphs. Also, the results of the copper assays, which were performed as per in 5.2.3.1.3 and 5.2.3.2, will be shown.

6.1.2.1 Mock Synthesis and Purification 1

The first mock synthesis and purification was a mean to gain insights regarding yield and behavior of LPEI during CEX and subsequent desalting via centrifugal filtration. ***Figure 13*** illustrates that, after applying the crude polymer to the ÄKTA-system, a separation into two distinct fractions occurs: 10 mL of fraction 1 and 19,5 mL of fraction 2 were collected. The second fraction contains the majority of the LPEI and is therefore selected for further purification (***Table 22***). A LPEI-loss of 4,63% is observed in

the first fraction, which is not suitable for further use. The calculated yield for fraction 2 exceeds 100%, which can be attributed to the assay variability discussed in section 6.1.1.3.

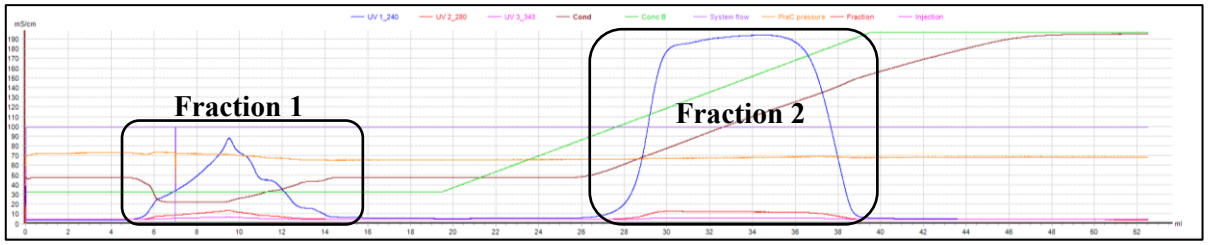

Figure 13 *Cation exchange chromatography diagram from* ***LPEI10kDa-Mock Synthesis and Purification 1*** *in HEPES buffer. 5ml of crude polymer was injected and subjected to chromatographic separation by ÄKTA. Y-axis plots conductivity and UV measurements are shown in colored lines (240nm blue, 280nm red and 343nm pink nm); blue line represents detected LPEI. Solid phase used was Macro-Prep High S Media and ÄKTA settings are described in* ***Table 7***

After desalting via centrifugal filtration as described in 5.2.3.2.1, it was determined that the pH does not show any fluctuations ranging between 8-9 and a significant amount of product loss is observed during the process. The results of this mock synthesis formed the basis of the second mock synthesis which had as a goal the reduction of polymer loss in fraction 1 by using higher dilutions of the crude polymer and investigation of product loss during centrifugal filtration.

Table 22 *Yields after ÄKTA Purification and Centrifugal Filtration of Mock Synthesis and Purification 1 determined via Copper Assay*

Weighed amount of LPEI [mg]	Fraction	Concentration of LPEI after CEX [µg/mL]	Content of LPEI after CEX [mg]	Yield after CEX [%]	Yield after CF [%]	
100,52	Fraction 1	481,81	4,81	4,63	Retentate	Filtrate
	Fraction 2	5331,25	103,96	103,42	22,57	77,43

6.1.2.2 Mock Synthesis and Purification 2.1

After gaining fundamental insights a second mock synthesis and purification was executed to compare small with big centrifugal filters in regards to desalting and also investigate the influence of washing cycles performed on the yield. Again, during CEX purification fraction 1 (33ml) and fraction 2 (29,5 ml) were collected. As observable in ***Figure 14*** and shown in ***Table 23***, further dilution of the crude polymer before applying onto the ÄKTA resulted in significantly lower LPEI loss in fraction 1. For this reason, it was decided that for all further mock syntheses as well as actual bi-/tri-conjugate syntheses high dilutions will be utilized for ÄKTA purification as a mean to reduce product loss in fraction 1.

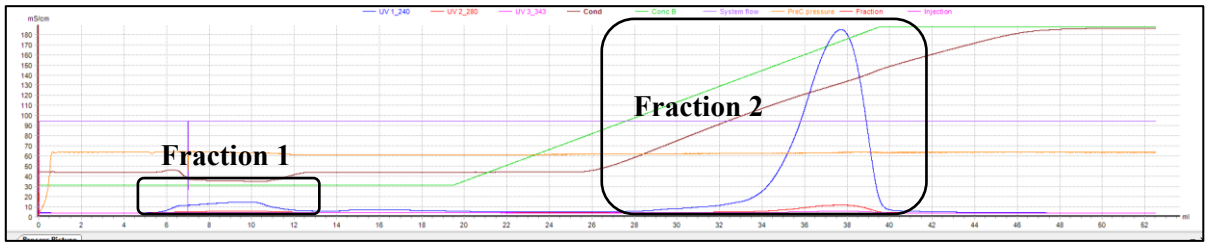

Figure 14 *Cation exchange chromatography diagram from* ***Run 1/2 of LPEI10kDa-Mock Synthesis and Purification 2.1*** *in HEPES buffer. 5ml of crude polymer was injected and subjected to chromatographic separation by ÄKTA. Y-axis plots conductivity and UV measurements are shown in colored lines (240nm blue, 280nm red and 343nm pink nm); blue line represents detected LPEI. Solid phase used was Macro-Prep High S Media and ÄKTA settings are described in* ***Table 7****; please note that the diagram of the second run* ***(2/2)*** *is listed in the Appendix*

Table 23 *Yields after CEX Purification of Mock Synthesis and Purification 2.1 calculated via Copper Assay*

Weighed amount of LPEI [mg]	Fraction	Concentration of LPEI after CEX [µg/mL]	Content of LPEI after CEX [mg]	Yield after CEX [%]
50,4	Fraction 1	8,06	0,27	0,54
	Fraction 2	1322,25	39,01	77,39

When comparing the 15 mL centrifugal filter with the 2 mL centrifugal filter, which both underwent just one washing cycle, it becomes evident that desalting with the 2 mL filter results in a higher yield (***Figure 15*** and ***Table 24***). However, the 2 mL centrifugal filter is not usable in the sense of efficiency when considering the high volumes of fraction 2 which need to be desalted. Coming to the second objective of this mock synthesis, the investigation of product loss during centrifugal filtration: the side-by-side comparison of the one-time washed and two-times washed 2 mL centrifugal filter demonstrate the increase in loss of product with increase in washing cycles (***Table 25***). For this observation, 2 possible root causes were assessed: loss due to washing of the product into the filtrate or loss due to the interaction of the cationic polymer with the centrifugal filter membrane as a function of contact time. In that sense, ***Table 25*** proves that the loss of product does increase and is a result of performed washing cycles.

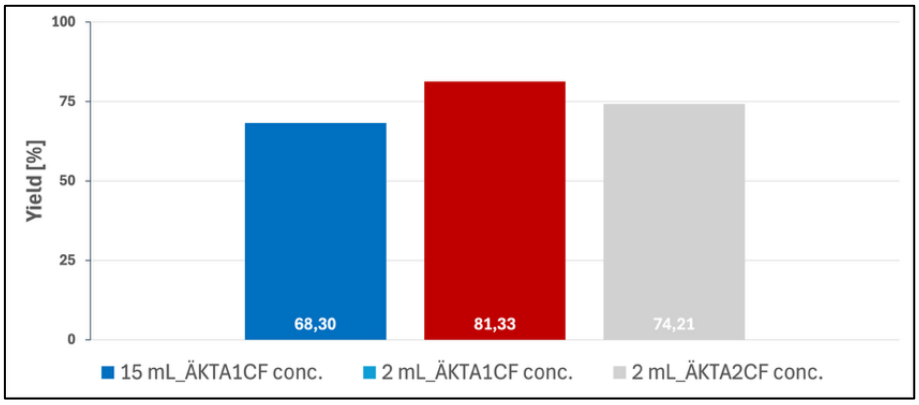

Figure 15 *Yields after Centrifugal Filtration of CEX-purified LPEI 10 kDa in Mock Synthesis and Purification 2.1 using different sized centrifugal filters and different amounts of washing cycles; yield in regards to applied amount of polymer onto the filter*

Table 24 *Yields after Centrifugal Filtration of CEX-purified LPEI 10 kDa in Mock Synthesis and Purification 2.1 using different sized centrifugal filters and different amounts of washing cycles*

Filter Capacity	Applied amount of LPEI [mg]	Amount of LPEI after 1 washing cycle [mg]	Amount of LPEI after 2 washing cycles [mg]
15 mL	19,83	13,55	
2 mL	2,64	2,15	
2 mL	2,64		1,96

Table 25 *Product loss during centrifugal filtration due to washing into filtrate and binding to filter membrane in Mock Synthesis and Purification 2.1*

Filter Capacity and amount of washing cycles	Retentate [%]	Loss in Filtrate [%]	Bound to Filter Membrane [%]
15 mL – 1 washing cycle	68,3	21,68	9,98
2 mL – 1 washing cycle	81,3	11,36	7,2
2 mL – 2 washing cycles	74,21	18,94	6,82

6.1.2.3 Mock Synthesis and Purification 2.2

In order to compare the desalting capacity between 1-time washed and 5-times washed LPEI as part of centrifugation filtration, the salt concentrations of the filtrate after each washing step were assessed using the ÄKTA-system. Furthermore, product loss was also characterized and put side by side. When examining the conductivity spectra, a clear trend emerges between the number of washing cycles performed and the resulting conductivity, and thus the salt concentration, of the samples. After 3 washing cycles, no further salt was detectable via the ÄKTA-system.

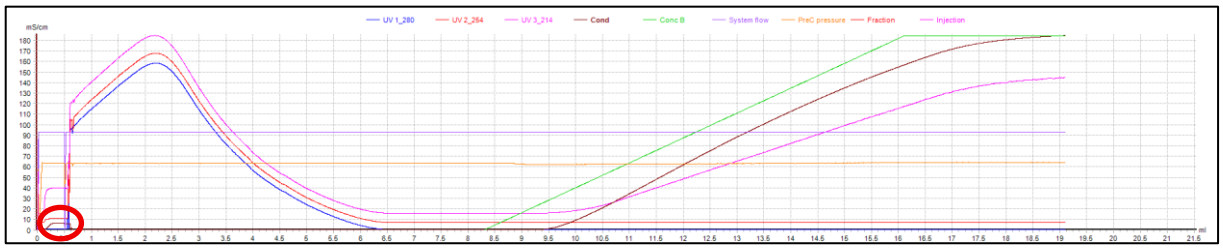

Figure 16 Filtrate after 1. Washing Cycle**; ÄKTA conductivity spectrums of **Mock Synthesis and Purification 2.2** in HEPES buffer; 0,5ml of sample was injected and subjected to conductivity measurement by ÄKTA. Y-axis plots conductivity and UV measurements are shown in colored lines (280nm blue, 214nm red and 254nm pink); blue line represents detected LPEI. Solid phase used was Macro-Prep High S Media and ÄKTA settings are described in ÄKTA **Table 8

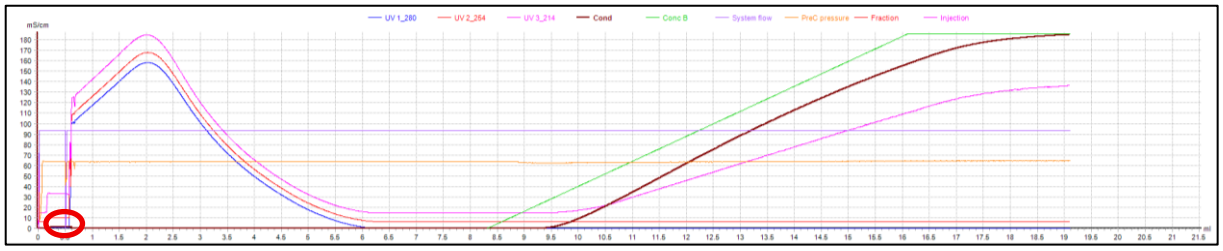

Figure 17 Filtrate after 2. Washing Cycle**; ÄKTA conductivity spectrums of **Mock Synthesis and Purification 2.2** in HEPES buffer; ÄKTA UV measurement (280 blue, 214 red and 254 pink nm); green line shows increasing salt concentration and brown line in correlation to the green line shows conductivity; solid phase: Macro-Prep High S Media; ÄKTA setting described in **Table 8

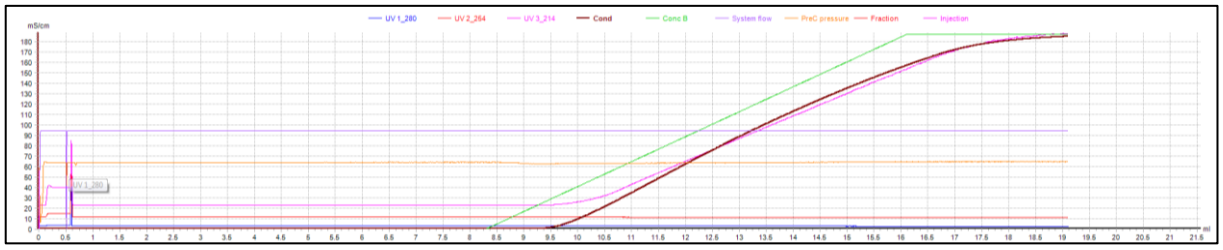

Figure 18 Filtrate after 3. Washing Cycle**; ÄKTA conductivity spectrums of **Mock Synthesis and Purification 2.2** in HEPES buffer; ÄKTA UV measurement (280 blue, 214 red and 254 pink nm); green line shows increasing salt concentration and brown line in correlation to the green line shows conductivity; solid phase: Macro-Prep High S Media; ÄKTA setting described in **Table 8

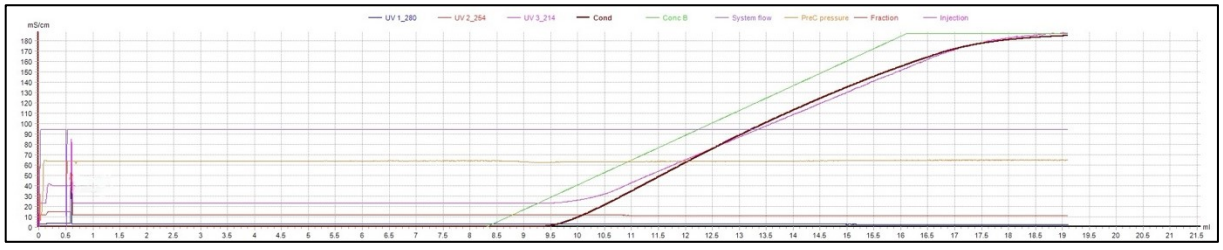

Figure 19 Filtrate after 4. Washing Cycle**; ÄKTA conductivity spectrums of **Mock Synthesis and Purification 2.2** in HEPES buffer; ÄKTA UV measurement (280 blue, 214 red and 254 pink nm); green line shows increasing salt concentration and brown line in correlation to the green line shows conductivity; solid phase: Macro-Prep High S Media; ÄKTA setting described in **Table 8

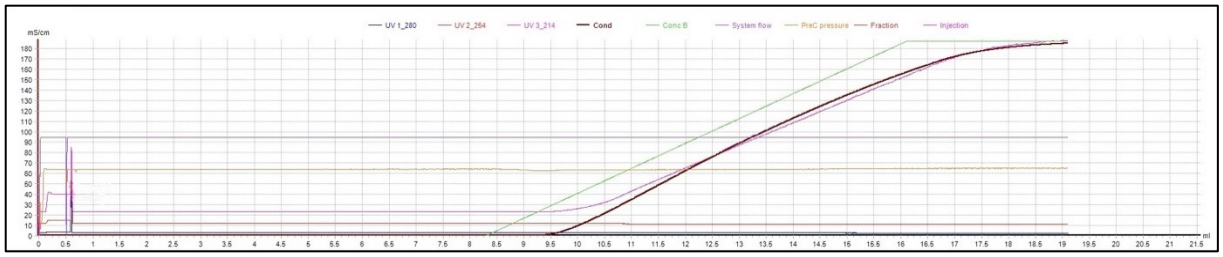

Figure 20 Filtrate after 5. Washing Cycle**; ÄKTA conductivity spectrums of **Mock Synthesis and Purification 2.2

in HEPES buffer; ÄKTA UV measurement (280 blue, 214 red and 254 pink nm); green line shows increasing salt concentration and brown line in correlation to the green line shows conductivity; solid phase: Macro-Prep High S Media; ÄKTA setting described in ***Table 8***

The yields shown in ***Table 26*** and ***Figure 21*** indicate a substantial loss of product associated with increasing numbers of washing cycles. After five washing cycles, the product loss was 46% higher than in the polymer subjected to only a single washing step. After these findings, the next step as a consequence was the comparison of conductivity between 1-time washed and 5-times washed polymer in correlation to its respective yield. This would then allow a sound decision regarding how many washing cycles should be performed during desalting to ensure low salt concentrations with reasonable amounts of product.

Table 26 *Comparison of yields after Centrifugal Filtration of ÄKTA-purified LPEI10kDa in Mock Synthesis and Purification 2.2 performing different amounts of washing cycles; yields were calculated in regards to applied amount of polymer at the beginning of desalting*

Applied amount of LPEI [mg]	LPEI amount after concentration [mg]	Washing Cycles performed	Amount of LPEI after washing cycles [mg]	Yield [%]	Loss in Filtrate [%]
19,83	16,78	1	13,55	68,3	31,7
2 mL	2,64	5	2,77	21,92	78,08

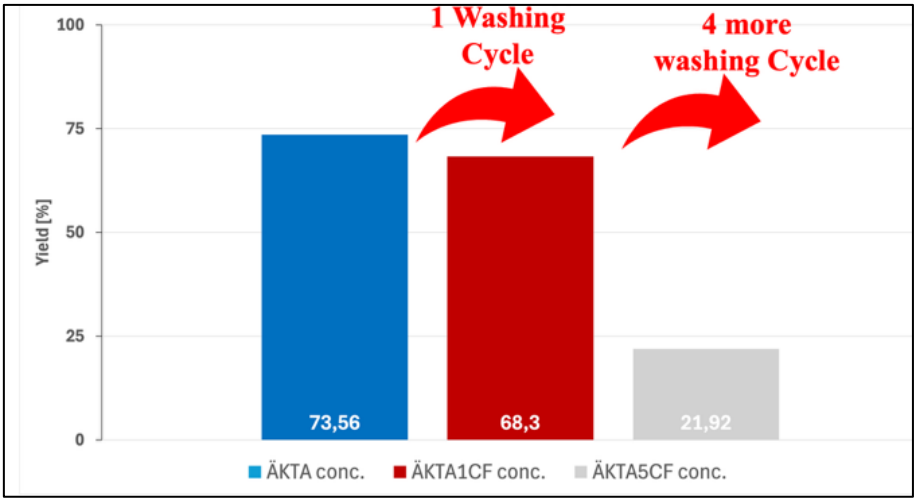

Figure 21 *Comparison of yields after Centrifugal Filtration of CEX-purified LPEI10kDa in Mock Synthesis and Purification 2.2 performing different amounts of washing cycles; yields were calculated in regards to applied amount of polymer at the beginning of desalting*

6.1.2.4 Mock Synthesis and Purification 3

A third mock synthesis and purification was performed to evaluate the agreement between the weighed amount of LPEI and the amount calculated from the copper assay, quantify LPEI yield losses associated with repeated centrifugal filter washing cycles, and compare the residual salt concentrations in fraction 2 and retentates subjected to one versus five washing cycles. Again, as part of the CEX fraction 1 (30 mL) and of fraction 2 (29,5 mL) were collected (***Figure 22***). After calculation of the LPEI contents in each fraction shown in ***Table 27***, it can be concluded that LPEI loss has been successfully reduced to an amount which does not need to be considered for further ÄKTA purifications. However, a difference in the weighed amount of LPEI and spectrophotometrically assessed amount of LPEI via copper assay, most likely as a result of method difference, was also observed.

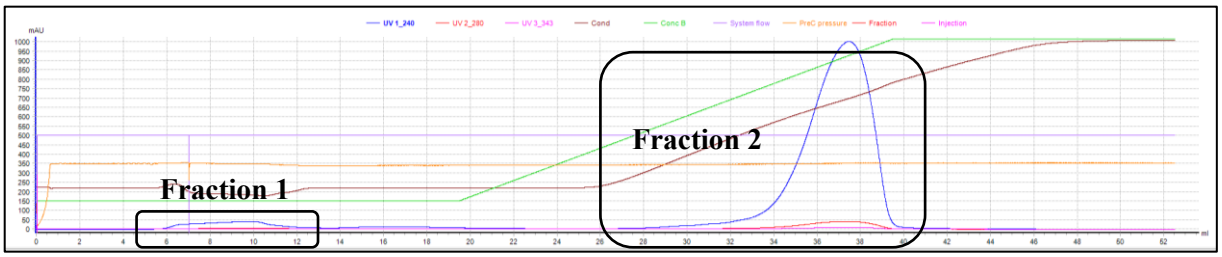

Figure 22 *Cation exchange chromatography diagram from* ***Run 1/2 of LPEI10kDa-Mock Synthesis and Purification 3*** *in HEPES buffer. 5ml of crude polymer was injected and subjected to chromatographic separation by ÄKTA. Y-axis plots milli-Absorbance-Units and UV measurements are shown in colored lines (240nm blue, 280nm red and 343nm pink nm); blue line represents detected LPEI. Solid phase used was Macro-Prep High S Media and ÄKTA settings are described in* ***Table 7****; please note that the diagram of the second run* ***(2/2)*** *is listed in the Appendix*

Table 27 *Yields after ÄKTA purification of Mock Synthesis 3 calculated via Copper Assay*

Weighed amount of LPEI [mg]	Redetermined amount of LPEI* [mg]	Fraction	Concentration of LPEI after CEX [µg/mL]	Content of LPEI after CEX [mg]	Yield after CEX [%]
50,09	48,1	Fraction 1	5,54	0,17	0,35
		Fraction 2	1419,8	41,88	87,08

**LPEI content determined in the crude polymer as described in 5.2.3.1.3 via copper assay*

The conductivity graphs from the filtrates (***Figure 24***) of each washing cycle validate the results from 6.1.2.3 and as for the fraction 2 (***Figure 23***) and retentates (***Figure 25*** *and* ***Figure 26***) the following has been shown: 1-time washing of ÄKTA-purified LPEI led to a reduction of 88% in AUC of the conductivity whereas, 5-times washed LPEI led to further reduction 63% in AUC of the conductivity.

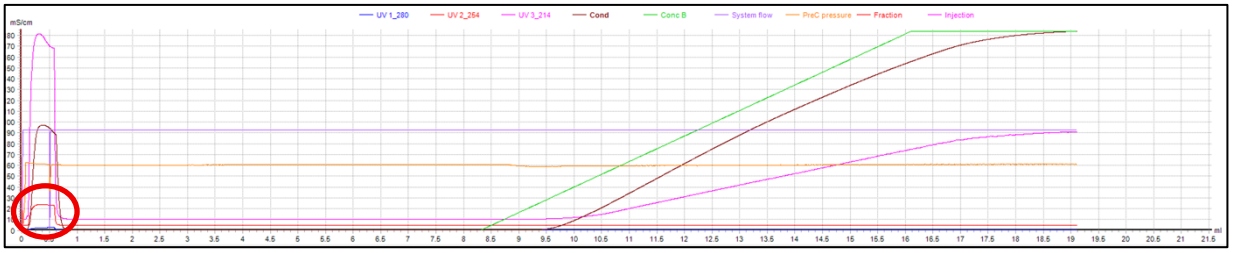

Figure 23 Fraction 2*; ÄKTA conductivity spectrums of* ***Mock Synthesis and Purification 3*** *in HEPES buffer; 0,5ml of sample was injected and subjected to conductivity measurement by ÄKTA. Y-axis plots conductivity and UV measurements are shown in colored lines (280nm blue, 214nm red and 254nm pink); blue line represents detected LPEI. Solid phase used was Macro-Prep High S Media and ÄKTA settings are described in ÄKTA* ***Table 8****; AUC of the marked section: 43,9 mL*mS/cm*

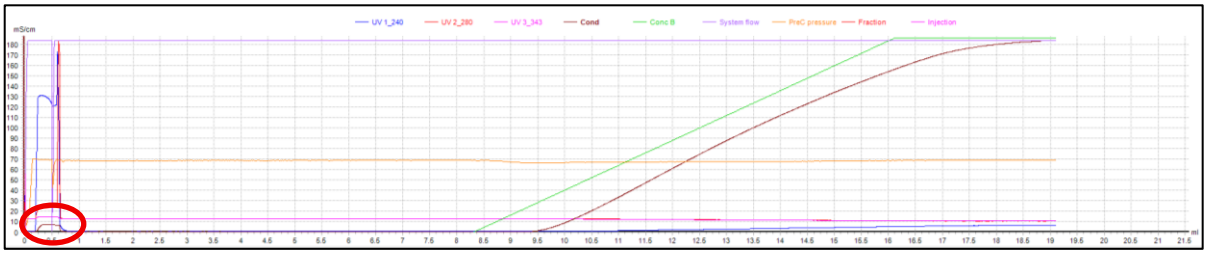

Figure 24 Filtrate after 1. Washing Cycle*; ÄKTA conductivity spectrums of* ***Mock Synthesis and Purification 3*** *in HEPES buffer; ÄKTA UV measurement (240 blue, 280 red and 343 pink nm); green line shows increasing salt concentration and brown line in correlation to the green line shows conductivity; solid phase: Macro-Prep High S Media; ÄKTA setting described in* ***Table 8****; please note that the spectrums of the filtrates after 2-5 washing cycles are listed in the Appendix*

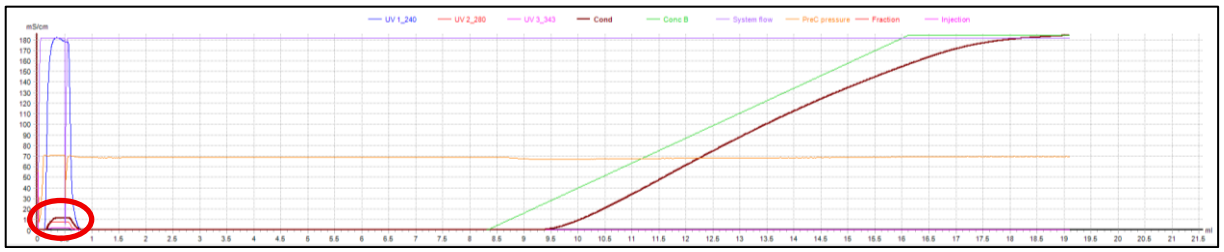

***Figure 25 Retentate after 1. Washing Cycle**; ÄKTA conductivity spectrums of **Mock Synthesis and Purification 3** in HEPES buffer; ÄKTA UV measurement (240 blue, 280 red and 343 pink nm); green line shows increasing salt concentration and brown line in correlation to the green line shows conductivity; solid phase: Macro-Prep High S Media; ÄKTA setting described in **Table 8**; AUC of the marked section: 5,21 mL*mS/cm*

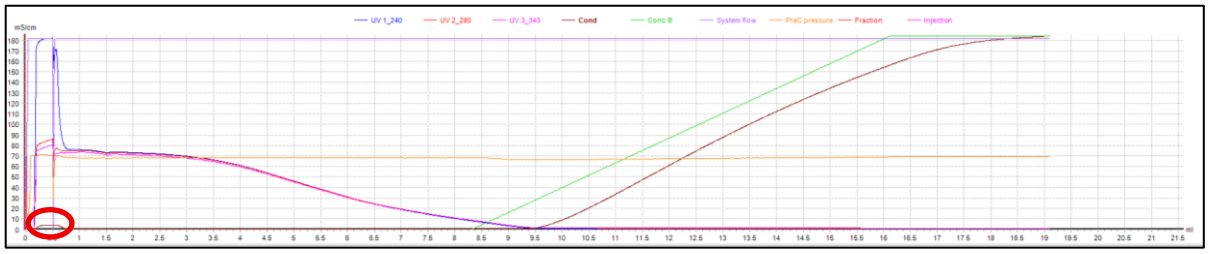

***Figure 26 Retentate after 5. Washing Cycle**; ÄKTA conductivity spectrums of **Mock Synthesis and Purification 3** in HEPES buffer; ÄKTA UV measurement (240 blue, 280 red and 343 pink nm); green line shows increasing salt concentration and brown line in correlation to the green line shows conductivity; solid phase: Macro-Prep High S Media; ÄKTA setting described in **Table 8**; AUC of the marked section: 1,91 mL*mS/cm*

A yield difference of 43% has been identified between the 1-time washed and 5-times washed polymer. With this last mock synthesis and purification, the results of 6.1.2.3 have also been validated in regards of yield difference between the 1-time and 5-time washed polymer, thus, the decision was made to set 1-time washing as part of desalting using centrifugal filters as a standard.

***Table 28** Comparison of yields after Centrifugal Filtration of ÄKTA-purified LPEI10kDa in Mock Synthesis 3 performing different amounts of washing cycles; yields were calculated in regards to applied amount of polymer at the beginning of desalting*

Applied amount of LPEI [mg]	LPEI amount after concentration [mg]	Washing Cycles performed	Amount of LPEI after washing cycles [mg]	Yield [%]	Loss in Filtrate [%]
20,74	14,91	1	12,08	81,03	19,97
20,74	16,66	5	6,36	38,17	61,83

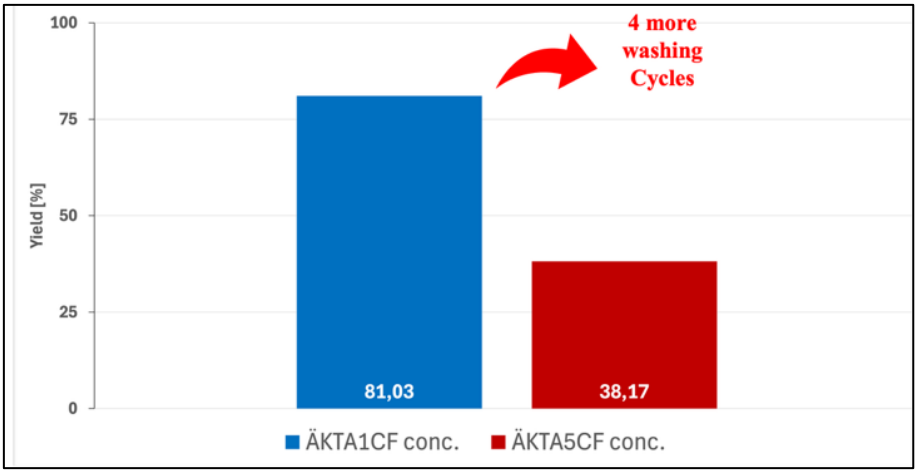

***Figure 27** Comparison of yields after Centrifugal Filtration of CEX-purified LPEI 10kDa in Mock Synthesis 3 performing different amounts of washing cycles; yields were calculated in regards to applied amount of polymer at the beginning of desalting*

6.1.2.5 Discussion – Mock Syntheses and Purifications 1-3

Key findings from mock syntheses and purifications 1-3 indicated that centrifugal filtration purification resulted in a significant loss of yield, with yield decreasing as the number of washing cycles increased. Smaller centrifugal filters provided higher yields compared with larger filters, although their applicability was limited by lower processing volumes. Five washing cycles resulted in a 47% greater yield loss compared with a single washing cycle, an effect that was independently confirmed in the third mock syntheses and purification by an observed 43% higher yield loss. After three washing cycles, residual salt in the filtrate was no longer detectable by conductivity measurements. A single washing cycle achieved an 88.13% reduction in salt concentration, whereas five washing cycles led to an additional 63.34% reduction in salt content in the retentate. Furthermore, the experimentally weighed amount of LPEI did not correspond to the amount calculated using the copper assay. All these findings made during mock syntheses and purification 1-3 described above led to the establishment of a final protocol for the bi-/tri-conjugate CEX purification and subsequent desalting via centrifugal filtration described in 5.2.4 - 5.2.7.

6.1.3 Synthesis of the LPEI-PEG-OPSS bi-conjugate

The synthesis of the bi-conjugate was executed as described in 5.2.4.

6.1.4 Purification of the LPEI-PEG-OPSS Bi-Conjugate

All insights gained from mock syntheses one to three made the basis for the real bi-/tri-conjugate synthesis procedure: CEX with the ÄKTA-system was performed using high dilutions of the crude conjugate, the LPEI content was redetermined via copper assay prior CEX and desalting using centrifugal filters included just one washing cycle.

6.1.4.1 ÄKTA Purification of LPEI-PEG-OPSS

The redetermination of LPEI content in the crude conjugate prior CEX demonstrated the high variability between weighed and spectrophotometrically assessed polymer amount (***Table 29***): for synthesis 1 164,43 mg were determined instead of the weighed 200 mg and 188,3 mg instead of 200 mg for synthesis 2. As part of the first synthesis, 67 mL of fraction 2 were collected from ÄKTA runs 1-4 (***Figure 28***) which was utilized for centrifugal filtration purification and 27 mL of fraction 2 from ÄKTA runs 5-7 (***Figure 29***) which was used for dialysis purification. For the second synthesis, 40 mL of fraction 2 each were used for centrifugal filtration (***Figure 30***) and dialysis (***Figure 31***) purification. In contrast to the mock syntheses and purification, fraction 1 of the bi-conjugates exhibited higher absorbance signals. This increase can be attributed to the presence of cleaved succinimide species in addition to the loss of LPEI. Furthermore, modifications to the ÄKTA gradient duration resulted in earlier elution and higher absorbance profiles.

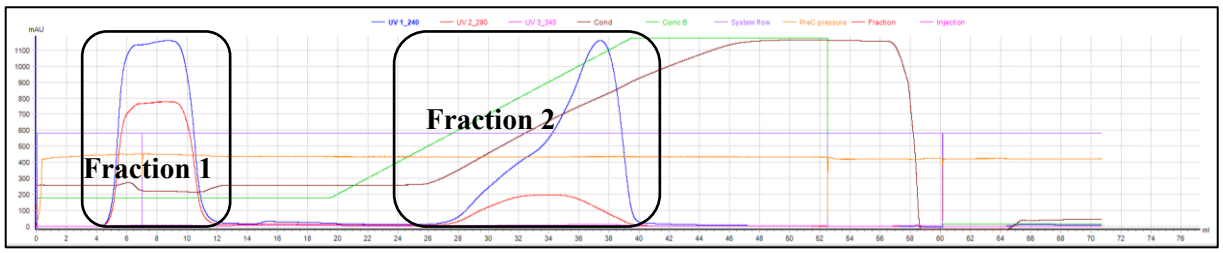

Figure 28 *Cation exchange chromatography diagram from* ***Run 1/8 of LPEI-PEG-OPSS Synthesis 1*** *in HEPES buffer. 5ml of crude polymer was injected and subjected to chromatographic separation by ÄKTA. Y-axis plots milli-Absorbance-Units and UV measurements are shown in colored lines (240nm blue, 280nm red and 343nm pink nm); blue line represents detected LPEI. Solid phase used was Macro-Prep High S Media and ÄKTA settings are described in* ***Table 7****;* ***Fraction 2 subject to Centrifugal Filtration Purification****; please note that the diagrams of the remaining runs (****2-4 and 6-8****) are listed in the Appendix*

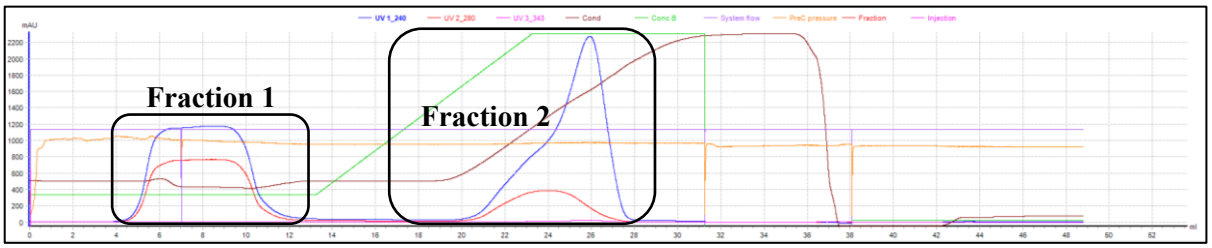

Figure 29 *Cation exchange chromatography diagram from* ***Run 5/8 of LPEI-PEG-OPSS Synthesis 1*** *in HEPES buffer. 5ml of crude polymer was injected and subjected to chromatographic separation by ÄKTA. Y-axis plots milli-Absorbance-Units and UV measurements are shown in colored lines (240nm blue, 280nm red and 343nm pink nm); blue line represents detected LPEI. Solid phase used was Macro-Prep High S Media and ÄKTA settings are described in* ***Table 11****;* ***Fraction 2 subject to Dialysis Purification****; please note that the diagrams of the remaining runs (****2-4 and 6-8****) are listed in the Appendix*

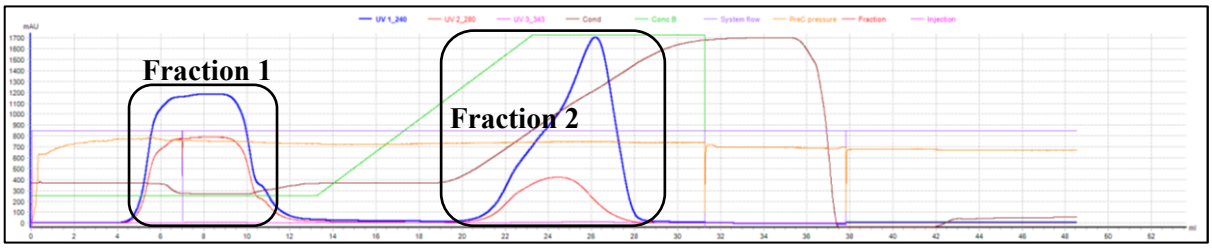

Figure 30 *Cation exchange chromatography diagram from* ***Run 1/8 of LPEI-PEG-OPSS Synthesis 2*** *in HEPES buffer. 5ml of crude polymer was injected and subjected to chromatographic separation by ÄKTA. Y-axis plots milli-Absorbance-Units and UV measurements are shown in colored lines (240nm blue, 280nm red and 343nm pink nm); blue line represents detected LPEI. Solid phase used was Macro-Prep High S Media and ÄKTA settings are described in* ***Table 11****;* ***Fraction 2 subject to Centrifugal Filtration Purification****; please note that the diagrams of the remaining runs (****2-4****) are listed in the Appendix*

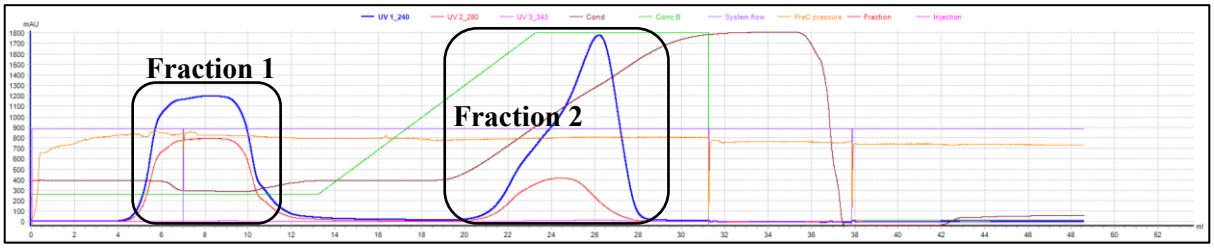

Figure 31 *Cation exchange chromatography diagram from* ***Run 5/8 of LPEI-PEG-OPSS Synthesis 2*** *in HEPES buffer. 5ml of crude polymer was injected and subjected to chromatographic separation by ÄKTA. Y-axis plots milli-Absorbance-Units and UV measurements are shown in colored lines (240nm blue, 280nm red and 343nm pink nm); blue line represents detected LPEI. Solid phase used was Macro-Prep High S Media and ÄKTA settings are described in* ***Table 11****;* ***Fraction 2 subject to Dialysis Purification****; please note that the diagrams of the remaining runs (****6-8****) are listed in the Appendix*

6.1.4.2 Desalting of LPEI-PEG-OPSS

The desalting results of the LPEI-bi-conjugate shown in ***Table 29*** and ***Figure 33*** highlight the significant difference in yield and molar ratio. In both syntheses a difference of approximately 30% is observed in regards of yield, suggesting a reproducible difference of the desalting methods. In the aspect of molar ratio, a trend is observed suggesting that bi-conjugates desalted via centrifugal filtration result in a higher OPSS to LPEI ratio. Comparing the conductivity measurements of centrifugally filtered LPEI (***Figure 25***, section 6.1.2.4) with those of the dialyzed LPEI bi-conjugate (***Figure 32***) demonstrates that dialysis provides an approximately 10,9-fold enhancement in desalting performance.

Table 29 *Comparison of yields after Desalting via Centrifugal Filtration and Dialysis of ÄKTA-purified LPEI-PEG-OPSS; yields were calculated in regards to applied amount of polymer at the beginning of desalting*

Synthesis	Weighed amount of LPEI [mg]	Redetermined amount of LPEI⁺ [mg]	Purification method	Yield of LPEI-PEG-OPSS [mg]	OPSS:LPEI molar ratio*
Synthesis 1	200	164,5	Centrifugal Filtration	49,88	0,84
			Dialysis	53,67	0,67
Synthesis 2	200	188,3	Centrifugal Filtration	41,53	1,21
			Dialysis	71,66	0,76

**Calculated as described in 5.2.2.3*
⁺LPEI content determined in the crude conjugate as described in 5.2.3.1.3 via copper assay

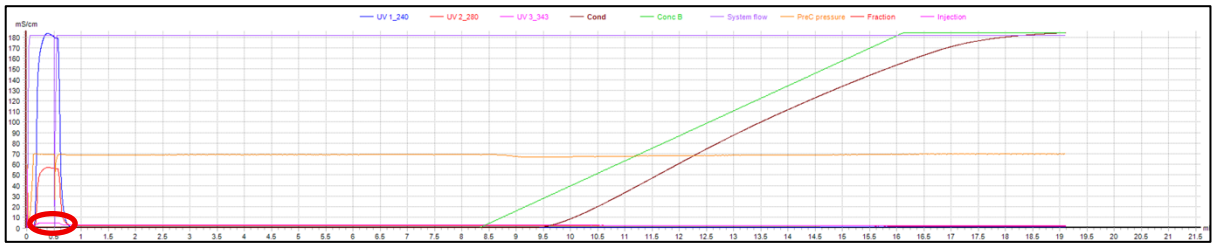

Figure 32 *ÄKTA conductivity spectrums of* ***Dialyzed Bi-Conjugate from Synthesis 1*** *in HEPES buffer; 0,5ml of sample was injected and subjected to conductivity measurement by ÄKTA. Y-axis plots conductivity and UV measurements are shown in colored lines (280nm blue, 214nm red and 254nm pink); blue line represents detected LPEI. Solid phase used was Macro-Prep High S Media and ÄKTA settings are described in ÄKTA* ***Table 8****; AUC of the marked section: 0,48 mL*mS/cm*

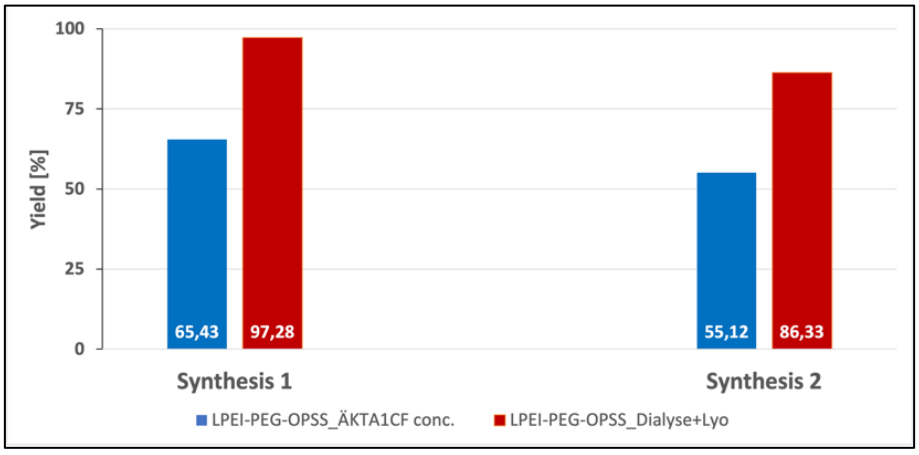

Figure 33 *Yields of bi-conjugates compared according to the desalting method utilized; Yields were calculated in regards to the applied amount of LPEI onto the filters*

6.1.4.3 Discussion – LPEI-PEG-OPSS Bi-Conjugate Synthesis and Purification

Methodological consistency proved to be critical, as discrepancies were observed between the weighed amounts of LPEI and the concentrations determined by the copper assay, directly affecting subsequent yield calculations. Reducing the gradient duration by half significantly improved process efficiency in terms of both time and eluent consumption; however, this modification also led to earlier elution and increased absorbance of the bi-conjugate during purification. Desalting by dialysis demonstrated superior performance with respect to both yield and salt removal efficiency. In contrast, centrifugally purified bi-conjugates exhibited higher OPSS:LPEI molar ratios.

6.1.5 Synthesis of the LPEI-PEG-CYS Tri-Conjugate

As described in 5.2.6 the coupling of the L-cysteine to the LPEI-PEG was monitored via spectrophotometer measurement. As ***Table 30*** and ***Table 31*** show, the coupling of the amino-acid is completed within the first minute after addition to the bi-conjugate solution.

Table 30 *Online Monitoring of L-Cysteine-Coupling during Synthesis 1; Absorption of split off 2-Thiopyridone measured at 343 nm; Blank/t=0 = LPEI-PEG-OPSS diluted in 20 mM HEPES + 10% v/v acetonitrile to a final concentration of 4-5 mg/mL and purged with argon gas*

LPEI-PEG-CYS for Centrifugal Filtration		LPEI-PEG-CYS for Dialysis	
Time [min]	**Absorption**	**Time [min]**	**Absorption**
0	0,087	0	0,186
+1	2,088	+1	2,140
+5	2,096	+5	2,138
+5	2,073	+5	2,137
+10	2,084	+10	2,131
+9	2,089	+9	2,119

Table 31 *Online Monitoring of L-Cysteine-Coupling during Synthesis 2; Absorption of split off 2-Thiopyridone measured at 343 n; Blank/t=0 = LPEI-PEG-OPSS diluted in 20 mM HEPES + 10% v/v acetonitrile to a final concentration of 4-5 mg/mL and purged with argon gas*

LPEI-PEG-CYS for Centrifugal Filtration		LPEI-PEG-CYS for Dialysis	
Time [min]	**Absorption**	**Time [min]**	**Absorption**
0	0,075	0	0,067
+1	2,113	+1	2,029
+5	2,113	+5	2,006
+15	2,104	+15	2,024
+10	2,103	+10	2,024

6.1.6 Purification of the LPEI-PEG-CYS Tri-Conjugate

Again, all insight gained from mock syntheses one to three made the basis for the actual tri-conjugate synthesis procedure: CEX purification was performed using high dilutions of the crude tri-conjugate and desalting using centrifugal filters included just one washing cycle.

6.1.6.1 ÄKTA Purification of LPEI-PEG-CYS

During the first synthesis, fraction 2 from ÄKTA runs 1-2 (20 mL) (***Figure 34***) were collected for purification by centrifugal filtration, and fraction 2 from ÄKTA run 3 (10 mL) (***Figure 35***) was used for dialysis. For the second synthesis, 10 mL of fraction 2 was processed by centrifugal filtration (***Figure 36***), while another 20 mL of fraction 2 underwent purification by dialysis (***Figure 37***). Inspection of the CEX chromatograms shows that the absorbance of fraction 1 is less pronounced, as it predominantly contains 2-thiopyridone and only negligible amounts of dissociated LPEI.

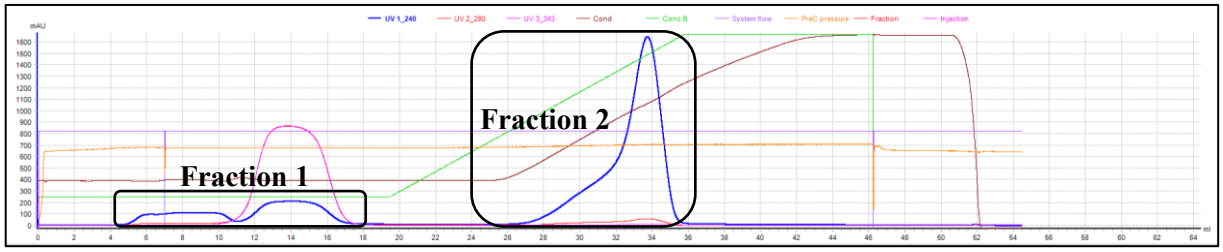

Figure 34 *Cation exchange chromatography diagram from* ***Run 1/2 of LPEI-PEG-CYS Synthesis 1 produced from centrifugally filtered Bi-Conjugate*** *in HEPES buffer. 5ml of crude polymer was injected and subjected to chromatographic separation by ÄKTA. Y-axis plots milli-Absorbance-Units and UV measurements are shown in colored lines (240nm blue, 280nm red and 343nm pink nm); blue line represents detected LPEI. Solid phase used was Macro-Prep High S Media and ÄKTA settings are described in* ***Table 16****;* ***Fraction 2 subject to Centrifugal Filtration Purification****; please note that the diagram of the remaining run (2) is listed in the Appendix*

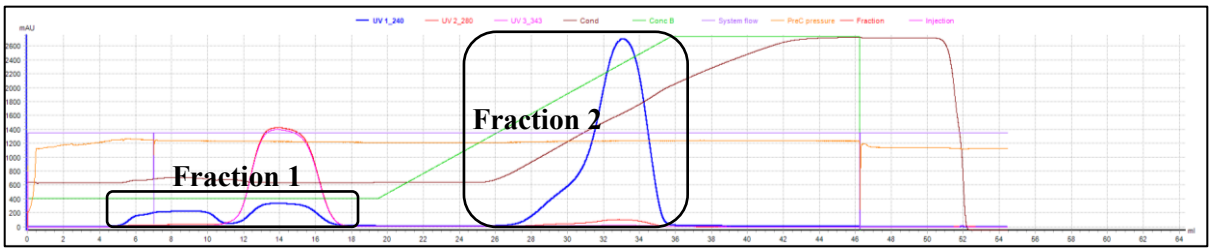

Figure 35 *Cation exchange chromatography diagram from* ***Run 1 of LPEI-PEG-CYS Synthesis 1 produced from dialyzed Bi-Conjugate*** *in HEPES buffer. 5ml of crude polymer was injected and subjected to chromatographic separation by ÄKTA. Y-axis plots milli-Absorbance-Units and UV measurements are shown in colored lines (240nm blue, 280nm red and 343nm pink nm); blue line represents detected LPEI. Solid phase used was Macro-Prep High S Media and ÄKTA settings are described in* ***Table 16****;* ***Fraction 2 subject to Dialysis Purification***

Figure 36 *Cation exchange chromatography diagram from* ***Run 1/2 of LPEI-PEG-CYS Synthesis 2 produced from centrifugally filtered Bi-Conjugate*** *in HEPES buffer. 5ml of crude polymer was injected and subjected to chromatographic separation by ÄKTA. Y-axis plots milli-Absorbance-Units and UV measurements are shown in colored lines (240nm blue, 280nm red and 343nm pink nm); blue line represents detected LPEI. Solid phase used was Macro-Prep High S Media and ÄKTA settings are described in* ***Table 16****;* ***Fraction 2 subject to Centrifugal Filtration Purification***

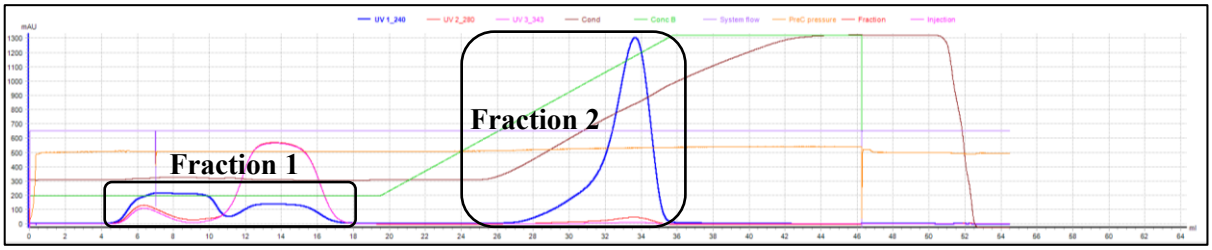

Figure 37 *Cation exchange chromatography diagram from* ***Run 1/2 of LPEI-PEG-CYS Synthesis 2 produced from dialyzed Bi-Conjugate*** *in HEPES buffer. 5ml of crude polymer was injected and subjected to chromatographic separation by ÄKTA. Y-axis plots milli-Absorbance-Units and UV measurements are shown in colored lines (240nm blue, 280nm red and 343nm pink nm); blue line represents detected LPEI. Solid phase used was Macro-Prep High S Media and ÄKTA settings are described in* ***Table 16****;* ***Fraction 2 subject to Dialysis Purification****; please note that the diagram of the remaining run (****2****) is listed in the Appendix*

6.1.6.2 Desalting of LPEI-PEG-CYS

Figure 38 resemble the results from the bi-conjugate desalting-process showcased in 6.1.4.2 in regards to the yield and molar ratio: again, the dialyzed product had a higher yield whereas the molar ratio is seen to be higher in the centrifugal filtered conjugate.

Table 32 *Comparison of yields after Desalting via Centrifugal Filtration and Dialysis of ÄKTA-purified LPEI-PEG-CYS; yields were calculated in regards to applied amount of polymer at the beginning of desalting*

Synthesis	Purification method	Used amount of LPEI-PEG-OPSS [mg]	Yield of LPEI-PEG-CYS [mg]	CYS:LPEI molar ratio*
Synthesis 1	Centrifugal Filtration	49,88	21,17	2,50
	Dialysis	53,67	30,55	0,67
Synthesis 2	Centrifugal Filtration	20,77	10,63	2,11
	Dialysis	35,83	24,67	1,04

**Calculated as described in 5.2.2.3*

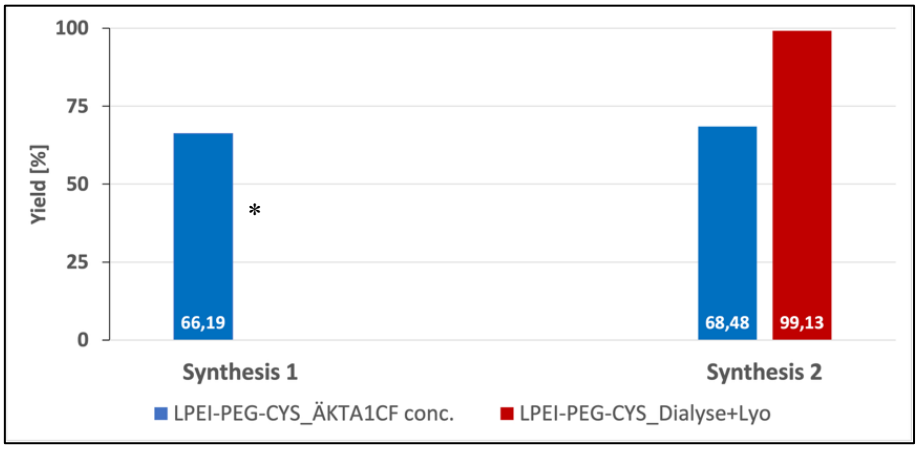

Yield calculation for the dialyzed tri-conjugate could not be performed since sampling was forgotten, however, similar relations to **Figure 33 can be expected when looking at the results of synthesis 2*

***Figure 38** Yields of tri-conjugates compared according to the desalting method utilized; Yields were calculated in regards to the applied amount of LPEI onto the filters*

6.1.6.3 Discussion – LPEI-PEG-CYS Tri-Conjugate Synthesis and Purification

The tri-conjugate synthesis yielded results comparable to those observed for the bi-conjugate synthesis with respect to the evaluation of the two desalting methods. While the molar ratios of the dialyzed tri-conjugate remained similar to those of the corresponding bi-conjugate, the centrifugally purified tri-conjugate exhibited even higher molar ratios suggesting a method depended effect.

6.1.7 DLS Characterization

The DLS characterization included the assessment of size of the polyplexes in the means of Z-average, as well as, the polydispersity as an indicator for homogeneity.

6.1.7.1 LPEI-pDNA-Polyplexes

This section elaborates the results from DLS measurements of LPEI 10 kDa with 40 and 10 µg/mL GLuc-pDNA. For each concentration N/P ratios 12 and 120 were assessed. Data analysis was restricted to measurements that fulfilled the quality criteria as per the DLS expert advice.

6.1.7.1.1 LPEI10kDa-pDNA-Polyplexes with a pDNA concentration of 40 µg/mL

The results from the DLS measurements shown in ***Table 33*** and ***Table 34*** (***Figure 39*** and ***Figure 40***) emphasize that higher N/P ratios using LPEI 10 kDa in combination with 40 µg/mL pDNA and higher dilutions result in smaller polyplexes. Since the PDIs are below 0,3, as explained in 3.3.3, the results can be considered as valid.

Table 33** Z-Average and Polydispersity-Index-Results from LPEI/pDNA-Polyplexes using 40 µg/mL pDNA assessed using DLS; DLS settings as described in **Table 19

N/P ratio	Dilution	Experiment 1		Experiment 2		Experiment 3	
		Z-Average	PDI	Z-Average	PDI	Z-Average	PDI
12	1:4	130,500	0,217	70,425	0,151	98,200	0,227
	1:10	121,550	0,247	107,060	0,262	148,975	0,209
120	1:4	125,950	0,181	118,200	0,220	89,618	0,259
	1:10	114,000	0,216	83,443	0,287	107,450	0,247

Table 34** Z-Average and Polydispersity-Index-Results averaged from all 3 LPEI/pDNA-Polyplex-DLS measurements; DLS settings as described in **Table 19

N/P ratio	Dilution	Average of all 3 experiments	
		Z-Average	PDI
12	1:4	99,708	0,198
	1:10	125,862	0,239
120	1:4	111,256	0,220
	1:10	101,631	0,250

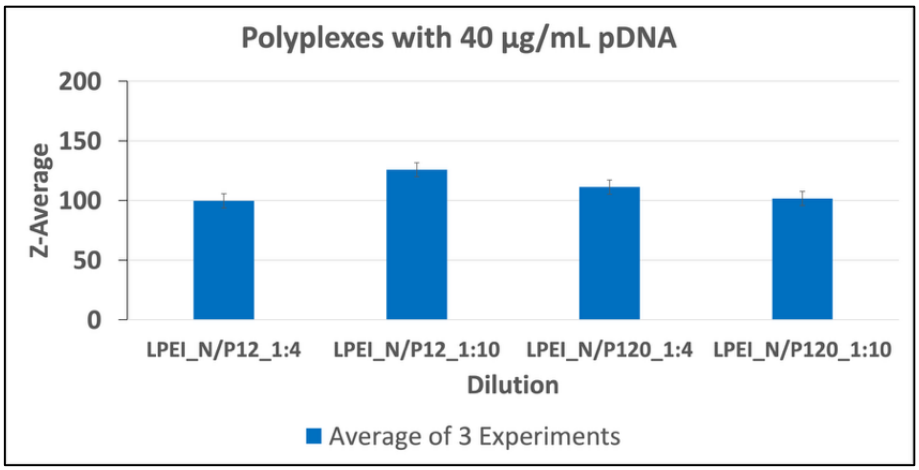

Figure 39 *DLS-Characterization; Z-Average of pDNA-polyplexes prepared with LPEI 10 kDa; numbers referring to the respective dilution used; polyplexes were prepared with a Gluc-pDNA concentration of 40 µg/mL and a N/P-ratio of 12 or 120*

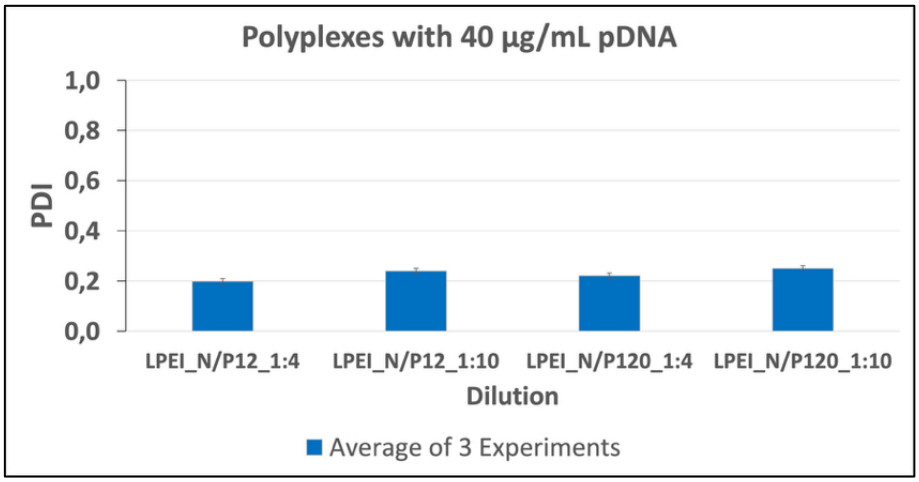

Figure 40 *DLS-Characterization; PDI of pDNA-polyplexes prepared with LPEI 10 kDa; numbers referring to the respective dilution used; polyplexes were prepared with a Gluc-pDNA concentration of 40 µg/mL and a N/P-ratio of 12 or 120*

6.1.7.1.2 LPEI10kDa-pDNA-Polyplexes with a pDNA concentration of 10 µg/mL

However, drawing conclusion from the DLS results using LPEI 10 kDa in combination with 10 µg/mL pDNA is difficult since the PDIs are mostly well above 0,3. Nonetheless, it can be stated that the Z-average is much smaller than their respective counterparts in 6.1.7.1.1.

Table 35 *Z-Average and Polydispersity-Index-Results from LPEI/pDNA-Polyplexes using 10 µg/mL pDNA assessed using DLS; DLS settings as described in* ***Table 19***

N/P ratio	Dilution	Experiment 1		Experiment 2		Experiment 3	
		Z-Average	PDI	Z-Average	PDI	Z-Average	PDI
12	1:4	69,583	0,374	100,865	0,274	104,867	0,304
	1:10	94,985	0,447	89,850	0,512	79,643	0,463
	1:40	132,950	0,608	84,223	0,863	145,650	0,407
120	1:4	84,868	0,445	88,040	0,282	89,485	0,320
	1:10	79,393	0,617	62,868	0,665	83,610	0,503
	1:40	81,490	0,944	24,965	1,000	40,283	0,799

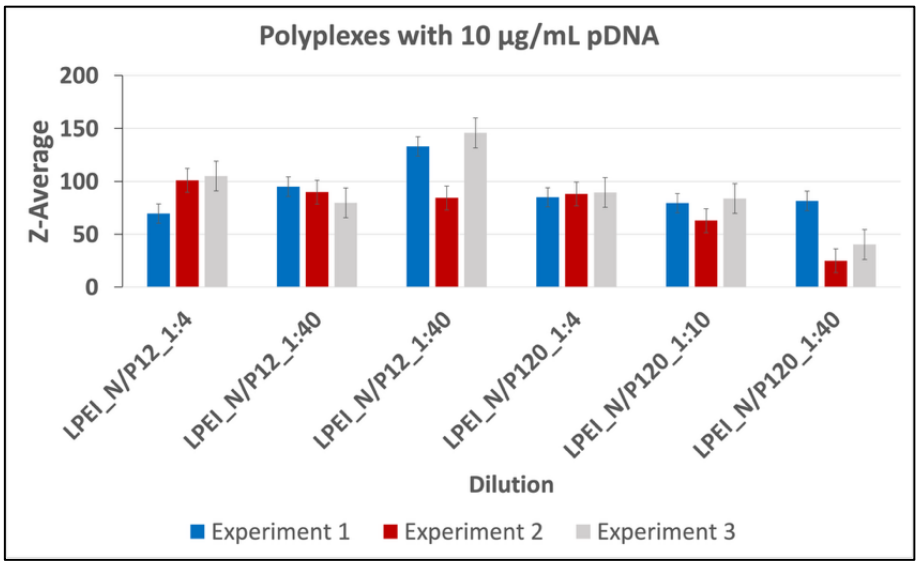

Figure 41 *DLS-Characterization; Z-Average of pDNA -polyplexes prepared with LPEI 10 kDa; numbers referring to the respective dilution used; polyplexes were prepared with a Gluc-pDNA concentration of 10 µg/mL and a N/P-ratio of 12 or 120*

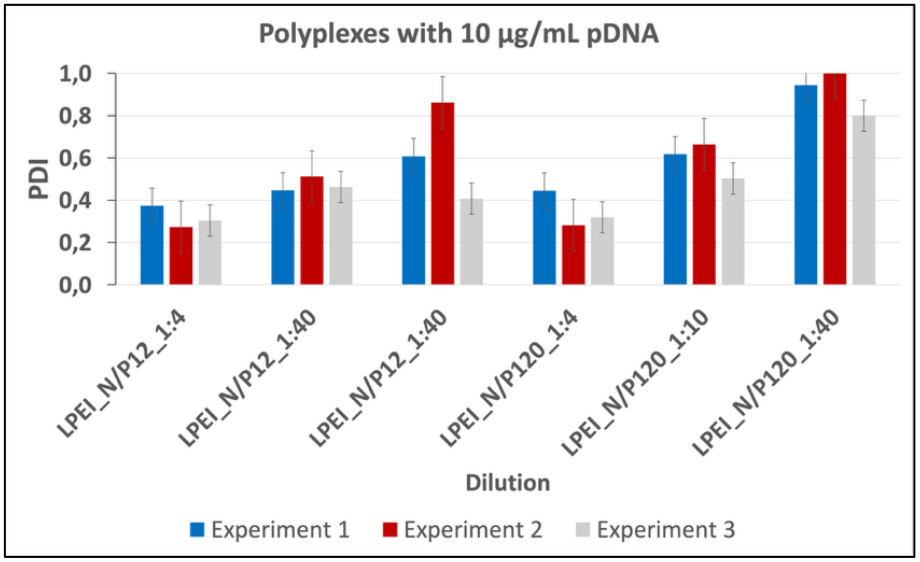

Figure 42 *DLS-Characterization; PDI of pDNA -polyplexes prepared with LPEI 10 kDa; numbers referring to the respective dilution used; polyplexes were prepared with a Gluc-pDNA concentration of 10 µg/mL and a N/P-ratio of 12 or 120*

6.1.7.2 Tri-Conjugate-mRNA-Polyplexes

This section elaborates the results from DLS measurements of LPEI 10 kDa, LPEI-PEG-CYS tri-conjugates desalted by dialysis or CF with 40 µg/mL GLuc-mRNA. For this purpose, the tri-conjugates from synthesis 2 were utilized for the purpose of tri-conjugate-mRNA-polyplexes. Data analysis was restricted to measurements that fulfilled the quality criteria as per the DLS expert advice.

6.1.7.2.1 LPEI-mRNA-Polyplexes with a N/P ratio of 12

As shown in ***Figure 43***, LPEI-mRNA polyplexes exhibited hydrodynamic diameters ranging from 100 to 150 nm, with acceptable PDIs of approximately 0,2-0,3. These results indicate efficient mRNA complexation by LPEI, as comparable particle sizes and PDIs were obtained for both dilutions and across independent experiments. In contrast, LPEI-PEG-CYS-mRNA polyplexes displayed greater variability in size. While LPC_CF showed a consistent hydrodynamic diameter of approximately 130 nm across both dilutions, LPC_D exhibited a size of approximately 70 nm at the 1:4 dilution and 135 nm at the 1:10 dilution. Moreover, the PDIs of the tri-conjugate polyplexes were predominantly above 0,3. These results suggest that PEGylation does impact polyplex homogeneity. With respect to particle size, LPEI- and LPC_CF-mRNA polyplexes showed comparable dimensions. Conversely, LPC_D-

mRNA polyplexes exhibited distinct size differences for at least one dilution, raising the question of whether the desalting method, which resulted in different CYS:LPEI molar ratios, impacts the polyplex formation process.

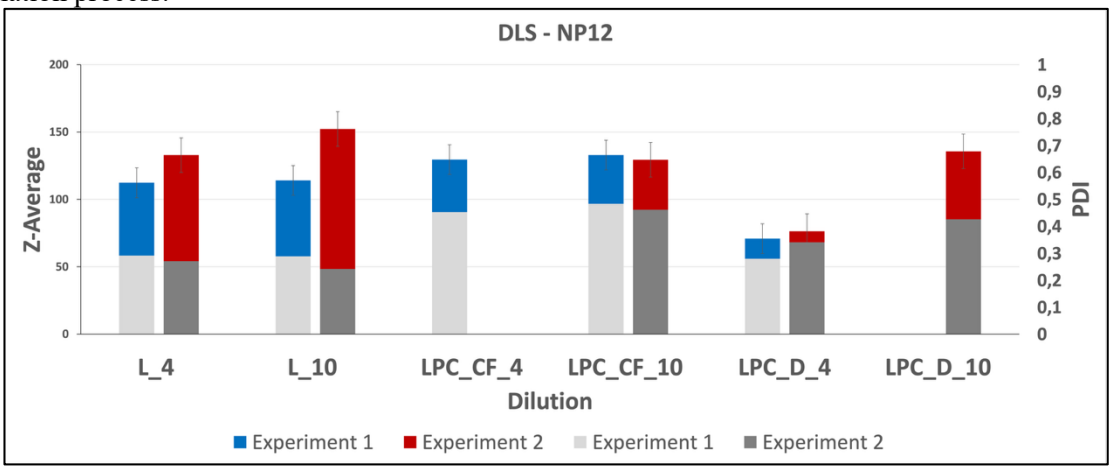

Figure 43 *DLS-Characterization of mRNA-polyplexes prepared with LPEI 10 kDa, LPC_CF and LPC_D; numbers referring to the respective dilution used; polyplexes were prepared with a Gluc-mRNA concentration of 40 µg/mL and a N/P-ratio of 12*

6.1.7.2.2 LPEI-mRNA-Polyplexes with a N/P ratio of 120

The characterization of tri-conjugate-mRNA polyplexes at a high N/P ratio of 120 was performed based on the findings reported by Herrero et al[36]. As shown in ***Figure 44***, none of the three polyplex types formed homogeneous particles, as indicated by PDIs consistently above 0,3, reflecting pronounced heterogeneity. Nevertheless, the hydrodynamic diameters ranged from 80 to 100 nm and were smaller compared with the corresponding polyplexes prepared at an N/P ratio of 12, in agreement with the observations of Herrero et al[36]. In contrast to 6.1.7.2.1, LPC_CF-mRNA polyplexes did not meet the data quality criteria recommended by the software expert advice and were therefore excluded from further analysis.

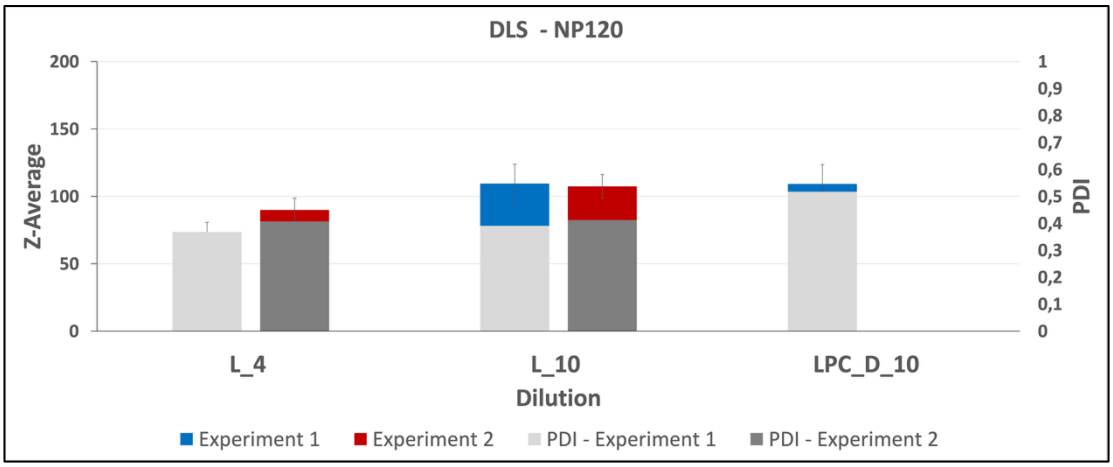

Figure 44 *DLS-Characterization of mRNA-polyplexes prepared with LPEI 10 kDa, LPC_CF and LPC_D; numbers referring to the respective dilution used; polyplexes were prepared with a Gluc-mRNA concentration of 40 µg/mL and a N/P-ratio of 120*

7 Conclusion and Outlook

The primary objectives of this study were to optimize the purification of LPEI-based tri-conjugates using cation-exchange chromatography and to compare dialysis and centrifugal filtration as desalting methods. In the process of achieving this goal, many insights have been made further optimizing the characterization of LPEI (6.1.1) as well as purification of LPEI-based conjugates (6.1.2 - 6.1.6): First, validation of the shelf-life of the copper-acetic solution used in the copper assay significantly increased the efficiency of subsequent LPEI characterization, which constituted an essential component of this project, by reducing both time and material consumption. Furthermore, the observed method variability demonstrates that the copper assay exhibits a measurable degree of variability. This variability should therefore be taken into account when applying the assay and interpreting the resulting data. With respect to the purification process, re-determination of the LPEI concentration by copper assay prior to loading onto the ÄKTA system for cation-exchange chromatography was established as a standard procedure for bi-conjugate purification (6.1.4). This step ensured greater accuracy in yield calculations by maintaining methodological consistency across the whole process. The shortening of the ÄKTA gradient times during CEX, as described in 6.1.4.1, has led to a significant increase in time efficiency and improved overall sustainability by reducing eluent buffer usage (***Figure 45***). In regards to establishing a standard procedure for desalting by centrifugal filtration, the cumulative knowledge from the mock syntheses 1-3 (6.1.2.1 - 6.1.2.4) led to the conclusion that 1 washing cycle led to significantly higher yields than 5 washing cycles while ensuring a reasonable salt concentration.

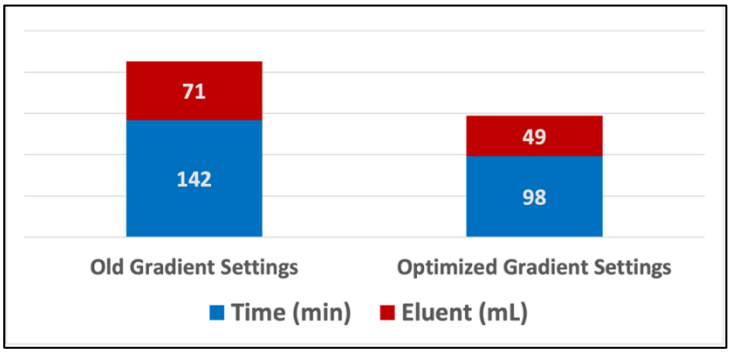

Figure 45 *Comparison of old ÄKTA gradient times as listed in* ***Table 7*** *and optimized ÄKTA gradient times as listed in* ***Table 11*** *in regards to time and eluent usage during CEX Purification*

With respect to the desalting process, the results presented and analyzed in sections 6.1.2 to 6.1.6 systematically elucidate the performance, strengths, and limitations of the respective desalting methods. When it comes to time efficiency, desalting via centrifugal filters is clearly the better method since it can be executed within a few hours, in contrast to 1,5 days when utilizing dialysis. However, the time efficiency comes with the drawback that centrifugal filtration results in lower yields (6.1.4.2 and 6.1.6.2) and has a lower desalting performance than dialysis shown in ***Figure 46*** (6.1.4.2). A significant observation made in this master's thesis was the difference in molar ratio between bi- and tri-conjugates desalted via centrifugal filtration or dialysis. Considering the results from 6.1.4.2 and 6.1.6, centrifugal filtration seems to lead to higher OPSS/CYS:LPEI ratios. One possible explanation for this might lay behind the synthesis process of LPEI with a specific molecular weight, in this case 10 kDa. The LPEI used in this study was synthesized by hydrolysis of the precursor polymer poly(2-ethyl-2-oxazoline), resulting in a heterogeneous molecular weight distribution that includes low-molecular-weight LPEI species (<10 kDa). During centrifugal filtration, centrifugal filter units with a molecular weight cut-off (MWCO) of 3 kDa were employed (***Figure 47***). Consequently, LPEI molecules with molecular weights below 3 kDa may have been lost during this purification step. Such loss would lead to an underestimation of the LPEI concentration as determined by the copper assay. This provides a plausible explanation for the higher calculated molar ratio observed for centrifugal filtration compared with dialysis, which was performed using a 1 kDa MWCO and, therefore, is less prone to the complete removal of low-molecular-weight species.

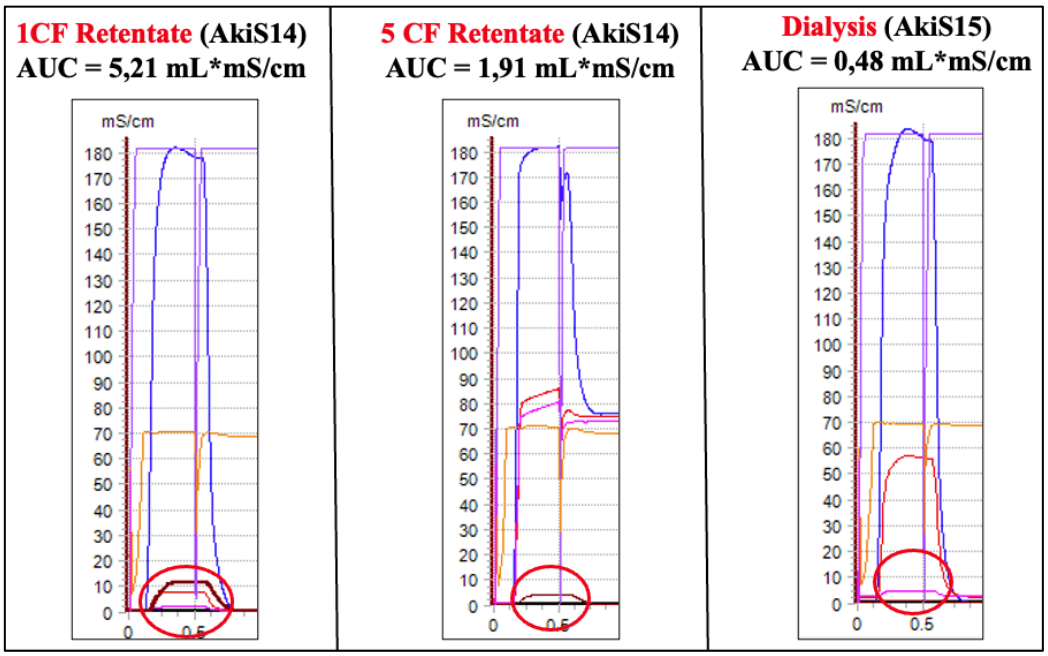

Figure 46 *Comparison of desalting performance between 1-time washed, 5-times washed and dialyzed LPEI in the aspect of conductivity measured via the ÄKTA-system as described in 5.2.3.1.4; brown line shows conductivity and is circled in red; solid phase: Macro-Prep High S Medi; AUC of the marked section: 0,48 mL*mS/cm; ÄKTA setting described in* ***Table 8****; these pictures are a zoomed in version of* ***Figure 25****,* ***Figure 26*** *and* ***Figure 32***

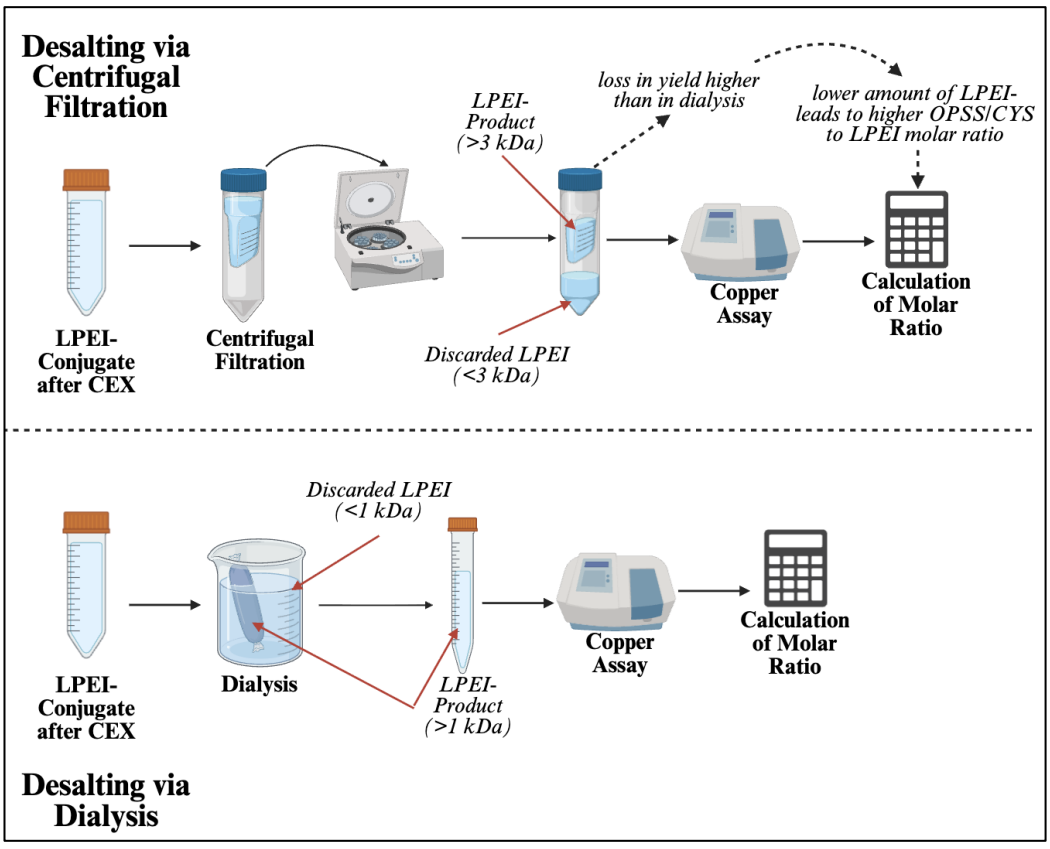

Figure 47 *Schematic illustration of the desalting processes in regards to loss of LPEI according the respective MWCO resulting in the difference in OPSS/CYS:LPEI molar ratio*

In regards to the DLS characterization, it can be concluded that higher N/P ratios generally result in smaller polyplex sizes, whereas lower pDNA concentrations are associated with increased heterogeneity. Additionally, indications of an influence of the desalting process, and potentially the resulting different CYS:LPEI molar ratio highlighted in this thesis, on the polyplex formation were observed. However, further investigations are required to draw definitive conclusions.

8 List of figures

Figure 1 Schematic illustration of the aims subject to this master's thesis; Created with BioRender.com 13

Figure 2 Schematic-Execution of the Copper Assay: Copper solution was added to the sample and the mixture was incubated for five minutes; absorption was measured at 285 nm using a spectrophotometer; created with BioRender.com.....18

Figure 3 Schematic-Execution of the DTT Assay: DTT reagent was added to the sample and the mixture was incubated for ten minutes; absorption was measured at 343 nm using a spectrophotometer; created with BioRender.com.....19

Figure 4 Schematic-Execution of the Mock Synthesis 1 as described in 5.2.3.2.1; created with BioRender.com 21

Figure 5 Schematic-Execution of the Mock Synthesis 2.1 as described in 5.2.3.2.2; F = Filtrate and R = Retentate; created with BioRender.com.....22

Figure 6 Schematic-Execution of the Mock Synthesis 3 as described in 5.2.3.2.4; F = Filtrate and R = Retentate; created with BioRender.com 23

Figure 7 Schematic-Execution of the Bi-Conjugate-Synthesis as described in 5.2.4 and 0; F = Filtrate and R = Retentate; created with BioRender.com 26

Figure 8 Schematic-Execution of the Tri-Conjugate-Synthesis as described in 5.2.6 and 5.2.7; F = Filtrate and R = Retentate; created with BioRender.com 28

Figure 9 Standard Curve of produced LPEI-Stock by measuring absorption of each dilution at 285 nm using a spectrophotometer 31

Figure 10 Comparison of 17-, 20- and 41-days old copper-acetic-buffer with freshly produced copper-acetic-buffer; measured absorption of each dilution at 285 nm using a spectrophotometer 31

Figure 11 Comparison of 4 different standard curves produced at different time points with the exact same LPEI-standard which was produced as described in 5.2.2.1.1 in regards to variation in absorption at 285 nm using a spectrophotometer; SC = Standard Curve.....32

Figure 12 Calculated variation of absorption for each dilution from all 4 standard curves shown in **Figure 11** 32

Figure 13 Cation exchange chromatography diagram from **LPEI10kDa-Mock Synthesis and Purification 1** in HEPES buffer. 5ml of crude polymer was injected and subjected to chromatographic separation by ÄKTA. Y-axis plots conductivity and UV measurements are shown in colored lines (240nm blue, 280nm red and 343nm pink nm); blue line represents detected LPEI. Solid phase used was Macro-Prep High S Media and ÄKTA settings are described in **Table 7**.....33

Figure 14 Cation exchange chromatography diagram from **Run 1/2 of LPEI10kDa-Mock Synthesis and Purification 2.1** in HEPES buffer. 5ml of crude polymer was injected and subjected to chromatographic separation by ÄKTA. Y-axis plots conductivity and UV measurements are shown in colored lines (240nm blue, 280nm red and 343nm pink nm); blue line represents detected LPEI. Solid phase used was Macro-Prep High S Media and ÄKTA settings are described in **Table 7**; please note that the diagram of the second run (**2/2**) is listed in the Appendix.....33

Figure 15 Yields after Centrifugal Filtration of CEX-purified LPEI 10 kDa in Mock Synthesis and Purification 2.1 using different sized centrifugal filters and different amounts of washing cycles; yield in regards to applied amount of polymer onto the filter.....34

Figure 16 Filtrate after 1. Washing Cycle; ÄKTA conductivity spectrums of **Mock Synthesis and Purification 2.2** in HEPES buffer; 0,5ml of sample was injected and subjected to conductivity measurement by ÄKTA. Y-axis plots conductivity and UV measurements are shown in colored lines (280nm blue, 214nm red and 254nm pink); blue line represents detected LPEI. Solid phase used was Macro-Prep High S Media and ÄKTA settings are described in ÄKTA **Table 8**..... 35

Figure 17 Filtrate after 2. Washing Cycle; ÄKTA conductivity spectrums of **Mock Synthesis and Purification 2.2** in HEPES buffer; ÄKTA UV measurement (280 blue, 214 red and 254 pink nm); green line shows increasing salt concentration and brown line in correlation to the green line shows conductivity; solid phase: Macro-Prep High S Media; ÄKTA setting described in **Table 8** 35

Figure 18 Filtrate after 3. Washing Cycle; ÄKTA conductivity spectrums of **Mock Synthesis and Purification 2.2** in HEPES buffer; ÄKTA UV measurement (280 blue, 214 red and 254 pink nm); green line shows increasing salt concentration and brown line in correlation to the green line shows conductivity; solid phase: Macro-Prep High S Media; ÄKTA setting described in **Table 8** 35

Figure 19 Filtrate after 4. Washing Cycle; ÄKTA conductivity spectrums of **Mock Synthesis and Purification 2.2** in HEPES buffer; ÄKTA UV measurement (280 blue, 214 red and 254 pink nm); green line shows increasing salt concentration and brown line in correlation to the green line shows conductivity; solid phase: Macro-Prep High S Media; ÄKTA setting described in **Table 8** 35

Figure 20 Filtrate after 5. Washing Cycle; ÄKTA conductivity spectrums of **Mock Synthesis and Purification 2.2** in HEPES buffer; ÄKTA UV measurement (280 blue, 214 red and 254 pink nm); green line shows increasing salt concentration and brown line in correlation to the green line shows conductivity; solid phase: Macro-Prep High S Media; ÄKTA setting described in **Table 8** 35

Figure 21 Comparison of yields after Centrifugal Filtration of CEX-purified LPEI10kDa in Mock Synthesis and Purification 2.2 performing different amounts of washing cycles; yields were calculated in regards to applied amount of polymer at the beginning of desalting 36

Figure 22 Cation exchange chromatography diagram from **Run 1/2 of LPEI10kDa-Mock Synthesis and Purification 3** in HEPES buffer. 5ml of crude polymer was injected and subjected to chromatographic separation by ÄKTA. Y-axis plots milli-Absorbance-Units and UV measurements are shown in colored lines (240nm blue, 280nm red and 343nm pink nm); blue line represents detected LPEI. Solid phase used was Macro-Prep High S Media and ÄKTA settings are described in **Table 7**; please note that the diagram of the second run (**2/2**) is listed in the Appendix..... 37

Figure 23 Fraction 2; ÄKTA conductivity spectrums of **Mock Synthesis and Purification 3** in HEPES buffer; 0,5ml of sample was injected and subjected to conductivity measurement by ÄKTA. Y-axis plots conductivity and UV measurements are shown in colored lines (280nm blue, 214nm red and 254nm pink); blue line represents detected LPEI. Solid phase used was Macro-Prep High S Media and ÄKTA settings are described in ÄKTA **Table 8**; AUC of the marked section: 43,9 mL*mS/cm 37

Figure 24 Filtrate after 1. Washing Cycle; ÄKTA conductivity spectrums of **Mock Synthesis and Purification 3** in HEPES buffer; ÄKTA UV measurement (240 blue, 280 red and 343 pink nm); green line shows increasing salt concentration and brown line in correlation to the green line shows conductivity; solid phase: Macro-Prep High S Media; ÄKTA setting described in **Table 8**; please note that the spectrums of the filtrates after 2-5 washing cycles are listed in the Appendix..... 37

Figure 25 Retentate after 1. Washing Cycle; ÄKTA conductivity spectrums of **Mock Synthesis and Purification 3** in HEPES buffer; ÄKTA UV measurement (240 blue, 280 red and 343 pink nm); green line shows increasing salt concentration and brown line in correlation to the green line shows conductivity; solid phase: Macro-Prep High S Media; ÄKTA setting described in **Table 8**; AUC of the marked section: 5,21 mL*mS/cm 38

Figure 26 Retentate after 5. Washing Cycle; ÄKTA conductivity spectrums of **Mock Synthesis and Purification 3** in HEPES buffer; ÄKTA UV measurement (240 blue, 280 red and 343 pink nm); green line shows increasing salt concentration and brown line in correlation to the green line shows conductivity; solid phase: Macro-Prep High S Media; ÄKTA setting described in **Table 8**; AUC of the marked section: 1,91 mL*mS/cm 38

Figure 27 Comparison of yields after Centrifugal Filtration of CEX-purified LPEI 10kDa in Mock Synthesis 3 performing different amounts of washing cycles; yields were calculated in regards to applied amount of polymer at the beginning of desalting 38

Figure 28 Cation exchange chromatography diagram from **Run 1/8 of LPEI-PEG-OPSS Synthesis 1** in HEPES buffer. 5ml of crude polymer was injected and subjected to chromatographic separation by ÄKTA. Y-axis plots milli-Absorbance-Units and UV measurements are shown in colored lines (240nm blue, 280nm red and 343nm pink nm); blue line represents detected LPEI. Solid phase used was Macro-Prep High S Media and ÄKTA settings are described in **Table 7**; **Fraction 2 subject to Centrifugal Filtration Purification**; please note that the diagrams of the remaining runs (**2-4 and 6-8**) are listed in the Appendix 39

Figure 29 Cation exchange chromatography diagram from **Run 5/8 of LPEI-PEG-OPSS Synthesis 1** in HEPES buffer. 5ml of crude polymer was injected and subjected to chromatographic separation by ÄKTA. Y-axis plots milli-Absorbance-Units and UV measurements are shown in colored lines (240nm blue, 280nm red and 343nm pink nm); blue line represents detected LPEI. Solid phase used was Macro-Prep High S Media and ÄKTA settings are described in **Table 11**; **Fraction 2 subject to Dialysis Purification**; please note that the diagrams of the remaining runs (**2-4 and 6-8**) are listed in the Appendix 40

Figure 30 Cation exchange chromatography diagram from **Run 1/8 of LPEI-PEG-OPSS Synthesis 2** in HEPES buffer. 5ml of crude polymer was injected and subjected to chromatographic separation by ÄKTA. Y-axis plots milli-Absorbance-Units and UV measurements are shown in colored lines (240nm blue, 280nm red and 343nm pink nm); blue line represents detected LPEI. Solid phase used was Macro-Prep High S Media and ÄKTA settings are described in **Table 11**; **Fraction 2 subject to Centrifugal Filtration Purification**; please note that the diagrams of the remaining runs (**2-4**) are listed in the Appendix 40

Figure 31 Cation exchange chromatography diagram from **Run 5/8 of LPEI-PEG-OPSS Synthesis 2** in HEPES buffer. 5ml of crude polymer was injected and subjected to chromatographic separation by ÄKTA. Y-axis plots milli-Absorbance-Units and UV measurements are shown in colored lines (240nm blue, 280nm red and 343nm pink nm); blue line represents detected LPEI. Solid phase used was Macro-Prep High S Media and ÄKTA settings are described in **Table 11**; **Fraction 2 subject to Dialysis Purification**; please note that the diagrams of the remaining runs (**6-8**) are listed in the Appendix 40

Figure 32 ÄKTA conductivity spectrums of **Dialyzed Bi-Conjugate from Synthesis 1** in HEPES buffer; 0,5ml of sample was injected and subjected to conductivity measurement by ÄKTA. Y-axis plots conductivity and UV measurements are shown in colored lines (280nm blue, 214nm red and 254nm pink); blue line represents detected LPEI. Solid phase used was Macro-Prep High S Media and ÄKTA settings are described in ÄKTA **Table 8**; AUC of the marked section: 0,48 mL*mS/cm 41

Figure 33 Yields of bi-conjugates compared according to the desalting method utilized; Yields were calculated in regards to the applied amount of LPEI onto the filters 41

Figure 34 Cation exchange chromatography diagram from **Run 1/2 of LPEI-PEG-CYS Synthesis 1 produced from centrifugally filtered Bi-Conjugate** in HEPES buffer. 5ml of crude polymer was injected and subjected to chromatographic separation by ÄKTA. Y-axis plots milli-Absorbance-Units and UV measurements are shown in colored lines (240nm blue, 280nm red and 343nm pink nm); blue line represents detected LPEI. Solid phase used was Macro-Prep High S Media and ÄKTA settings are described in **Table 16**; **Fraction 2 subject to Centrifugal Filtration Purification**; please note that the diagram of the remaining run (**2**) is listed in the Appendix 42

Figure 35 Cation exchange chromatography diagram from **Run 1 of LPEI-PEG-CYS Synthesis 1 produced from dialyzed Bi-Conjugate** in HEPES buffer. 5ml of crude polymer was injected and subjected to chromatographic separation by ÄKTA. Y-axis plots milli-Absorbance-Units and UV measurements are shown in colored lines (240nm blue, 280nm red and 343nm pink nm); blue line represents detected LPEI. Solid phase used was Macro-Prep High S Media and ÄKTA settings are described in **Table 16**; **Fraction 2 subject to Dialysis Purification** 43

Figure 36 Cation exchange chromatography diagram from **Run 1/2 of LPEI-PEG-CYS Synthesis 2 produced from centrifugally filtered Bi-Conjugate** in HEPES buffer. 5ml of crude polymer was injected and subjected to chromatographic separation by ÄKTA. Y-axis plots milli-Absorbance-Units and UV measurements are shown in colored lines (240nm blue, 280nm red and 343nm pink nm); blue line represents detected LPEI. Solid phase used was Macro-Prep High S Media and ÄKTA settings are described in **Table 16**; **Fraction 2 subject to Centrifugal Filtration Purification** 43

Figure 37 Cation exchange chromatography diagram from **Run 1/2 of LPEI-PEG-CYS Synthesis 2 produced from dialyzed Bi-Conjugate** in HEPES buffer. 5ml of crude polymer was injected and subjected to chromatographic separation by ÄKTA. Y-axis plots milli-Absorbance-Units and UV measurements are shown in colored lines (240nm blue, 280nm red and 343nm pink nm); blue line represents detected LPEI. Solid phase used was Macro-Prep High S Media and ÄKTA settings are described in **Table 16**; **Fraction 2 subject to Dialysis Purification**; please note that the diagram of the remaining run (**2**) is listed in the Appendix 43

Figure 38 Yields of tri-conjugates compared according to the desalting method utilized; Yields were calculated in regards to the applied amount of LPEI onto the filters 44

Figure 39 DLS-Characterization; Z-Average of pDNA-polyplexes prepared with LPEI 10 kDa; numbers referring to the respective dilution used; polyplexes were prepared with a Gluc-pDNA concentration of 40 µg/mL and a N/P-ratio of 12 or 120 45

Figure 40 DLS-Characterization; PDI of pDNA-polyplexes prepared with LPEI 10 kDa; numbers referring to the respective dilution used; polyplexes were prepared with a Gluc-pDNA concentration of 40 µg/mL and a N/P-ratio of 12 or 120..... 45

Figure 41 DLS-Characterization; Z-Average of pDNA -polyplexes prepared with LPEI 10 kDa; numbers referring to the respective dilution used; polyplexes were prepared with a Gluc-pDNA concentration of 10 µg/mL and a N/P-ratio of 12 or 120 46

Figure 42 DLS-Characterization; PDI of pDNA -polyplexes prepared with LPEI 10 kDa; numbers referring to the respective dilution used; polyplexes were prepared with a Gluc-pDNA concentration of 10 µg/mL and a N/P-ratio of 12 or 120..... 46

Figure 43 DLS-Characterization of mRNA-polyplexes prepared with LPEI 10 kDa, LPC_CF and LPC_D; numbers referring to the respective dilution used; polyplexes were prepared with a Gluc-mRNA concentration of 40 µg/mL and a N/P-ratio of 12 47

Figure 44 DLS-Characterization of mRNA-polyplexes prepared with LPEI 10 kDa, LPC_CF and LPC_D; numbers referring to the respective dilution used; polyplexes were prepared with a Gluc-mRNA concentration of 40 µg/mL and a N/P-ratio of 120 47

Figure 45 Comparison of old ÄKTA gradient times as listed in **Table 7** and optimized ÄKTA gradient times as listed in **Table 11** in regards to time and eluent usage during CEX Purification 48

Figure 46 Comparison of desalting performance between 1-time washed, 5-times washed and dialyzed LPEI in the aspect of conductivity measured via the ÄKTA-system as described in 5.2.3.1.4; brown line shows conductivity and is circled in red; solid phase: Macro-Prep High S Medi; AUC of the marked section: 0,48 mL*mS/cm; ÄKTA setting described in **Table 8**; these pictures are a zoomed in version of **Figure 25**, **Figure 26** and **Figure 32** 49

Figure 47 Schematic illustration of the desalting processes in regards to loss of LPEI according the respective MWCO resulting in the difference in OPSS/CYS:LPEI molar ratio 49

Figure 48 Cation exchange chromatography diagram from **Run 2/2 of LPEI10kDa-Mock Synthesis and Purification 2.1** in HEPES buffer. 5ml of crude polymer was injected and subjected to chromatographic separation by ÄKTA. Y-axis plots conductivity and UV measurements are shown in colored lines (240nm blue, 280nm red and 343nm pink nm); blue line represents detected LPEI. Solid phase used was Macro-Prep High S Media and ÄKTA settings are described in **Table 7**.....61

Figure 49 Cation exchange chromatography diagram from **Run 2/2 of LPEI10kDa-Mock Synthesis and Purification 3** in HEPES buffer. 5ml of crude polymer was injected and subjected to chromatographic separation by ÄKTA. Y-axis plots milli-Absorbance-Units and UV measurements are shown in colored lines (240nm blue, 280nm red and 343nm pink nm); blue line represents detected LPEI. Solid phase used was Macro-Prep High S Media and ÄKTA settings are described in **Table 7** 61

Figure 50 Filtr**ate after 2. Washing Cycle**; ÄKTA conductivity spectrums of **Mock Synthesis and Purification 3** in HEPES buffer; ÄKTA UV measurement (240 blue, 280 red and 343 pink nm); green line shows increasing salt concentration and brown line in correlation to the green line shows conductivity; solid phase: Macro-Prep High S Media; ÄKTA setting described in **Table 8** 61

Figure 51 Filtrate after 3. Washing Cycle; ÄKTA conductivity spectrums of **Mock Synthesis and Purification 3** in HEPES buffer; ÄKTA UV measurement (240 blue, 280 red and 343 pink nm); green line shows increasing salt concentration and brown line in correlation to the green line shows conductivity; solid phase: Macro-Prep High S Media; ÄKTA setting described in **Table 8** 61

Figure 52 Filtrate after 4. Washing Cycle; ÄKTA conductivity spectrums of **Mock Synthesis and Purification 3** in HEPES buffer; ÄKTA UV measurement (240 blue, 280 red and 343 pink nm); green line shows increasing salt concentration and brown line in correlation to the green line shows conductivity; solid phase: Macro-Prep High S Media; ÄKTA setting described in **Table 8** 62

Figure 53 Filtrate after 5. Washing Cycle; ÄKTA conductivity spectrums of **Mock Synthesis and Purification 3** in HEPES buffer; ÄKTA UV measurement (240 blue, 280 red and 343 pink nm); green line shows increasing salt concentration and brown line in correlation to the green line shows conductivity; solid phase: Macro-Prep High S Media; ÄKTA setting described in **Table 8** 62

Figure 54 Cation exchange chromatography diagram from **Run 2/8 of LPEI-PEG-OPSS Synthesis 1** in HEPES buffer. 5ml of crude polymer was injected and subjected to chromatographic separation by ÄKTA. Y-axis plots milli-Absorbance-Units and UV measurements are shown in colored lines (240nm blue, 280nm red and 343nm pink nm); blue line represents detected LPEI. Solid phase used was Macro-Prep High S Media and ÄKTA settings are described in **Table 7**; Fraction 2 subject to Centrifugal Filtration Purification; 62

Figure 55 Cation exchange chromatography diagram from **Run 3/8 of LPEI-PEG-OPSS Synthesis 1** in HEPES buffer. 5ml of crude polymer was injected and subjected to chromatographic separation by ÄKTA. Y-axis plots milli-Absorbance-Units and UV measurements are shown in colored lines (240nm blue, 280nm red and 343nm pink nm); blue line represents detected LPEI. Solid phase used was Macro-Prep High S Media and ÄKTA settings are described in **Table 7**; Fraction 2 subject to Centrifugal Filtration Purification; 62

Figure 56 Cation exchange chromatography diagram from **Run 4/8 of LPEI-PEG-OPSS Synthesis 1** in HEPES buffer. 5ml of crude polymer was injected and subjected to chromatographic separation by ÄKTA. Y-axis plots milli-Absorbance-Units and UV measurements are shown in colored lines (240nm blue, 280nm red and 343nm pink nm); blue line represents detected LPEI. Solid phase used was Macro-Prep High S Media and ÄKTA settings are described in **Table 7**; Fraction 2 subject to Centrifugal Filtration Purification; 63

Figure 57 Cation exchange chromatography diagram from **Run 6/8 of LPEI-PEG-OPSS Synthesis 1** in HEPES buffer. 5ml of crude polymer was injected and subjected to chromatographic separation by ÄKTA. Y-axis plots milli-Absorbance-Units and UV measurements are shown in colored lines (240nm blue, 280nm red

and 343nm pink nm); blue line represents detected LPEI. Solid phase used was Macro-Prep High S Media and ÄKTA settings are described in **Table 11**; Fraction 2 subject to Dialysis Purification; 63

Figure 58 Cation exchange chromatography diagram from **Run 7/8 of LPEI-PEG-OPSS Synthesis 1** in HEPES buffer. 5ml of crude polymer was injected and subjected to chromatographic separation by ÄKTA. Y-axis plots milli-Absorbance-Units and UV measurements are shown in colored lines (240nm blue, 280nm red and 343nm pink nm); blue line represents detected LPEI. Solid phase used was Macro-Prep High S Media and ÄKTA settings are described in **Table 11**; Fraction 2 subject to Dialysis Purification; 63

Figure 59 Cation exchange chromatography diagram from **Run 8/8 of LPEI-PEG-OPSS Synthesis 1** in HEPES buffer. 5ml of crude polymer was injected and subjected to chromatographic separation by ÄKTA. Y-axis plots milli-Absorbance-Units and UV measurements are shown in colored lines (240nm blue, 280nm red and 343nm pink nm); blue line represents detected LPEI. Solid phase used was Macro-Prep High S Media and ÄKTA settings are described in **Table 11**; Fraction 2 was not processed further due to insufficient amount of crude conjugate which was nonetheless applied 63

Figure 60 Cation exchange chromatography diagram from **Run 2/8 of LPEI-PEG-OPSS Synthesis 2** in HEPES buffer. 5ml of crude polymer was injected and subjected to chromatographic separation by ÄKTA. Y-axis plots milli-Absorbance-Units and UV measurements are shown in colored lines (240nm blue, 280nm red and 343nm pink nm); blue line represents detected LPEI. Solid phase used was Macro-Prep High S Media and ÄKTA settings are described in **Table 11**; Fraction 2 subject to Centrifugal Filtration Purification 64

Figure 61 Cation exchange chromatography diagram from **Run 3/8 of LPEI-PEG-OPSS Synthesis 2** in HEPES buffer. 5ml of crude polymer was injected and subjected to chromatographic separation by ÄKTA. Y-axis plots milli-Absorbance-Units and UV measurements are shown in colored lines (240nm blue, 280nm red and 343nm pink nm); blue line represents detected LPEI. Solid phase used was Macro-Prep High S Media and ÄKTA settings are described in **Table 11**; Fraction 2 subject to Centrifugal Filtration Purification 64

Figure 62 Cation exchange chromatography diagram from **Run 4/8 of LPEI-PEG-OPSS Synthesis 2** in HEPES buffer. 5ml of crude polymer was injected and subjected to chromatographic separation by ÄKTA. Y-axis plots milli-Absorbance-Units and UV measurements are shown in colored lines (240nm blue, 280nm red and 343nm pink nm); blue line represents detected LPEI. Solid phase used was Macro-Prep High S Media and ÄKTA settings are described in **Table 11**; Fraction 2 subject to Centrifugal Filtration Purification 64

Figure 63 Cation exchange chromatography diagram from **Run 6/8 of LPEI-PEG-OPSS Synthesis 2** in HEPES buffer. 5ml of crude polymer was injected and subjected to chromatographic separation by ÄKTA. Y-axis plots milli-Absorbance-Units and UV measurements are shown in colored lines (240nm blue, 280nm red and 343nm pink nm); blue line represents detected LPEI. Solid phase used was Macro-Prep High S Media and ÄKTA settings are described in **Table 11**; Fraction 2 subject to Dialysis Purification 64

Figure 64 Cation exchange chromatography diagram from **Run 7/8 of LPEI-PEG-OPSS Synthesis 2** in HEPES buffer. 5ml of crude polymer was injected and subjected to chromatographic separation by ÄKTA. Y-axis plots milli-Absorbance-Units and UV measurements are shown in colored lines (240nm blue, 280nm red and 343nm pink nm); blue line represents detected LPEI. Solid phase used was Macro-Prep High S Media and ÄKTA settings are described in **Table 11**; Fraction 2 subject to Dialysis Purification 65

Figure 65 Cation exchange chromatography diagram from **Run 8/8 of LPEI-PEG-OPSS Synthesis 2** in HEPES buffer. 5ml of crude polymer was injected and subjected to chromatographic separation by ÄKTA. Y-axis plots milli-Absorbance-Units and UV measurements are shown in colored lines (240nm blue, 280nm red and 343nm pink nm); blue line represents detected LPEI. Solid phase used was Macro-Prep High S Media and ÄKTA settings are described in **Table 11**; Fraction 2 subject to Dialysis Purification 65

Figure 66 Cation exchange chromatography diagram from **Run 1/2 of LPEI-PEG-CYS Synthesis 1 produced from centrifugally filtered Bi-Conjugate** in HEPES buffer. 5ml of crude polymer was injected and subjected to chromatographic separation by ÄKTA. Y-axis plots milli-Absorbance-Units and UV measurements are shown in colored lines (240nm blue, 280nm red and 343nm pink nm); blue line represents detected LPEI. Solid

phase used was Macro-Prep High S Media and ÄKTA settings are described in **Table 16**; Fraction 2 subject to Centrifugal Filtration Purification 65

Figure 67 Cation exchange chromatography diagram from **Run 2/2 of LPEI-PEG-CYS Synthesis 2 produced from dialyzed Bi-Conjugate** in HEPES buffer. 5ml of crude polymer was injected and subjected to chromatographic separation by ÄKTA. Y-axis plots milli-Absorbance-Units and UV measurements are shown in colored lines (240nm blue, 280nm red and 343nm pink nm); blue line represents detected LPEI. Solid phase used was Macro-Prep High S Media and ÄKTA settings are described in **Table 16**; Fraction 2 subject to Dialysis Purification 65

9 List of Tables

Table 1 List of used chemicals 14

Table 2 List of used materials 15

Table 3 List of used devices 16

Table 4 List of used software 16

Table 5 Dilution Table used for the Copper Assay Standard Curve 17

Table 6 Amounts of Reagents used in each Mock Synthesis and Purification 20

Table 7 ÄKTA Settings used for Mock Synthesis 1-3 and Synthesis 1 (Run 1-4) 20

Table 8 ÄKTA Settings for Conductivity Measurement 21

Table 9 Reagents used for the Bi-Conjugate Synthesis 24

Table 10 Collected Fraction 2 from ÄKTA Purification of Synthesis 1 and 2 24

Table 11 Optimized ÄKTA settings to increase time efficiency used for Synthesis 1 and 2 24

Table 12 Centrifugal Filtration of the Bi-Conjugate from Synthesis 1 and 2 25

Table 13 Dialysis and Lyophilization of the Bi-Conjugate from Synthesis 1 and 2 25

Table 14 Reagents used for the Tri-Conjugate-Synthesis 27

Table 15 Collected Fraction 1 and 2 from ÄKTA Purification of Synthesis 1 and 2 27

Table 16 ÄKTA settings for Tri-Conjugate-Synthesis 27

Table 17 Centrifugal Filtration of the Tri-Conjugate 28

Table 18 Dialysis and Lyophilization of the Tri-Conjugate 28

Table 19 Settings used for Dynamic-Light-Scattering Measurements 29

Table 20 LPEI-pDNA-Polyplex-Preparation 29

Table 21 Tri-Conjugate-Polyplex-Preparation 30

Table 22 Yields after ÄKTA Purification and Centrifugal Filtration of Mock Synthesis and Purification 1 determined via Copper Assay 33

Table 23 Yields after CEX Purification of Mock Synthesis and Purification 2.1 calculated via Copper Assay 33

Table 24 Yields after Centrifugal Filtration of CEX-purified LPEI 10 kDa in Mock Synthesis and Purification 2.1 using different sized centrifugal filters and different amounts of washing cycles 34

Table 25 Product loss during centrifugal filtration due to washing into filtrate and binding to filter membrane in Mock Synthesis and Purification 2.1 34

Table 26 Comparison of yields after Centrifugal Filtration of ÄKTA-purified LPEI10kDa in Mock Synthesis and Purification 2.2 performing different amounts of washing cycles; yields were calculated in regards to applied amount of polymer at the beginning of desalting 36

Table 27 Yields after ÄKTA purification of Mock Synthesis 3 calculated via Copper Assay..... 37

Table 28 Comparison of yields after Centrifugal Filtration of ÄKTA-purified LPEI10kDa in Mock Synthesis 3 performing different amounts of washing cycles; yields were calculated in regards to applied amount of polymer at the beginning of desalting 38

Table 29 Comparison of yields after Desalting via Centrifugal Filtration and Dialysis of ÄKTA-purified LPEI-PEG-OPSS; yields were calculated in regards to applied amount of polymer at the beginning of desalting .. 41

Table 30 Online Monitoring of L-Cysteine-Coupling during Synthesis 1; Absorption of split off 2-Thiopyridone measured at 343 nm; Blank/t=0 = LPEI-PEG-OPSS diluted in 20 mM HEPES + 10% v/v acetonitrile to a final concentration of 4-5 mg/mL and purged with argon gas..... 42

Table 31 Online Monitoring of L-Cysteine-Coupling during Synthesis 2; Absorption of split off 2-Thiopyridone measured at 343 n; Blank/t=0 = LPEI-PEG-OPSS diluted in 20 mM HEPES + 10% v/v acetonitrile to a final concentration of 4-5 mg/mL and purged with argon gas..... 42

Table 32 Comparison of yields after Desalting via Centrifugal Filtration and Dialysis of ÄKTA-purified LPEI-PEG-CYS; yields were calculated in regards to applied amount of polymer at the beginning of desalting 43

Table 33 Z-Average and Polydispersity-Index-Results from LPEI/pDNA-Polyplexes using 40 µg/mL pDNA assessed using DLS; DLS settings as described in **Table 19** 44

Table 34 Z-Average and Polydispersity-Index-Results averaged from all 3 LPEI/pDNA-Polyplex-DLS measurements; DLS settings as described in **Table 19** 44

Table 35 Z-Average and Polydispersity-Index-Results from LPEI/pDNA-Polyplexes using 10 µg/mL pDNA assessed using DLS; DLS settings as described in **Table 19** 45

10 References

1. Huang, S., Que, H., Wang, M. & Wei, X. mRNA vaccines as cancer therapies. *Chin. Med. J. (Engl.)* **137**, 2979–2995 (2024).
2. Liu, B., Zhou, H., Tan, L., Siu, K. T. H. & Guan, X.-Y. Exploring treatment options in cancer: tumor treatment strategies. *Signal Transduct. Target. Ther.* **9**, 175 (2024).
3. Cheng, Z., Li, M., Dey, R. & Chen, Y. Nanomaterials for cancer therapy: current progress and perspectives. *J. Hematol. Oncol.J Hematol Oncol* **14**, 85 (2021).
4. Hanahan, D. & Weinberg, R. A. Hallmarks of Cancer: The Next Generation. *Cell* **144**, 646–674 (2011).
5. Pérez-Herrero, E. & Fernández-Medarde, A. Advanced targeted therapies in cancer: Drug nanocarriers, the future of chemotherapy. *Eur. J. Pharm. Biopharm.* **93**, 52–79 (2015).
6. Ferrara, N. Pathways mediating VEGF-independent tumor angiogenesis. *Cytokine Growth Factor Rev.* **21**, 21–26 (2010).
7. Hanahan, D. & Folkman, J. Patterns and Emerging Mechanisms Review of the Angiogenic Switch during Tumorigenesis.
8. Klymkowsky, M. W. & Savagner, P. Epithelial-Mesenchymal Transition. *Am. J. Pathol.* **174**, 1588–1593 (2009).
9. Talmadge, J. E. & Fidler, I. J. AACR Centennial Series: The Biology of Cancer Metastasis: Historical Perspective. *Cancer Res.* **70**, 5649–5669 (2010).
10. Li, H., Min, L., Du, H., Wei, X. & Tong, A. Cancer mRNA vaccines: clinical application progress and challenges. *Cancer Lett.* **625**, 217752 (2025).
11. Hanahan, D. Hallmarks of Cancer: New Dimensions. *Cancer Discov.* **12**, 31–46 (2022).
12. Kaur, R., Bhardwaj, A. & Gupta, S. Cancer treatment therapies: traditional to modern approaches to combat cancers. *Mol. Biol. Rep.* **50**, 9663–9676 (2023).
13. Cross, D. & Burmester, J. K. Gene Therapy for Cancer Treatment: Past, Present and Future. *Clin. Med. Res.* **4**, 218–227 (2006).
14. Szeto, G. L. & Finley, S. D. Integrative Approaches to Cancer Immunotherapy. *Trends Cancer* **5**, 400–410 (2019).

15. Vishweshwaraiah, Y. L. & Dokholyan, N. V. mRNA vaccines for cancer immunotherapy. *Front. Immunol.* **13**, 1029069 (2022).
16. Tsimberidou, A. M., Fountzilas, E., Nikanjam, M. & Kurzrock, R. Review of precision cancer medicine: Evolution of the treatment paradigm. *Cancer Treat. Rev.* **86**, 102019 (2020).
17. Yao, R., Xie, C. & Xia, X. Recent progress in mRNA cancer vaccines. *Hum. Vaccines Immunother.* **20**, 2307187 (2024).
18. Mondal, M., Guo, J., He, P. & Zhou, D. Recent advances of oncolytic virus in cancer therapy. *Hum. Vaccines Immunother.* **16**, 2389–2402 (2020).
19. Wei, G., Wang, Y., Yang, G., Wang, Y. & Ju, R. Recent progress in nanomedicine for enhanced cancer chemotherapy. *Theranostics* **11**, 6370–6392 (2021).
20. Beck, J. D. *et al.* mRNA therapeutics in cancer immunotherapy. *Mol. Cancer* **20**, 69 (2021).
21. Liu, C. *et al.* mRNA-based cancer therapeutics. *Nat. Rev. Cancer* **23**, 526–543 (2023).
22. Zong, Y., Lin, Y., Wei, T. & Cheng, Q. Lipid Nanoparticle (LNP) Enables mRNA Delivery for Cancer Therapy. *Adv. Mater.* **35**, 2303261 (2023).
23. Mainini, F. & Eccles, M. R. Lipid and Polymer-Based Nanoparticle siRNA Delivery Systems for Cancer Therapy. *Molecules* **25**, 2692 (2020).
24. Pandey, A. P. & Sawant, K. K. Polyethylenimine: A versatile, multifunctional non-viral vector for nucleic acid delivery. *Mater. Sci. Eng. C* **68**, 904–918 (2016).
25. Yao, Z. *et al.* Targeted delivery systems of siRNA based on ionizable lipid nanoparticles and cationic polymer vectors. *Biotechnol. Adv.* **81**, 108546 (2025).
26. Rödl, W., Taschauer, A., Schaffert, D., Wagner, E. & Ogris, M. Synthesis of Polyethylenimine-Based Nanocarriers for Systemic Tumor Targeting of Nucleic Acids. in *Nanotechnology for Nucleic Acid Delivery* (eds Ogris, M. & Sami, H.) vol. 1943 83–99 (Springer New York, New York, NY, 2019).
27. Sabin, J., Alatorre-Meda, M., Miñones, J., Domínguez-Arca, V. & Prieto, G. New insights on the mechanism of polyethylenimine transfection and their implications on gene therapy and DNA vaccines. *Colloids Surf. B Biointerfaces* **210**, 112219 (2022).

28. Bauer, M. *et al.* Rethinking the impact of the protonable amine density on cationic polymers for gene delivery: A comparative study of partially hydrolyzed poly(2-ethyl-2-oxazoline)s and linear poly(ethylene imine)s. *Eur. J. Pharm. Biopharm.* **133**, 112–121 (2018).
29. Ungaro, F., De Rosa, G., Miro, A. & Quaglia, F. Spectrophotometric determination of polyethylenimine in the presence of an oligonucleotide for the characterization of controlled release formulations. *J. Pharm. Biomed. Anal.* **31**, 143–149 (2003).
30. Boeckle, S. *et al.* Purification of polyethylenimine polyplexes highlights the role of free polycations in gene transfer. *J. Gene Med.* **6**, 1102–1111 (2004).
31. Rockwell, L. *et al.* Cation exchange as a single polishing step for conjugated peptides. *Biotechnol. Prog.* **38**, e3238 (2022).
32. Taschauer, A. *et al.* Up-Scaled Synthesis and Characterization of Nonviral Gene Delivery Particles for Transient *In Vitro* and *In Vivo* Transgene Expression. *Hum. Gene Ther. Methods* **27**, 87–97 (2016).
33. Johnsen, E. *et al.* A critical evaluation of Amicon Ultra centrifugal filters for separating proteins, drugs and nanoparticles in biosamples. *J. Pharm. Biomed. Anal.* **120**, 106–111 (2016).
34. Kidambi, P. R. *et al.* Nanoporous Atomically Thin Graphene Membranes for Desalting and Dialysis Applications. *Adv. Mater.* **29**, 1700277 (2017).
35. Filippov, S. K. *et al.* Dynamic light scattering and transmission electron microscopy in drug delivery: a roadmap for correct characterization of nanoparticles and interpretation of results. *Mater. Horiz.* **10**, 5354–5370 (2023).
36. Moreno Herrero, J. *et al.* Compact polyethylenimine-complexed mRNA vaccines. *Nat. Nanotechnol.* **20**, 1323–1331 (2025).

11 Appendix

11.1 Ad Mock Synthesis and Purification 2.1

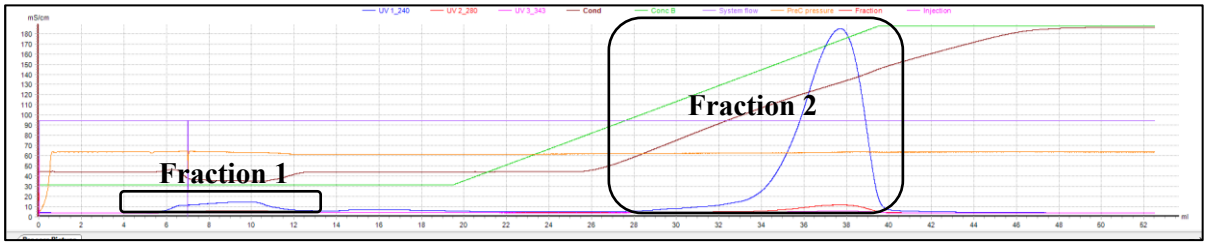

Figure 48 *Cation exchange chromatography diagram from* ***Run 2/2 of LPEI10kDa-Mock Synthesis and Purification 2.1*** *in HEPES buffer. 5ml of crude polymer was injected and subjected to chromatographic separation by ÄKTA. Y-axis plots conductivity and UV measurements are shown in colored lines (240nm blue, 280nm red and 343nm pink nm); blue line represents detected LPEI. Solid phase used was Macro-Prep High S Media and ÄKTA settings are described in* ***Table 7***

11.2 Ad Mock Synthesis and Purification 3

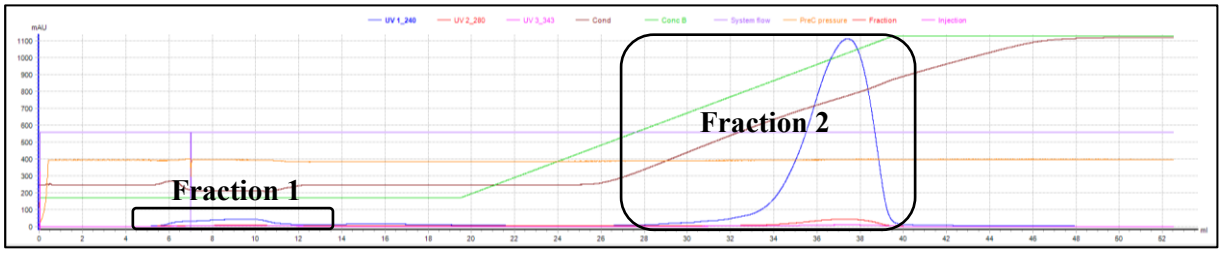

Figure 49 *Cation exchange chromatography diagram from* ***Run 2/2 of LPEI10kDa-Mock Synthesis and Purification 3*** *in HEPES buffer. 5ml of crude polymer was injected and subjected to chromatographic separation by ÄKTA. Y-axis plots milli-Absorbance-Units and UV measurements are shown in colored lines (240nm blue, 280nm red and 343nm pink nm); blue line represents detected LPEI. Solid phase used was Macro-Prep High S Media and ÄKTA settings are described in* ***Table 7***

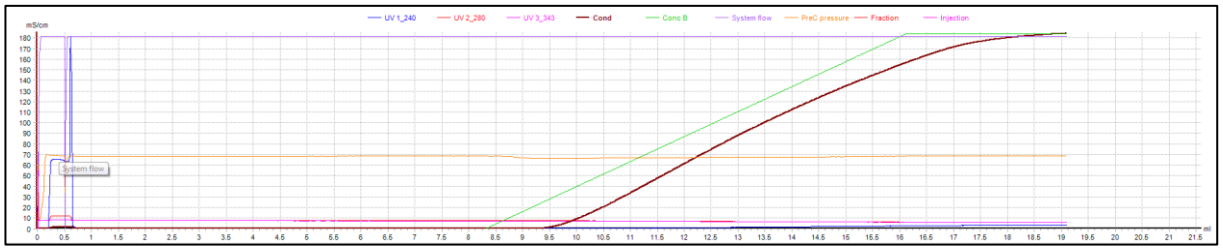

Figure 50 *Filtr****ate after 2. Washing Cycle****; ÄKTA conductivity spectrums of* ***Mock Synthesis and Purification 3*** *in HEPES buffer; ÄKTA UV measurement (240 blue, 280 red and 343 pink nm); green line shows increasing salt concentration and brown line in correlation to the green line shows conductivity; solid phase: Macro-Prep High S Media; ÄKTA setting described in* ***Table 8***

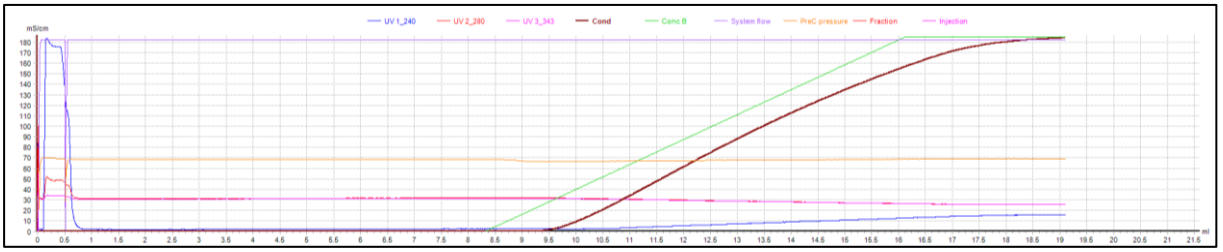

Figure 51 Filtrate after 3. Washing Cycle*; ÄKTA conductivity spectrums of* ***Mock Synthesis and Purification 3*** *in HEPES buffer; ÄKTA UV measurement (240 blue, 280 red and 343 pink nm); green line shows increasing salt concentration and brown line in correlation to the green line shows conductivity; solid phase: Macro-Prep High S Media; ÄKTA setting described in* ***Table 8***

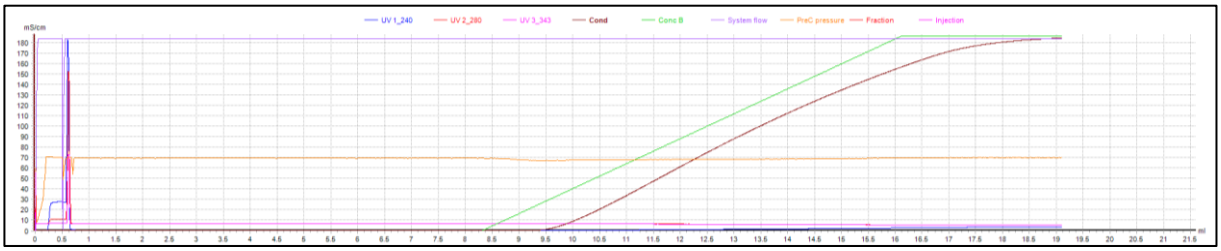

Figure 52 Filtrate after 4. Washing Cycle**; ÄKTA conductivity spectrums of **Mock Synthesis and Purification 3** in HEPES buffer; ÄKTA UV measurement (240 blue, 280 red and 343 pink nm); green line shows increasing salt concentration and brown line in correlation to the green line shows conductivity; solid phase: Macro-Prep High S Media; ÄKTA setting described in **Table 8

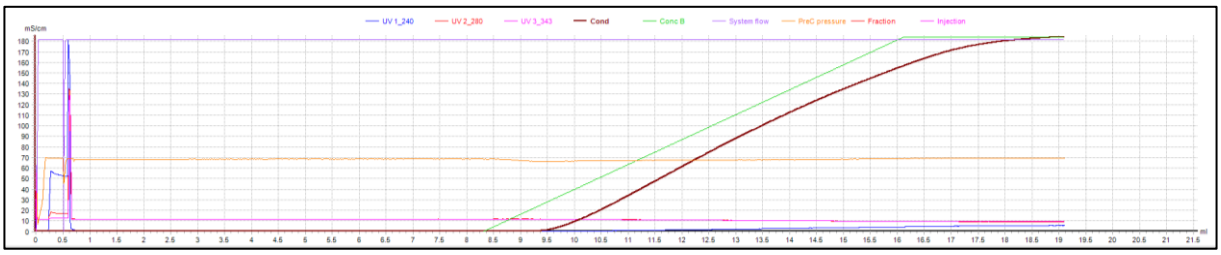

Figure 53 Filtrate after 5. Washing Cycle**; ÄKTA conductivity spectrums of **Mock Synthesis and Purification 3** in HEPES buffer; ÄKTA UV measurement (240 blue, 280 red and 343 pink nm); green line shows increasing salt concentration and brown line in correlation to the green line shows conductivity; solid phase: Macro-Prep High S Media; ÄKTA setting described in **Table 8

11.3 Ad ÄKTA Purification of LPEI-PEG-OPSS

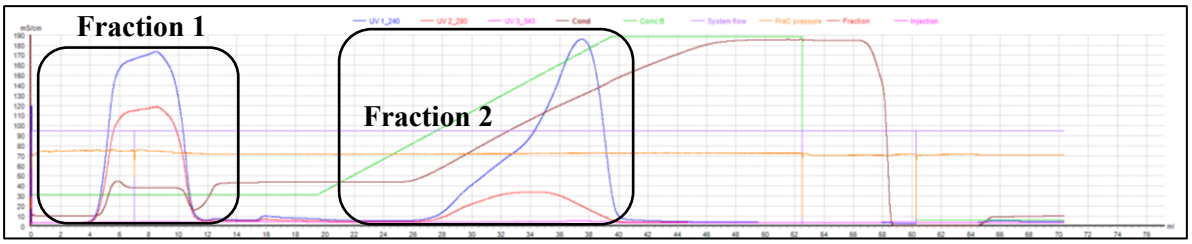

***Figure 54** Cation exchange chromatography diagram from **Run 2/8 of LPEI-PEG-OPSS Synthesis 1** in HEPES buffer. 5ml of crude polymer was injected and subjected to chromatographic separation by ÄKTA. Y-axis plots milli-Absorbance-Units and UV measurements are shown in colored lines (240nm blue, 280nm red and 343nm pink nm); blue line represents detected LPEI. Solid phase used was Macro-Prep High S Media and ÄKTA settings are described in **Table 7**; Fraction 2 subject to Centrifugal Filtration Purification;*

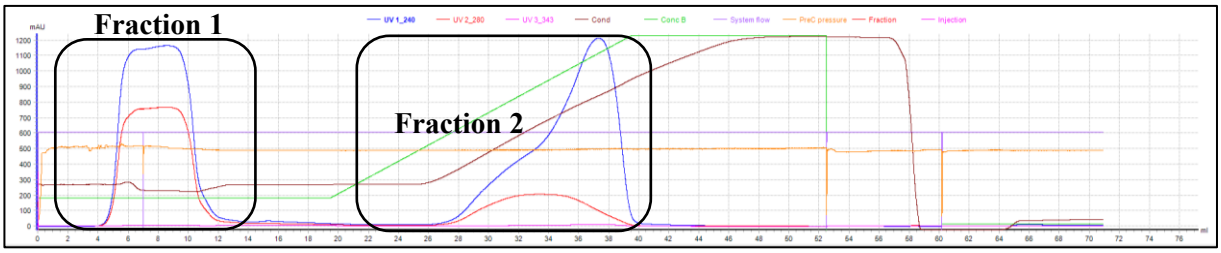

***Figure 55** Cation exchange chromatography diagram from **Run 3/8 of LPEI-PEG-OPSS Synthesis 1** in HEPES buffer. 5ml of crude polymer was injected and subjected to chromatographic separation by ÄKTA. Y-axis plots milli-Absorbance-Units and UV measurements are shown in colored lines (240nm blue, 280nm red and 343nm pink nm); blue line represents detected LPEI. Solid phase used was Macro-Prep High S Media and ÄKTA settings are described in **Table 7**; Fraction 2 subject to Centrifugal Filtration Purification;*

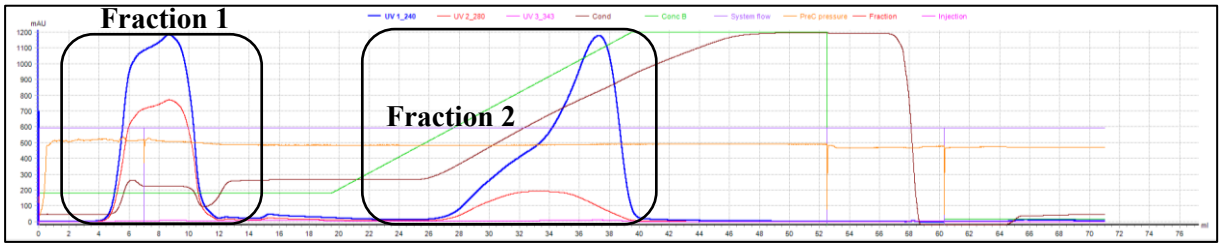

Figure 56 *Cation exchange chromatography diagram from* ***Run 4/8 of LPEI-PEG-OPSS Synthesis 1*** *in HEPES buffer. 5ml of crude polymer was injected and subjected to chromatographic separation by ÄKTA. Y-axis plots milli-Absorbance-Units and UV measurements are shown in colored lines (240nm blue, 280nm red and 343nm pink nm); blue line represents detected LPEI. Solid phase used was Macro-Prep High S Media and ÄKTA settings are described in* ***Table 7****; Fraction 2 subject to Centrifugal Filtration Purification;*

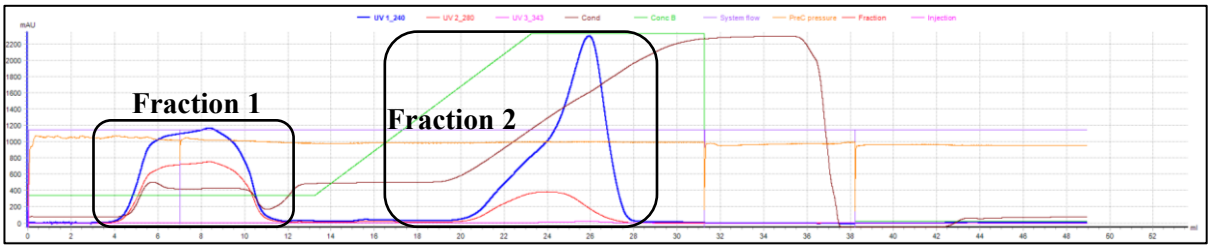

Figure 57 *Cation exchange chromatography diagram from* ***Run 6/8 of LPEI-PEG-OPSS Synthesis 1*** *in HEPES buffer. 5ml of crude polymer was injected and subjected to chromatographic separation by ÄKTA. Y-axis plots milli-Absorbance-Units and UV measurements are shown in colored lines (240nm blue, 280nm red and 343nm pink nm); blue line represents detected LPEI. Solid phase used was Macro-Prep High S Media and ÄKTA settings are described in* ***Table 11****; Fraction 2 subject to Dialysis Purification;*

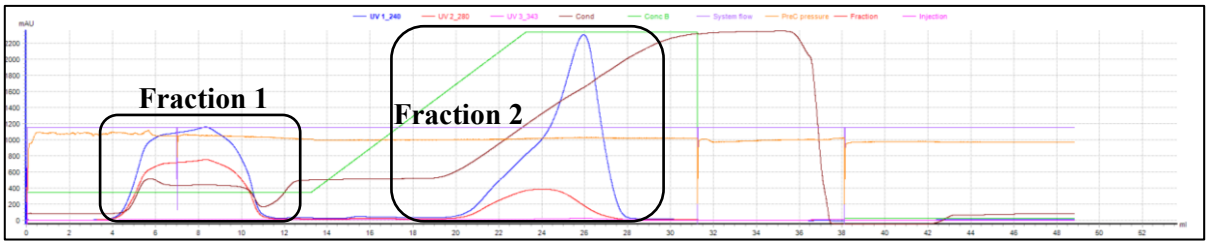

Figure 58 *Cation exchange chromatography diagram from* ***Run 7/8 of LPEI-PEG-OPSS Synthesis 1*** *in HEPES buffer. 5ml of crude polymer was injected and subjected to chromatographic separation by ÄKTA. Y-axis plots milli-Absorbance-Units and UV measurements are shown in colored lines (240nm blue, 280nm red and 343nm pink nm); blue line represents detected LPEI. Solid phase used was Macro-Prep High S Media and ÄKTA settings are described in* ***Table 11****; Fraction 2 subject to Dialysis Purification;*

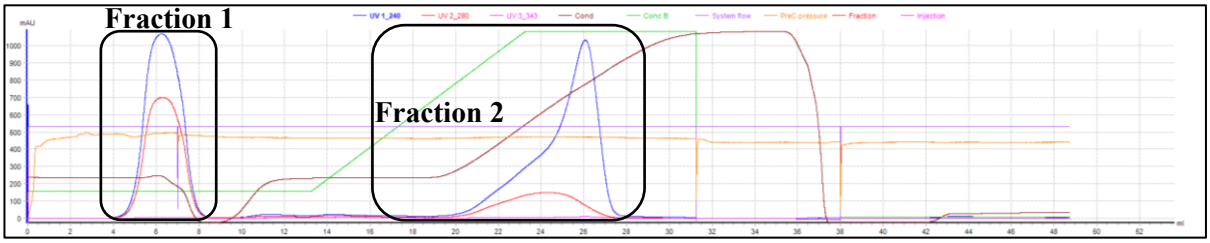

Figure 59 *Cation exchange chromatography diagram from* ***Run 8/8 of LPEI-PEG-OPSS Synthesis 1*** *in HEPES buffer. 5ml of crude polymer was injected and subjected to chromatographic separation by ÄKTA. Y-axis plots milli-Absorbance-Units and UV measurements are shown in colored lines (240nm blue, 280nm red and 343nm pink nm); blue line represents detected LPEI. Solid phase used was Macro-Prep High S Media and ÄKTA settings are described in* ***Table 11****; Fraction 2 was not processed further due to insufficient amount of crude conjugate which was nonetheless applied*

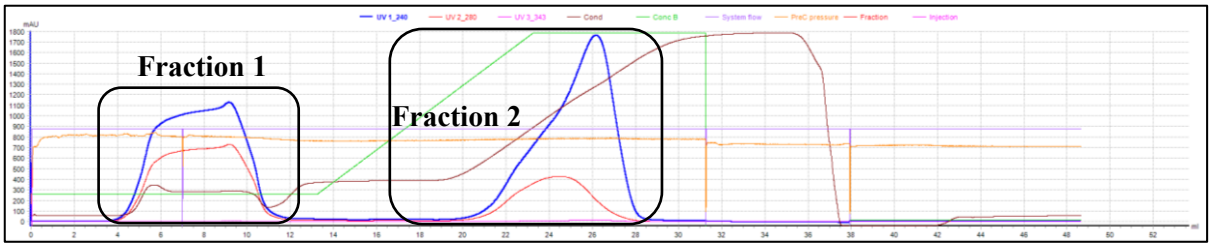

Figure 60 *Cation exchange chromatography diagram from* ***Run 2/8 of LPEI-PEG-OPSS Synthesis 2*** *in HEPES buffer. 5ml of crude polymer was injected and subjected to chromatographic separation by ÄKTA. Y-axis plots milli-Absorbance-Units and UV measurements are shown in colored lines (240nm blue, 280nm red and 343nm pink nm); blue line represents detected LPEI. Solid phase used was Macro-Prep High S Media and ÄKTA settings are described in* ***Table 11****; Fraction 2 subject to Centrifugal Filtration Purification*

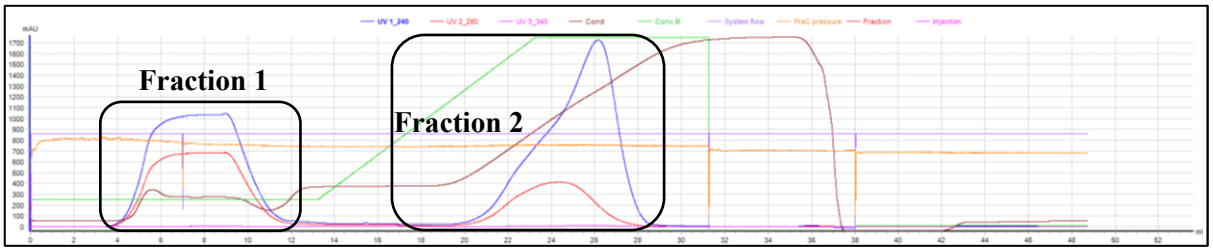

Figure 61 *Cation exchange chromatography diagram from* ***Run 3/8 of LPEI-PEG-OPSS Synthesis 2*** *in HEPES buffer. 5ml of crude polymer was injected and subjected to chromatographic separation by ÄKTA. Y-axis plots milli-Absorbance-Units and UV measurements are shown in colored lines (240nm blue, 280nm red and 343nm pink nm); blue line represents detected LPEI. Solid phase used was Macro-Prep High S Media and ÄKTA settings are described in* ***Table 11****; Fraction 2 subject to Centrifugal Filtration Purification*

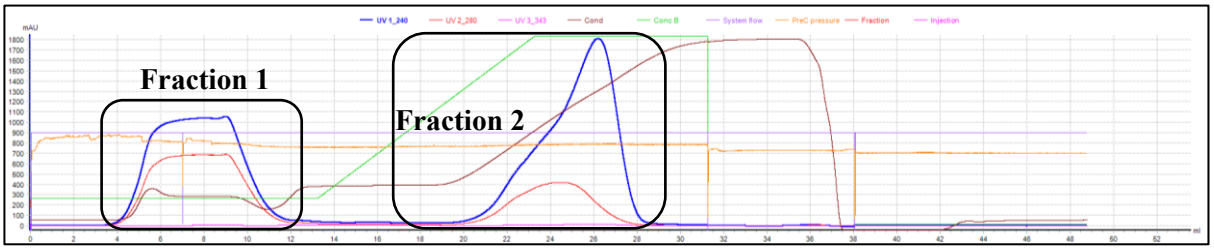

Figure 62 *Cation exchange chromatography diagram from* ***Run 4/8 of LPEI-PEG-OPSS Synthesis 2*** *in HEPES buffer. 5ml of crude polymer was injected and subjected to chromatographic separation by ÄKTA. Y-axis plots milli-Absorbance-Units and UV measurements are shown in colored lines (240nm blue, 280nm red and 343nm pink nm); blue line represents detected LPEI. Solid phase used was Macro-Prep High S Media and ÄKTA settings are described in* ***Table 11****; Fraction 2 subject to Centrifugal Filtration Purification*

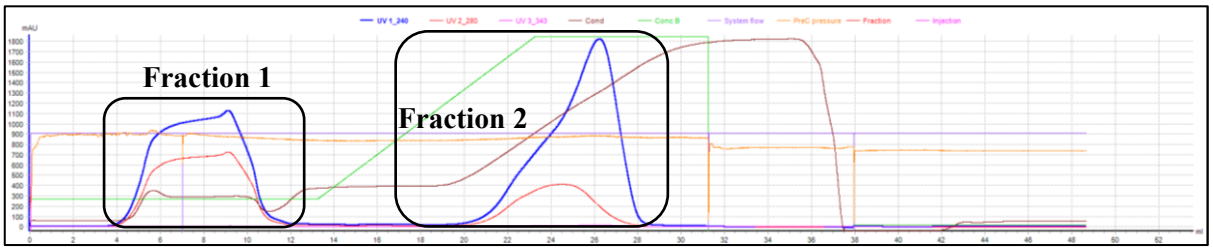

Figure 63 *Cation exchange chromatography diagram from* ***Run 6/8 of LPEI-PEG-OPSS Synthesis 2*** *in HEPES buffer. 5ml of crude polymer was injected and subjected to chromatographic separation by ÄKTA. Y-axis plots milli-Absorbance-Units and UV measurements are shown in colored lines (240nm blue, 280nm red and 343nm pink nm); blue line represents detected LPEI. Solid phase used was Macro-Prep High S Media and ÄKTA settings are described in* ***Table 11****; Fraction 2 subject to Dialysis Purification*

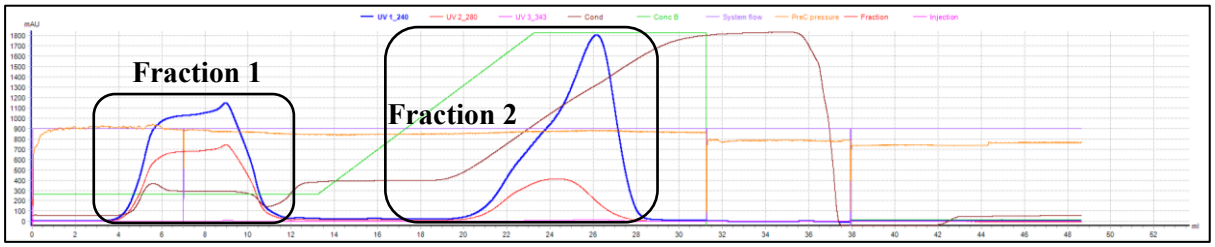

Figure 64 *Cation exchange chromatography diagram from* ***Run 7/8 of LPEI-PEG-OPSS Synthesis 2*** *in HEPES buffer. 5ml of crude polymer was injected and subjected to chromatographic separation by ÄKTA. Y-axis plots milli-Absorbance-Units and UV measurements are shown in colored lines (240nm blue, 280nm red and 343nm pink nm); blue line represents detected LPEI. Solid phase used was Macro-Prep High S Media and ÄKTA settings are described in* ***Table 11****; Fraction 2 subject to Dialysis Purification*

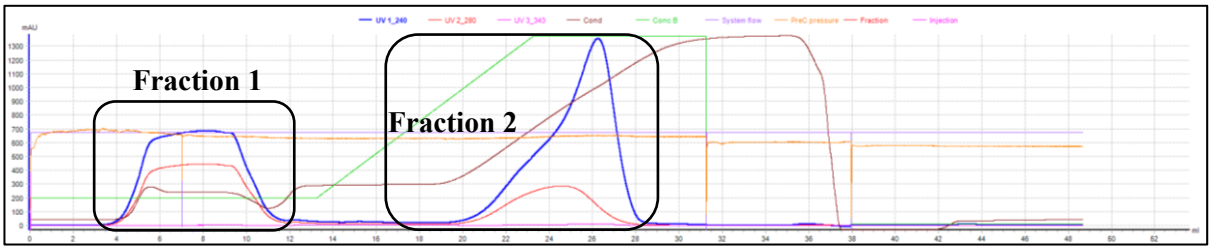

Figure 65 *Cation exchange chromatography diagram from* ***Run 8/8 of LPEI-PEG-OPSS Synthesis 2*** *in HEPES buffer. 5ml of crude polymer was injected and subjected to chromatographic separation by ÄKTA. Y-axis plots milli-Absorbance-Units and UV measurements are shown in colored lines (240nm blue, 280nm red and 343nm pink nm); blue line represents detected LPEI. Solid phase used was Macro-Prep High S Media and ÄKTA settings are described in* ***Table 11****; Fraction 2 subject to Dialysis Purification*

11.4 Ad Purification of the LPEI-PEG-CYS Tri-Conjugate

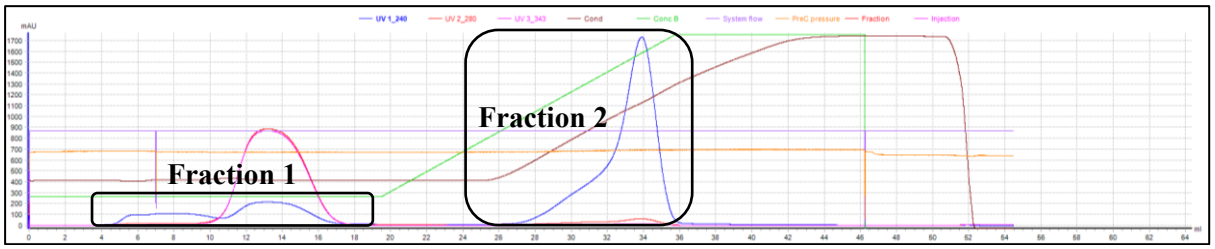

Figure 66 *Cation exchange chromatography diagram from* ***Run 1/2 of LPEI-PEG-CYS Synthesis 1 produced from centrifugally filtered Bi-Conjugate*** *in HEPES buffer. 5ml of crude polymer was injected and subjected to chromatographic separation by ÄKTA. Y-axis plots milli-Absorbance-Units and UV measurements are shown in colored lines (240nm blue, 280nm red and 343nm pink nm); blue line represents detected LPEI. Solid phase used was Macro-Prep High S Media and ÄKTA settings are described in* ***Table 16****; Fraction 2 subject to Centrifugal Filtration Purification*

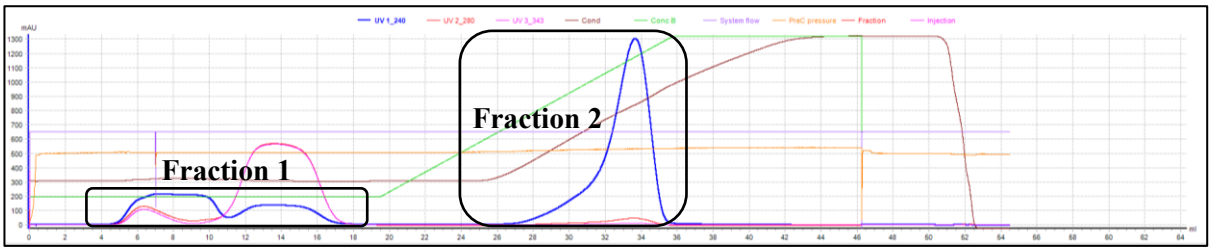

Figure 67 *Cation exchange chromatography diagram from* ***Run 2/2 of LPEI-PEG-CYS Synthesis 2 produced from dialyzed Bi-Conjugate*** *in HEPES buffer. 5ml of crude polymer was injected and subjected to chromatographic separation by ÄKTA. Y-axis plots milli-Absorbance-Units and UV measurements are shown in colored lines (240nm blue, 280nm red and 343nm pink nm); blue line represents detected LPEI. Solid phase used was Macro-Prep High S Media and ÄKTA settings are described in* ***Table 16****; Fraction 2 subject to Dialysis Purification*